ORNL/TM-2004/290

Thermophysical Properties of Heat Resistant Shielding Material

December 2004

W. D. Porter
H. Wang

UT-BATTELLE

2-537

Metals and Ceramics Division

THERMOPHYSICAL PROPERTIES OF HEAT RESISTANT SHIELDING MATERIAL

W. D. Porter and H. Wang

Date Published: December 2004

2-540

CONTENTS

LIST OF FIGURES

2-544

LIST OF TABLES

2-546

1. INTRODUCTION

This project was aimed at determining thermal conductivity, specific heat and thermal expansion of a heat resistant shielding material for neutron absorption applications. These data are critical in predicting the structural integrity of the shielding under thermal cycling and mechanical load. The measurements of thermal conductivity and specific heat were conducted in air at five different temperatures (-31°F, 73.4°F, 140°F, 212°F and 302°F). The transient plane source (TPS) method was used in the tests. Thermal expansion tests were conducted using push rod dilatometry over the continuous range from -40°F (-40°C) to 302°F (150°C).

2. EXPERIMENTAL

2.1 THERMAL CONDUCTIVITY AND VOLUMETRIC SPECIFIC HEAT

The Hot Disk Thermal Constants Analyzer was used to measure both thermal conductivity and specific heat of the samples.[1-3] The recently upgraded system (Fig. 1) uses a bridge to balance out changes in heater resistance at different temperatures. Two samples are needed for the measurement. A Kapton sensor/heater is sandwiched between the two samples. For the heat resistant shielding material, each measurement took 80 s during which the interface was heated up by a constant power output of 0.05 W. The overall temperature rise was kept under 5°C. Thermal conductivity and volumetric specific heat can be calculated from the interface temperature vs. time plot using the Hot Disk® software.

Six heat resistant shielding samples, Thermo Electron RM&P Catalog No. 277-4, were provided and were paired up in random. Each pair was measured at room temperature at HTML. The system was then taken to Building 4508 where a freezer (at -31°F) was available. After the freezer test, the specimens were tested in a box furnace at three elevated temperatures. To reach thermal equilibrium, the specimens were left in the freezer or furnace for at least 2.5 hr before measurements were started.
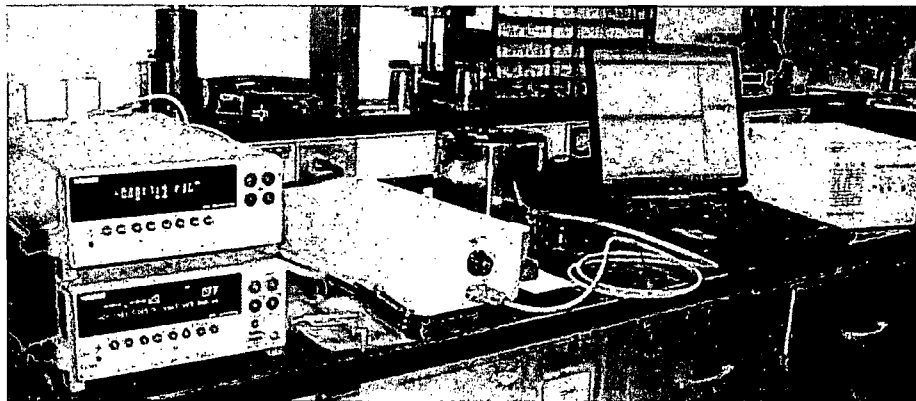

Fig. 1. Hot Disk System.

1

2.2 THERMAL EXPANSION

Specimens of cast Type 277-4 cement were received and tested by staff of the High Temperature Materials Laboratory at ORNL. The specimens were received in two shipments and consisted of three separate pours (lots) of the material. Lot 1 contained one specimen, poured in a one-piece mold, and having a diameter of ~5.5 mm. Lot 2 contained 7 specimens, poured in a split two-piece mold, also with a diameter of ~5.5 mm. Lot 3 had 5 specimens with a diameter of ~12.5 mm. No specimens from Lot 3 were used for measurements. The nominal length of all specimens was 25 mm.

Thermal expansion measurements were conducted using a Theta Industries dual push rod dilatometer. The testing followed the constant ramping procedure of ASTM E-228 for "Linear Thermal Expansion of Solid Materials with a Vitreous Silica Dilatometer."[4] A cryogenic furnace, cooled with helium gas bubbled through liquid nitrogen and heated by nichrome wires, was used with a silica specimen holder and push rods. A type K thermocouple in direct contact with the specimen was used to measure the specimen temperature. NIST Tungsten SRM 737 was used for the reference standard in the differential measurements. The specimens were tested over the range of -40°C to 150°C using heating rates of 3°C/min. The reference temperature for all expansion calculations was 20°C. A 5 cc/min flowrate of helium was used inside the specimen enclosure during the tests. This was a separate stream of helium from that used for cooling the cryogenic furnace. The displacements of the specimen and reference rods were determined by an LVDT housed in a constant temperature enclosure which also contained the RTD used for cold junction compensation of the specimen thermocouple signal.

The temperature schedule for the measurement tests was as follows:

1. Cool specimen to ~15°C prior to starting test using cooled helium.
2. Start data collection and heat specimen to 40°C. (Expansion is automatically zeroed as the specimen temperature goes through the 20°C reference temperature.)
3. Cool to -40°C at a nominal rate of 3°C/min.
4. Heat to 150°C.
5. Cool to -40°C at a nominal rate of 3°C/min.
6. Heat to 25°C and end test.

The schedule used allowed any hysteresis of the specimen expansion behavior to be noted.

3. RESULTS

3.1 THERMAL CONDUCTIVITY AND VOLUMETRIC SPECIFIC HEAT

Thermal conductivity values of the three pairs of samples are shown in Table 1 and the Thermal Conductivity vs. Temperature plot is shown in Fig. 2. Three measurements were taken at each temperature for each pair of samples. There is some scatter among the pairs (<5% between 3 measurements at the same temperature, 3-10% among the pairs) but they all showed similar changes over the temperature range. Since the specimens had to be taken out several times at each temperature, their exposure to air and thermal cycles was not controlled.

2

Table 1. Thermal conductivity (W/m•K)

Temperature (F)	Pair A	Pair B	Pair C
-31	0.96	0.97	0.92
73.4	1.00	0.97	1.05
140	0.87	0.75	0.87
212	0.64	0.62	0.58
302	0.67	0.59	0.64
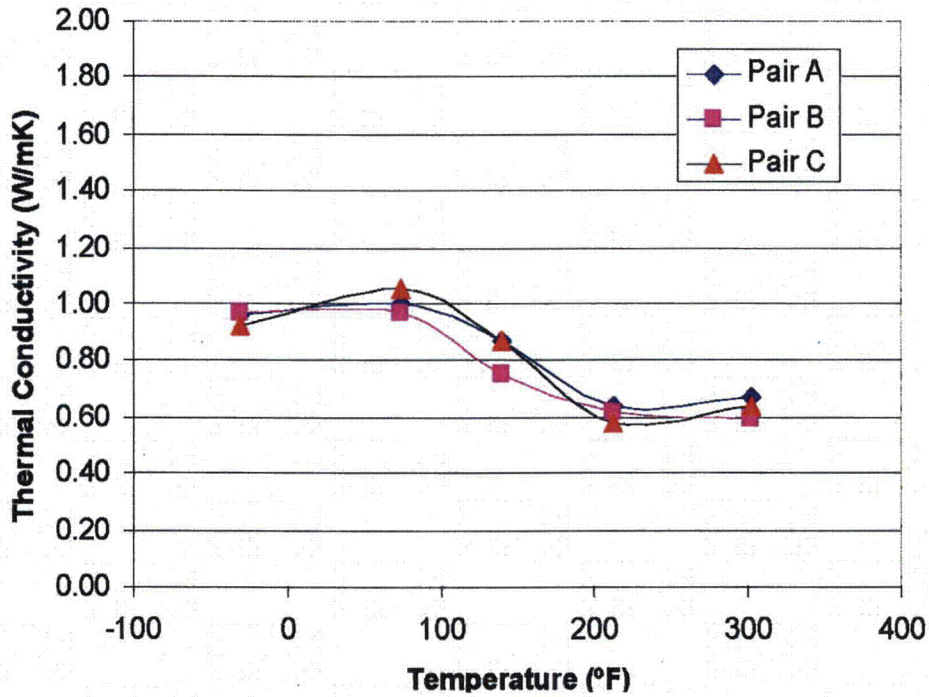
Fig 2. Thermal conductivity of Thermo Electron RM&P Catalog No. 277-4.

The volumetric specific heats were also obtained in the calculation. The value is a product of specific heat and density with the unit of $10^6 J/m^3•K$, as shown in Table 2 and Fig. 3. Since the weight of the samples exceeded the limit of the balance in the lab we were not able to measure the density of the specimens accurately. If the density is known ($1.68*10^6 g/m^3$ from product literature), the specific heat values can be calculated simply by dividing the current experimental value by density.

3

Table 2. Volumetric Specific Heat (MJ/m³•K)

Temperature (F)	Pair A	Pair B	Pair C
-31	0.92	0.80	0.92
73.4	1.33	1.27	1.32
140	1.71	1.68	1.65
212	1.72	1.67	1.72
302	1.99	2.14	2.01
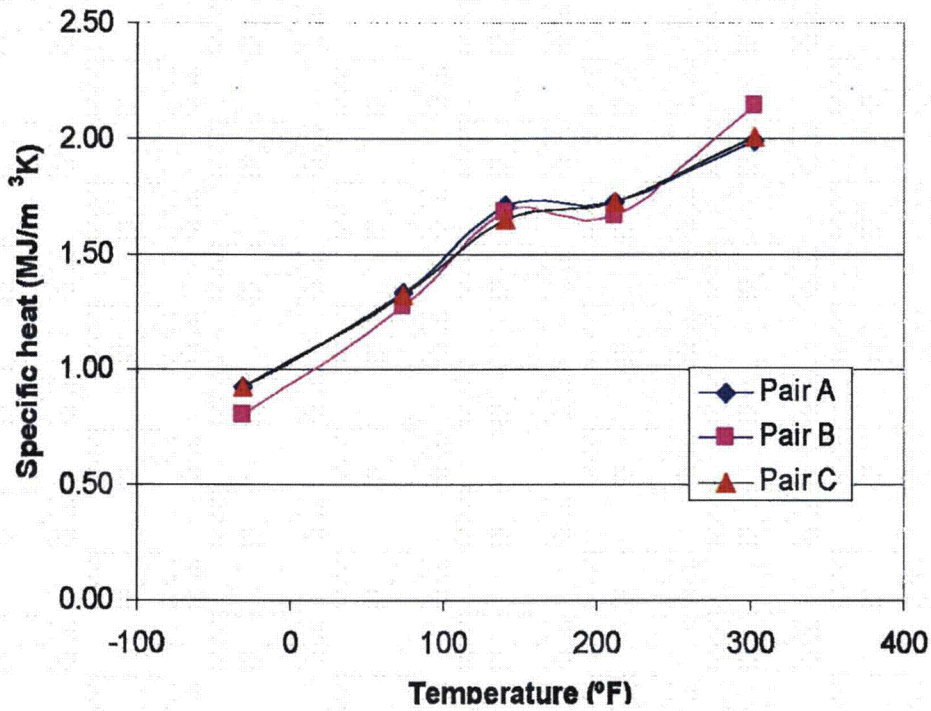
Fig. 3. Volumetric specific heat vs. temperature.

Since the three pairs of specimens were randomly grouped, we averaged the results to show the material properties. The values are shown in Table 3 and the plots are shown in Figures 4-5.

4

Table 3. Average values of k and Cp

Temperature (°F)	Average k (W/m·K)	Average Cp (MJ/m³·K)
-31	0.95	0.88
73.4	1.01	1.31
140	0.83	1.68
212	0.61	1.70
302	0.63	2.05
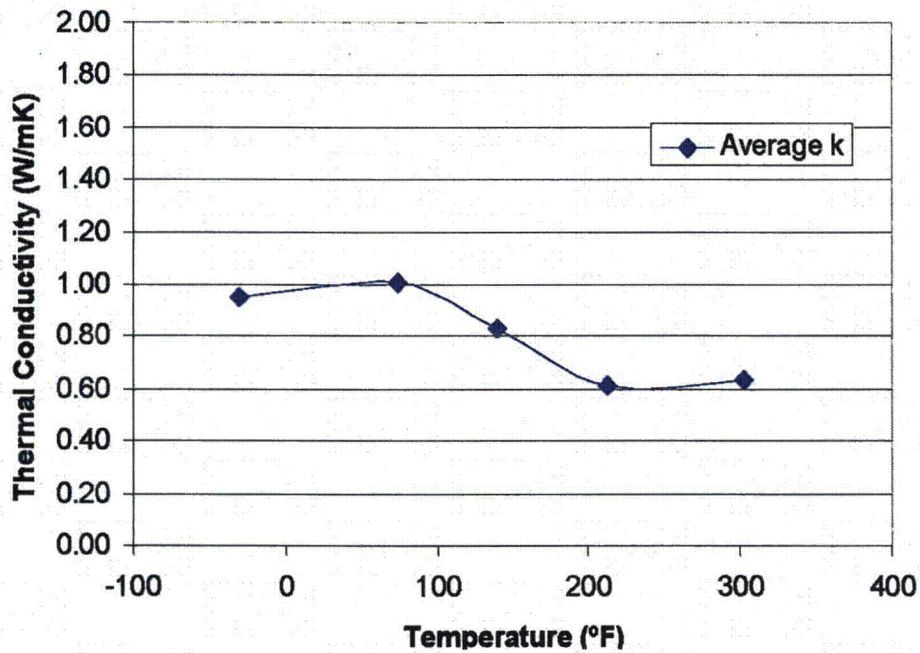
Fig. 4. Average thermal conductivity of Thermo Electron RM&P No. 277-4.

5
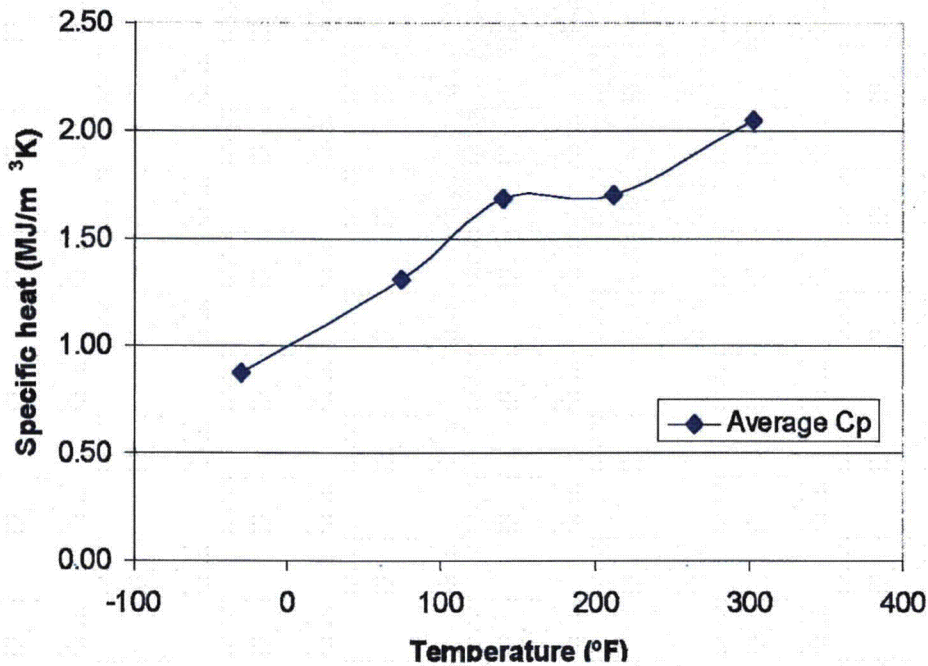
Fig. 5. Average volumetric specific heat of Thermo Electron RM&P Catalog No. 277-4.

3.2 THERMAL EXPANSION

One specimen from Lot 1 and four specimens from Lot 2 were tested. The thermal expansion results of the five specimens are shown in Fig. 6. Three Lot 2 specimen results grouped almost on top of each other. The fourth Lot 2 specimen deviated from the other three at temperatures greater than about 100°C. The single specimen from Lot 1 behaved markedly different than the Lot 2 specimens when heated above 50°C. The expansion behavior during cooling was very similar for all five specimens tested. All specimens tested exhibited a permanent strain (shrinkage) as a result of heating above 50°C. Measured data for the expansion of the five specimens taken from the initial heating from -40°C to 150°C can be found in Table 4. Also shown in Table 4 are values for the Mean Coefficient of Thermal Expansion (MCTE) calculated from 20°C. MCTE is defined as:

$$\text{MCTE} = (\text{expansion @ } T) / (T - 20) \tag{1}$$

where T is the temperature in °C.

6
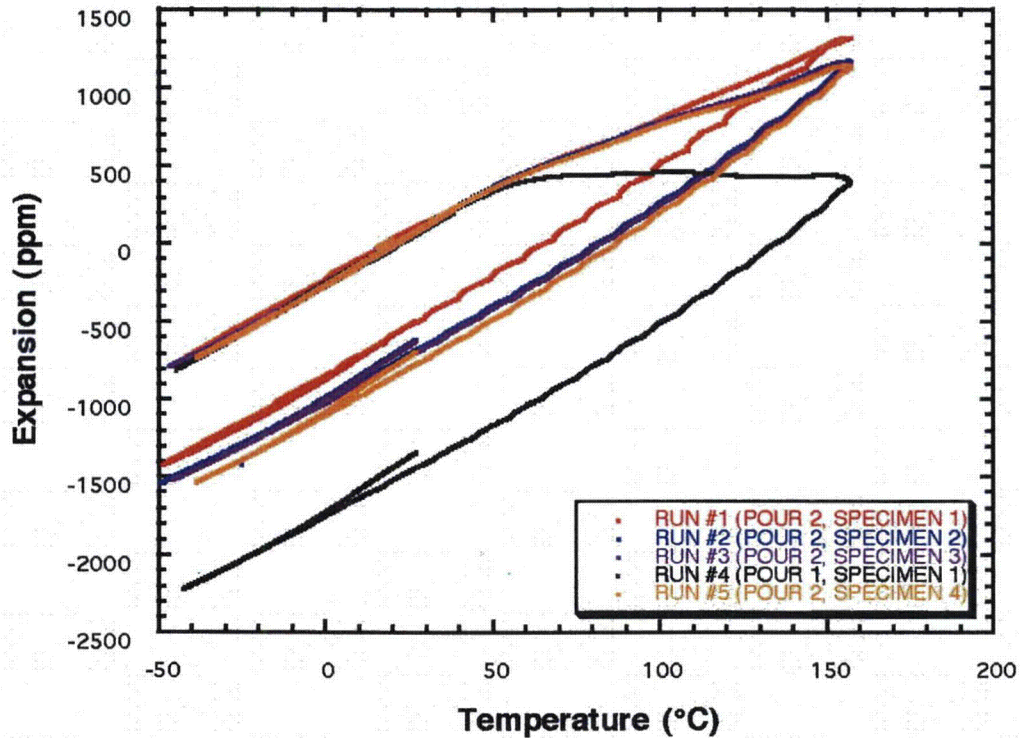
Fig. 6. Thermal expansion of Type 277-4 cement material as a function of temperature.

Table 4. Measured thermal expansion values and Mean CTE for Type 277-4 specimens

Temperature, °C	Run #1		Run #2		Run #3		Run #4		Run #5	
	exp, ppm	MCTE, ppm/°C	exp, ppm	MCTE, ppm/°C	exp, ppm	MCTE, ppm/°C	exp, ppm	MCTE, ppm/°C	exp, ppm	MCTE, ppm/°C
-40	-741	12.4	-727	12.1	-725	12.1	-759	12.6	-753	12.6
-20	-517	12.9	-500	12.5	-498	12.4	-519	13.0	-520	13.0
0	-266	13.3	-251	12.6	-247	12.3	-251	12.5	-260	13.0
20	0		0		0		0		0	
40	239	12.0	252	12.6	245	12.3	240	12.0	248	12.4
60	463	11.6	466	11.6	455	11.4	410	10.2	458	11.5
80	628	10.5	622	10.4	611	10.2	448	7.5	605	10.1
100	797	10.0	778	9.7	772	9.7	465	5.8	757	9.5
120	983	9.8	907	9.1	905	9.1	447	4.5	882	8.8
140	1166	9.7	1050	8.8	1042	8.7	434	3.6	1019	8.5
150	1271	9.8	1136	8.7	1126	8.7	449	3.4	1108	8.5

7

2-553

The expansion data in the interval -40 to 150°C for 3 of the Lot 2 specimens (Run #2, #3 and #5) were pooled and then sorted in ascending order by temperature. A moving average smoothing routine with a 31-point window (corresponds to less than 1°C temperature interval) was used to smooth both the temperature and expansion data. A cubic spline fit through this pooled, sorted and smoothed data set was then used to generate values for the expansion at increments of 1°C as shown in Table 5. The spline fit indicated an expansion of 1.6 ppm at 20°C. Since by definition the expansion is zero at the 20°C reference temperature, the values of Table 5 have been offset by this amount.

Table 5. Expansion values at even intervals estimated from cubic spline fit of pooled, sorted and smoothed data from Runs 2, 3, and 5.

TEMPERATURE, °C	ESTIMATED EXPANSION, ppm	ESTIMATED MCTE, ppm/°C	TEMPERATURE, °C	ESTIMATED EXPANSION, ppm	ESTIMATED MCTE, ppm/°C
-37	-706	12.4	5	-190	12.7
-36	-695	12.4	6	-177	12.7
-35	-683	12.4	7	-165	12.7
-34	-671	12.4	8	-152	12.7
-33	-661	12.5	9	-139	12.7
-32	-649	12.5	10	-126	12.7
-31	-638	12.5	11	-114	12.7
-30	-625	12.5	12	-101	12.7
-29	-614	12.5	13	-88	12.7
-28	-603	12.6	14	-76	12.7
-27	-591	12.6	15	-63	12.6
-26	-578	12.6	16	-50	12.6
-25	-567	12.6	17	-37	12.6
-24	-555	12.6	18	-25	12.6
-23	-544	12.7	19	-12	12.6
-22	-532	12.7	20	0	12.6
-21	-519	12.7	21	12	12.6
-20	-508	12.7	22	25	12.6
-19	-496	12.7	23	38	12.7
-18	-484	12.7	24	50	12.6
-17	-470	12.7	25	63	12.6
-16	-458	12.7	26	75	12.6
-15	-446	12.8	27	88	12.6
-14	-433	12.8	28	100	12.6
-13	-420	12.8	29	113	12.6
-12	-408	12.8	30	125	12.5
-11	-395	12.7	31	137	12.5
-10	-382	12.8	32	150	12.5
-9	-369	12.7	33	162	12.5
-8	-356	12.7	34	174	12.5
-7	-344	12.7	35	186	12.4
-6	-331	12.7	36	198	12.4
-5	-317	12.7	37	210	12.4
-4	-304	12.7	38	222	12.4
-3	-292	12.7	39	235	12.4
-2	-279	12.7	40	246	12.3
-1	-267	12.7	41	258	12.3
0	-254	12.7	42	270	12.3
1	-241	12.7	43	281	12.3
2	-228	12.7	44	293	12.2
3	-216	12.7	45	305	12.2
4	-203	12.7	46	316	12.2

8

Table 5. (Continued)

TEMPERATURE, °C	ESTIMATED EXPANSION, ppm	ESTIMATED MCTE, ppm/°C	TEMPERATURE, °C	ESTIMATED EXPANSION, ppm	ESTIMATED MCTE, ppm/°C
47	327	12.1	99	759	9.62
48	338	12.1	100	767	9.60
49	349	12.1	101	776	9.58
50	360	12.0	102	783	9.55
51	371	12.0	103	790	9.53
52	381	11.9	104	797	9.50
53	392	11.9	105	804	9.46
54	402	11.8	106	812	9.44
55	412	11.8	107	818	9.40
56	421	11.7	108	825	9.38
57	431	11.7	109	831	9.34
58	440	11.6	110	837	9.31
59	449	11.5	111	844	9.28
60	458	11.5	112	850	9.25
61	466	11.4	113	856	9.21
62	475	11.3	114	862	9.18
63	483	11.3	115	867	9.13
64	492	11.2	116	873	9.10
65	500	11.1	117	879	9.06
66	508	11.0	118	885	9.03
67	515	11.0	119	890	8.99
68	523	10.9	120	897	8.97
69	530	10.8	121	902	8.94
70	538	10.8	122	908	8.91
71	545	10.7	123	914	8.88
72	552	10.6	124	920	8.85
73	559	10.6	125	926	8.82
74	566	10.5	126	933	8.81
75	573	10.4	127	939	8.78
76	581	10.4	128	946	8.76
77	588	10.3	129	953	8.74
78	596	10.3	130	959	8.72
79	603	10.2	131	966	8.71
80	611	10.2	132	974	8.70
81	619	10.1	133	980	8.68
82	626	10.1	134	987	8.67
83	634	10.1	135	996	8.66
84	642	10.0	136	1003	8.65
85	650	10.0	137	1011	8.64
86	658	9.98	138	1019	8.64
87	666	9.94	139	1026	8.63
88	673	9.91	140	1034	8.62
89	681	9.88	141	1043	8.62
90	689	9.86	142	1051	8.62
91	697	9.83	143	1059	8.62
92	705	9.79	144	1068	8.62
93	713	9.78	145	1076	8.62
94	720	9.74	146	1085	8.62
95	728	9.72	147	1094	8.62
96	736	9.69	148	1104	8.63
97	744	9.67	149	1113	8.64
98	752	9.64	150	1122	8.63

9

Figure 7 compares the pooled experimental expansion data with the smoothed data and the cubic spline fit. The relative residuals of the spline fit are shown in Fig. 8. It can be seen that the estimated expansion values from the spline fit are within 0.2% of the smoothed data.
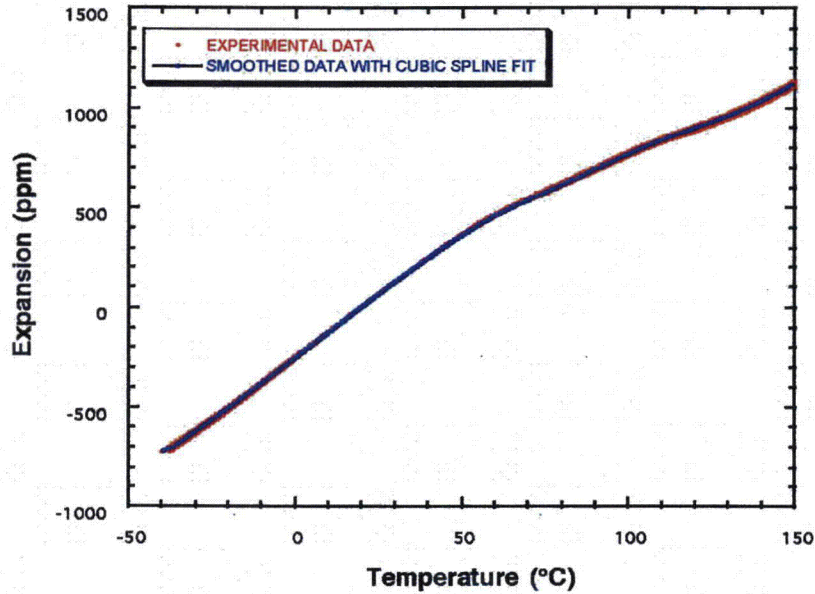

Fig. 7. Comparison of smoothed data and cubic spline fit of smoothed data to raw pooled experimental data for thermal expansion of Type 277-4 cement material as a function of temperature.
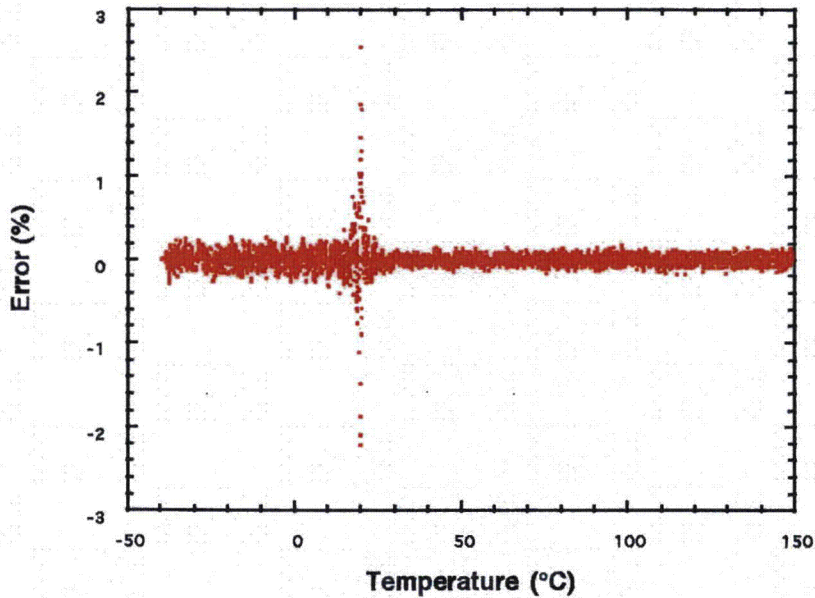

Fig. 8. Relative residuals of cubic spline fit used to estimate expansion values tabulated in Table 5.

10

The estimated expansion at the 1°C increments was used to calculate the MCTE values shown in Table 5. The value of MCTE at 20°C cannot be calculated because of a division by zero condition; therefore, the average of the 19 and 21°C MCTE values is listed in Table 5. Figure 9 shows a plot of the MCTE values from Table 5 along with a 9th order polynomial used to fit the values. The MCTE at any temperature in the range -37 to 150°C can be calculated using

$$MCTE\ (ppm/°C) = 12.699164 - 0.0073715235*T + 0.00018778752*T^2$$
$$+ 1.517514e\text{-}05*T^3 - 6.6945913e\text{-}07*T^4 - 2.4414824e\text{-}09*T^5$$
$$+ 2.7529257*T^6 - 3.4686036e\text{-}12*T^7 + 1.7626873e\text{-}14*T^8$$
$$- 3.2800845e\text{-}17*T^9 \tag{2}$$

It is strongly cautioned that Eq. (2) cannot be used to extrapolate MCTE values outside the measured range and describes the behavior only during an initial heating. Figure 10 shows the relative residuals for Eq. (2) using 8 significant digits for the polynomial coefficients compared to the MCTE values from Table 5. It can be seen that Eq. (2) generates the MCTE values of Table 5 to within better than 1% over the temperature range measured in this study.

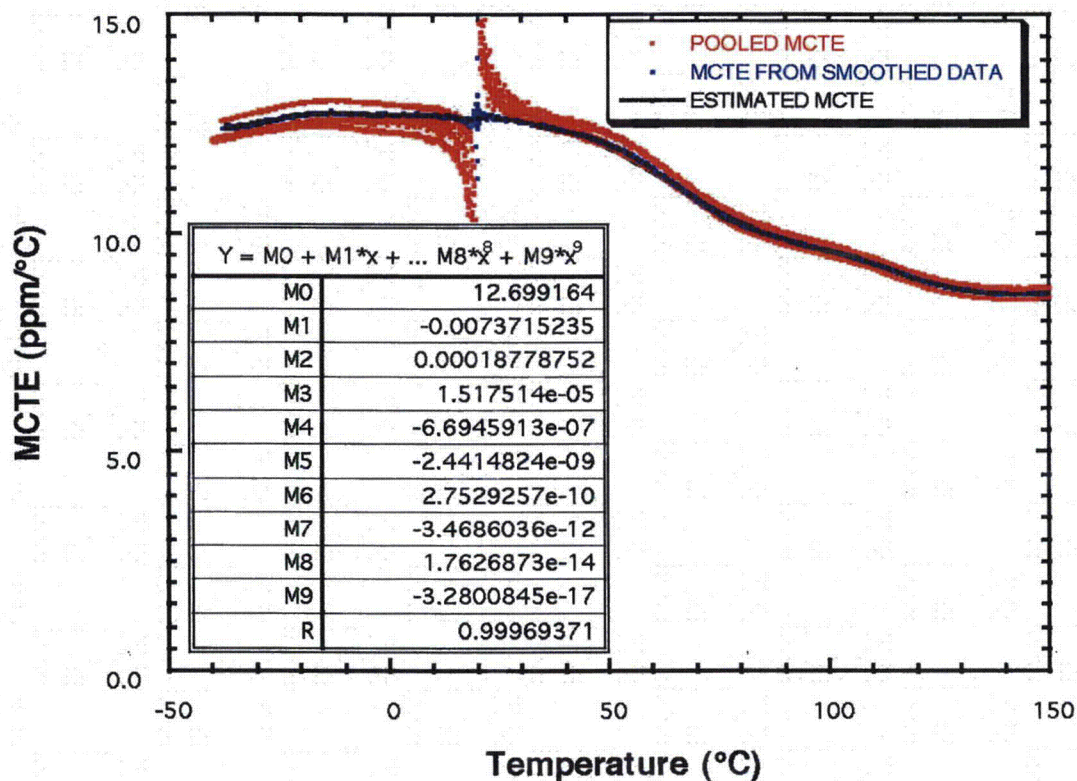| Y = M0 + M1*x + ... M8*x⁸ + M9*x⁹	
M0	12.699164
M1	-0.0073715235
M2	0.00018778752
M3	1.517514e-05
M4	-6.6945913e-07
M5	-2.4414824e-09
M6	2.7529257e-10
M7	-3.4686036e-12
M8	1.7626873e-14
M9	-3.2800845e-17
R	0.99969371

Fig. 9. Comparison of MCTE calculated from estimated expansion with MCTE calculated from smoothed expansion data and raw pooled MCTE values. Also shown is a 9th order polynomial fit of the MCTE calculated from the estimated expansion values of Table 5.

11

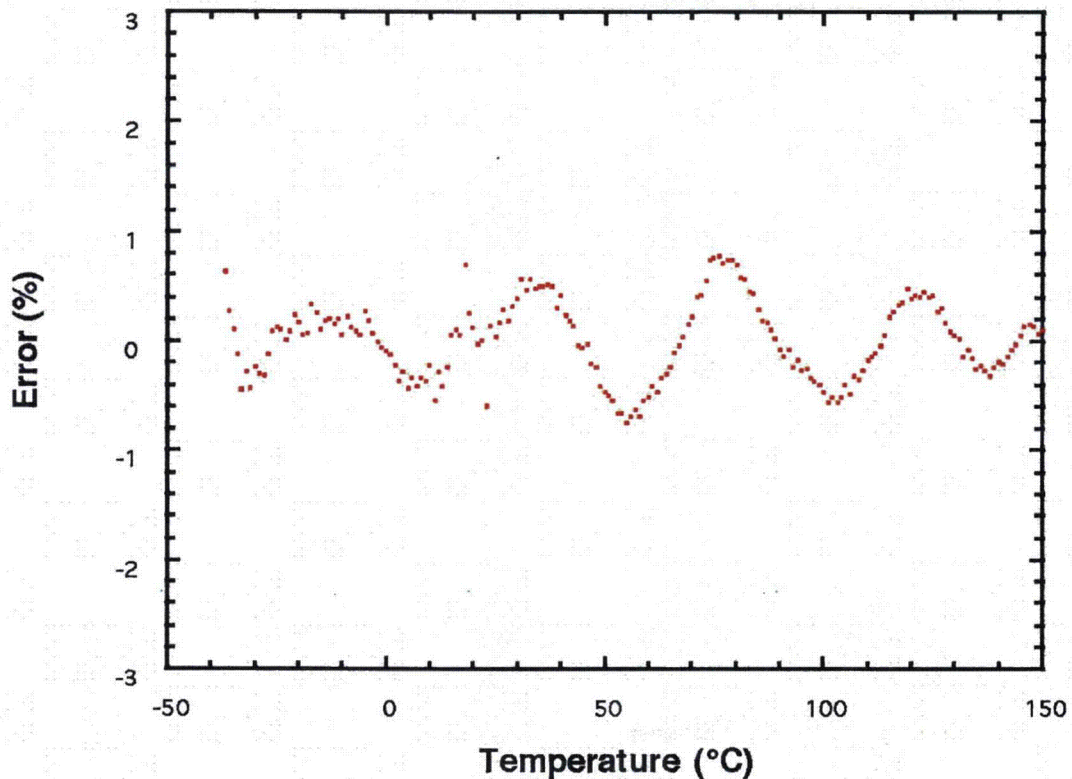Y/LF-717/Rev 2/ES-3100 HEU SAR/Ch-2/rlw/3-6-08

Fig. 10. Relative residuals of the 9th order polynomial fit of the estimated MCTE values using 8 significant digits for the coefficients as shown in Eq. (2).

After non-reversible behavior was demonstrated by the first specimen tested, the remaining four specimens were weighed before and after the expansion testing to determine any changes in mass resulting from heating the specimens. All specimens exhibited a weight loss of ~1.3% with individual results shown in Table 6. The initial density for the specimens tested is listed in Table 7. The Lot 1 specimen (Run #4) appeared to have a higher density than the Lot 2 specimens.

Table 6. Weight loss (%) behavior during testing

Run #1 (Lot 2, Specimen 1)	Not measured
Run #2 (Lot 2, Specimen 2)	-1.39
Run #3 (Lot 2, Specimen 3)	-1.24
Run #4 (Lot 1, Specimen 1)	-1.29
Run #5 (Lot 2, Specimen 4)	-1.34

12

Table 7. Initial density (10^6 g/m^3) of specimens tested

Run #1 (Lot 2, Specimen 1)	Not measured
Run #2 (Lot 2, Specimen 2)	1.47
Run #3 (Lot 2, Specimen 3)	1.50
Run #4 (Lot 1, Specimen 1)	1.60
Run #5 (Lot 2, Specimen 4)	1.48

4. SUMMARY

Two thermophysical properties, thermal conductivity and volumetric specific heat, were measured using the Hot Disk® method. The results among three random pairs of samples are consistent. All the specimens exhibited the same variations as a function of temperature.

The thermal expansion behavior was determined using a push rod dilatometer. Two specimens were considered to be outliers. Data from the remaining 3 specimens were pooled and the MCTE was described by a 9th order polynomial equation to within 1%.

All specimens lost about 1.3% during the expansion testing. Measured density of the specimens was found to be about $1.50*10^6$ g/m^3 for Lot 2 and about $1.60*10^6$ g/m^3 for Lot 1.

Since the material tested in this study undergoes irreversible changes the first time it is heated above 50°C, the data reported is valid only for the first time the material is heated above 50°C and must not be used to describe subsequent heating cycles.

REFERENCES

1. S.E. Gustafsson, E. Karawacki and M.N., Khan, *J. Phys. D.: Appl. Phys.* **12**, 1411(1979).
2. S.E. Gustafsson, *Rev. Sci. Instrum.* **62**, 797(1991).
3. V. Bohac, M.K. Gustavsson, L. Kubicar and S.E. Gustafsson, *Rev. Sci. Instrum.* **71**, 2452(2000).
4. ASTM E-228-95, "Standard Test Method for Linear Thermal Expansion of Solid Materials With a Vitreous Silica Dilatometer," *Annual Book of Standards* **Vol. 14.02**, ASTM International, West Conshohocken, PA(2003).

13

2-560

INTERNAL DISTRIBUTION

1.	C. M. Amonett, 9111, MS8201	19.	D. T. Johnson, 9110, MS8238
2.	J. C. Anderson, 9113, MS8208	20.	D. B. Miller, 9113, MS8206
3.	J. G. Arbital, 9113, MS8206	21.	A. E. Pasto
4.	P. A. Bales, 9113, MS8206	22.	R. G. Perkins, 9113, MS8208
5.	E. E. Bloom	23-27.	W. D. Porter
6-7.	G. A. Byington, 9111, MS8201	28.	G. B. Singleton, 9113, MS8206
8.	S. N Cramer, 9113, MS8208	29.	R. H. Smith, 9110, MS8238
9.	M. D. Crenshaw, 9110, MS8238	30.	D. P. Sooter, 9111, MS8201
10.	J. F. DeClue, 9110, MS8238	31.	S. K. Thomas, 9201-2, MS8073
11.	R. B. Dinwiddie	32.	D. A. Tollefson, 9110, MS8238
12.	G. W. Eckert, 9119, MS8234	33.	S. B. Turner, 9110, MS8238
13-14.	M. L. Goins, 9112, MS8201	34-38.	H. Wang
15.	K. D. Handy, 9201-2, MS8073	39.	T. L. Warren, 9113, MS8206
16.	C. N. Heatherly, 9113, MS8208	40.	Central Research Library
17.	S. T. Holder, 9113, MS8208	41.	ORNL Laboratory Records-RC
18.	C. R. Hubbard	42-43.	ORNL Laboratory Records-OSTI

2-562

BWXT Y12
A BWXT/Bechtel Enterprise

Y-12
NATIONAL
SECURITY
COMPLEX

Mechanical Properties of 277-4

B. F. Smith
Technology Development

G. A. Byington
Mechanical and Manufacturing Engineering

January 19, 2005

Prepared by the
Y-12 National Security Complex
P.O. Box 2009
Oak Ridge, Tennessee, 37831-8169
Managed by BWXT Y-12, L.L.C.
for the
U.S. DEPARTMENT OF ENERGY
under contract DE-AC05-00OR22800

MECHANICAL PROPERTIES OF 277-4

B. F. Smith
Technology Development

G. A. Byington
Mechanical and Manufacturing Engineering

Date of Issue: January 19, 2005

CONTENTS

iii

LIST OF FIGURES

LIST OF TABLES

iv

INTRODUCTION

It was desired to reduce the costs associated with a shipping container by replacing Eagle Picher BoroBond4 with a lighter, less expensive material. Thermo Electron Corporation Catalog 277-4 material met both of these requirements. At 105 lb/ft³, 277-4 is significantly less dense than BoroBond4, which has a density of 123 lb/ft³. Before the container could be certified, a number of tests had to be performed on the material. These included measuring coefficient of thermal expansion, thermal conductivity, and specific heat. Other tests included thermogravimetric analysis, neutron transmission, and outgassing. Several mechanical properties were needed, including compressive strength, tensile strength, modulus of elasticity, and Poisson's ratio. This study focuses on the mechanical properties of 277-4 at three temperatures: -40°F, 70°F, and 100°F.

EXPERIMENTAL PROCEDURE

The procedure for measuring the compressive strength was based on ASTM C109-02, *Standard Test Method for Compressive Strength of Hydraulic Cement Mortars (Using 2-in. or [50-mm] Cube Specimens).*[1] Two batches of cubes were cast on October 4 and October 11. Tensile specimens were cast at the same time; they will be described below. Eighteen cubes were delivered to the mechanical testing lab on November 1. The density of each cube was measured using a scale and calipers. Each cube was assigned a number according to the following system:

[Compression or Tension][Date of cast][Mix time in minutes]-[Arbitrary number]

Thus, specimen C1043-1 is a compression specimen that was cast on October 4. It was mixed for three minutes prior to pouring. In addition to providing compressive strength values, these cube specimens were used for measuring the modulus of elasticity and Poisson's ratio of the material. Stress-strain curves were needed for calculating the modulus. Also, accurate measurements of transverse strain were required for Poisson's ratio. Measuring stress is relatively straightforward, but measuring strain of cement is more complex. It was decided to use 90° tee rosette strain gages to measure axial strain and transverse strain simultaneously. Originally, two rosettes were to be adhered to each specimen on opposite faces, however, time constraints prohibited this. Only one rosette was attached to each cube. During strain gage application, each cube experienced the same thermal treatment while curing the precoat and gage adhesive. See the Appendix for detailed application procedures. Six cubes were tested at -40°F, six were tested at 70°F (room temperature), and six were tested at 100°F. Prior to testing, each specimen had to soak at the appropriate temperature long enough to ensure the center was at the test temperature. The -40°F cubes were thermally "shocked" at -50°F for approximately 23 h. Three of the 100°F cubes were heated at 110°F for 3.5 h. The other three 100°F cubes were heated at 120°F for 45 min.

The tensile test was based on ASTM C307-03, *Standard Test Method for Tensile Strength of Chemical-Resistant Mortar, Grouts, and Monolithic Surfacings.*[2] The briquet specimen described in this method has a "dogbone" shape and is approximately three inches long and has a reduced section of one inch wide by one inch thick. A photograph of one is shown in Figure 1. These specimens were cast and delivered at the same time as the compression cubes. These specimens have a discontinuous cross-section, so generating stress-strain curves from them would be difficult. For this reason, strain gages were not attached to them. The tensile test was used only for determining tensile strength. Six briquets were tested at -40°F, six were tested at 70°F (room temperature), and six were tested at 100°F. All briquets were soaked for the same lengths of time and at the same temperatures as the cubes, even though calculations for thermal equilibrium were based on the cube geometry. The only exception to this was that none of the 100°F briquets were soaked at 120°F.

1
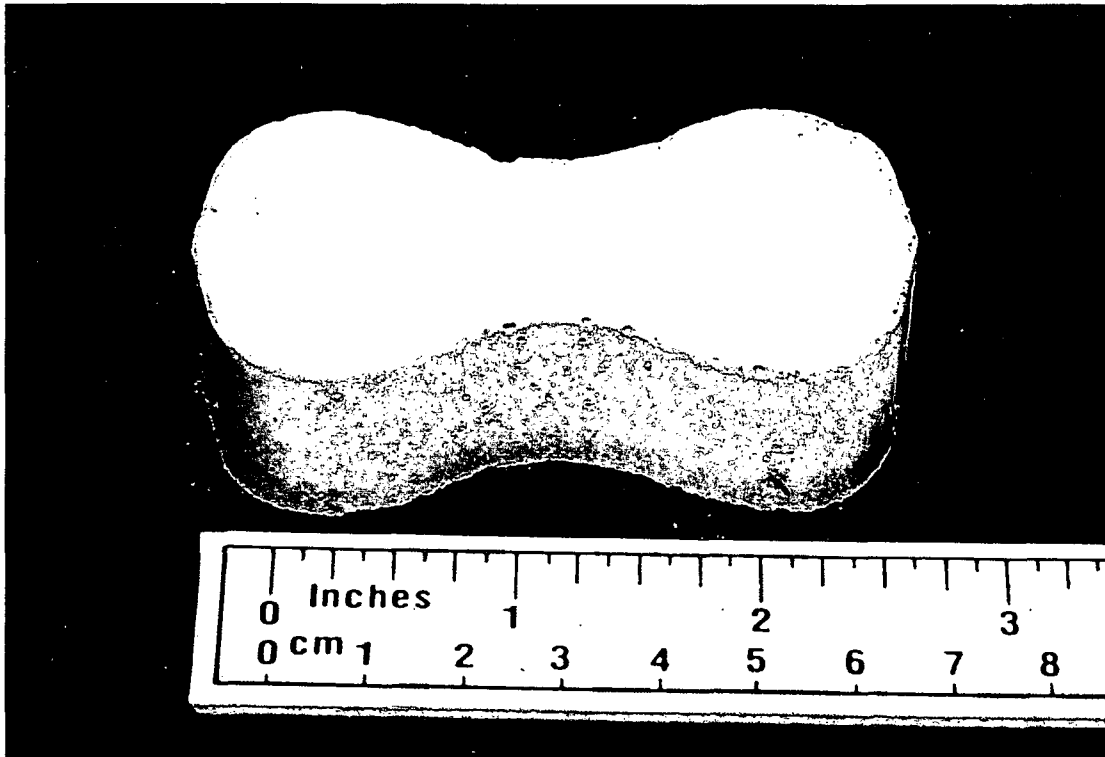
Fig. 1. Tensile specimen

RESULTS

Tables 1 through 3 give room temperature densities and compressive strength values at the three temperatures being considered. Tables 4 through 6 give tensile strength values at the same three temperatures.

Table 1. Compressive strengths of 277-4 at 100°F

Cube ID	Density @ Room Temp (lb/ft^3)	Compressive Strength (psi)
C10043-2	99.76	746.2
C10043-5	99.96	854.4
C10113-9	100.65	1185.2
C10043-6	101.01	777.3
C10043-3	101.24	711.3
C10043-4	101.32	727.9
Average	100.66	833.7

2

2-569

Table 2. Compressive strengths of 277-4 at 70°F

Cube ID	Density @ Room Temp (lb/ft³)	Compressive Strength (psi)
C10043-1	101.37	757.5
C10113-8	101.80	1073.0
C10113-2	101.95	977.9
C10113-3	102.22	1043.4
C10113-4	102.32	1041.8
C10113-7	102.65	1004.3
Average	102.05	983.0

Table 3. Compressive strengths of 277-4 at -40°F

Cube ID	Density @ Room Temp (lb/ft³)	Compressive Strength (psi)
C10113-6	103.67	1250.7
C10113-5	104.36	1253.8
C10113-1	104.55	1227.4
C10043-7	108.97	1013.4
C10043-9	109.80	1176.9
C10043-8	109.91	1072.8
Average	106.88	1165.8

Table 4. Tensile strengths of 277-4 at 100°F

Briquet ID	Location of Fracture	Tensile Strength (psi)
T10113-4	Grip	255.9
T10113-5	Grip	232.6
T10113-6	Middle	238.5
T10043-4	Middle	161.4
T10043-5	Grip	144.5
T10043-6	Grip	225.1
Average		209.7

Table 5. Tensile strengths of 277-4 at 70°F

Briquet ID	Location of Fracture	Tensile Strength (psi)
T10113-1	Grip	170.1
T10113-2	Middle	129.1
T10113-3	Grip	145.2
T10043-1	Middle	226.0
T10043-2	Middle	241.2
T10043-3	Grip	192.1
Average		184.0

3

Table 6. Tensile strengths of 277-4 at -40°F

Briquet ID	Location of Fracture	Tensile Strength (psi)
T10113-7	Middle	341.1
T10113-8	Middle	286.7
T10113-9	Grip	206.7
T10043-7	Middle	201.7
T10043-8	Grip	180.7
T10043-9	Grip	191.2
Average		234.7

The stress-strain curves for several of the specimens turn back when fracture begins. However, the stress continues to increase as the strain decreases, generating a "hook" at the top of the curve. ASTM C 109 defines the strength as the maximum stress achieved during the test, regardless of the strain behavior. In order to simplify modulus calculations, the turned back portion of the stress-strain curve was cut out. The strength was still calculated using the maximum stress reading, per C 109. In order to evaluate each of the data curves, a straight line interpolation was used to generate points at discrete strain levels. An increment of 100 microstrain was used up to 400 microstrain. Beyond 400 microstrain, an increment of 200 microstrain was used until the end of the curve. Dividing each curve in this manner resulted in uniform strain curves ranging from 16 to 26 points, depending on the total compression of the specimen. This data decimation technique reduces the number of data points from approximately 200 and allows a simple average to be computed for each sample group at the same strain levels. The simple average curves had large discontinuities where each constituent curve in that group ended. An upper bounding curve was generated by taking the maximum stress value for each strain value of the -40°F sample. Similarly, a lower bounding curve was generated by taking the minimum stress value of the 100°F sample for each strain value.

To unify the data handling and for input into modeling software, composite 10 point curves were generated for the minimum and maximum bounding curves and for the 70°F average curve . An approximated arclength parameterization technique was used for interpolating between the data points. This approximation was generated by calculating delta arclength parameter (ΔS) segments. The delta arclength parameter segments were calculated by adding the fractional change in strain with the corresponding fractional change in stress and dividing the sum by 2. See equation 1. This parameterization approximation technique works best on functions. The plotting scale has no effect on the results because the delta arclength parameter segments are the percent differences or fractional changes between each of the strain and stress data points. Summing all of the fractional changes of the strain will generate a value of 1. Summing all of the fractional changes of the stress will also generate a value of 1.

$$\Delta S = \left(\frac{\Delta strain}{totalstrain} + \frac{\Delta stress}{totalstress} \right) \bigg/ 2 \qquad (1)$$

By iteratively summing the delta arclength parameter (ΔS) segments the fractional arclength parameter (S) was calculated according to equation 2.

$$S = \sum_{0}^{n} \Delta S \qquad (2)$$

4

The fractional arclength parameter indicates the location along the curve, such that at the origin S equals zero and at the end of the curve S equals one. Now one can use a straight line interpolation to map the arclength parameter S to both strain and stress. At every 10 percent of the arclength parameter, both strain and stress were calculated using a straight line interpolation. This method was applied to the upper and lower bounding curves and the 70°F average curve. Tables 7 through 9 give the numerical values, while Figure 2 shows them graphically. In addition to the boundary curves, Figure 3 shows the decimated stress-strain curves for all specimens used in calculations. Several specimens were rejected due to abnormally shaped curves. It is possible these anomalous curves were due to imperfect strain gage application. Often, after seemingly adequate surface preparation, small peaks would be apparent underneath the gage. These peaks could have caused the strange readings in the rejected specimens.

Table 7. Ten-point stress-strain curve summary, lower bound

Strain (microstrain)	Stress (psi)
0.0	0.0
257.5	103.7
527.0	205.5
885.0	293.5
1320.1	369.4
1814.8	436.0
2347.5	496.6
2887.8	556.0
3431.8	614.9
4003.7	669.3
4600.0	720.0

Table 8. Ten-point stress-strain curve summary, 70°F average

Strain (microstrain)	Stress (psi)
0.0	0.0
219.8	150.3
490.0	289.7
797.6	421.2
1155.4	541.8
1565.4	651.3
2042.0	746.5
2552.4	834.4
3262.3	879.4
3935.3	932.4
4600.0	987.2

5

Table 9. Ten-point stress-strain curve summary, upper bound

Strain (microstrain)	Stress (psi)
0.0	0.0
101.1	201.3
251.8	378.8
390.9	561.9
579.6	721.1
762.8	883.1
1002.9	1017.6
1305.2	1122.2
1663.2	1200.1
2108.4	1236.1
2600.0	1249.7

Values of Young's modulus for each temperature were calculated using the first nonzero data point and the origin. The modulus is reported in Table 10. Poisson's ratio was determined from the plot of transverse strain versus axial strain. Poisson's ratio is the slope of the linear portion of this plot. Table 11 gives Poisson's ratio at each temperature.

Table 10. Young's modulus values

Temperature	Modulus (Mpsi)
100°F	0.4027
70°F	0.6838
-40°F	1.991

Table 11. Poisson's ratio of 277-4 at three temperatures

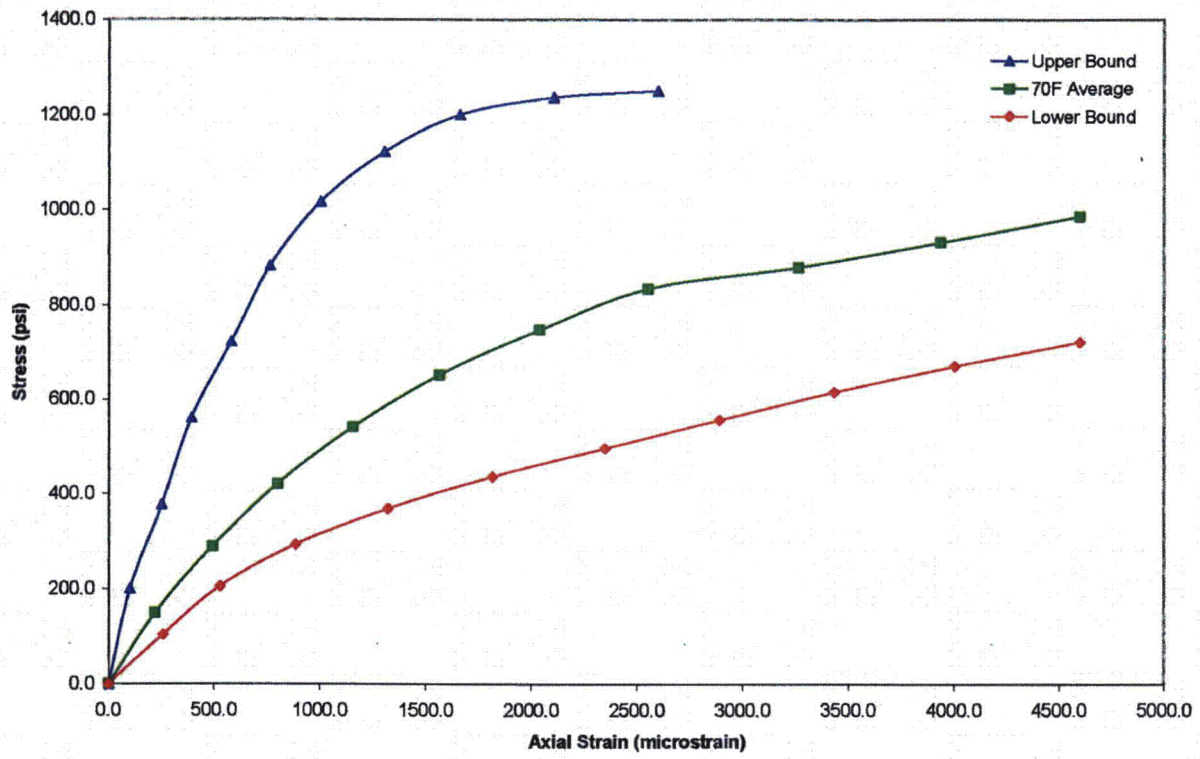| Temperature	Poisson's Ratio	Standard Deviation
100°F	0.25	0.045
70°F	0.28	0.105
-40°F	0.33	0.088

6

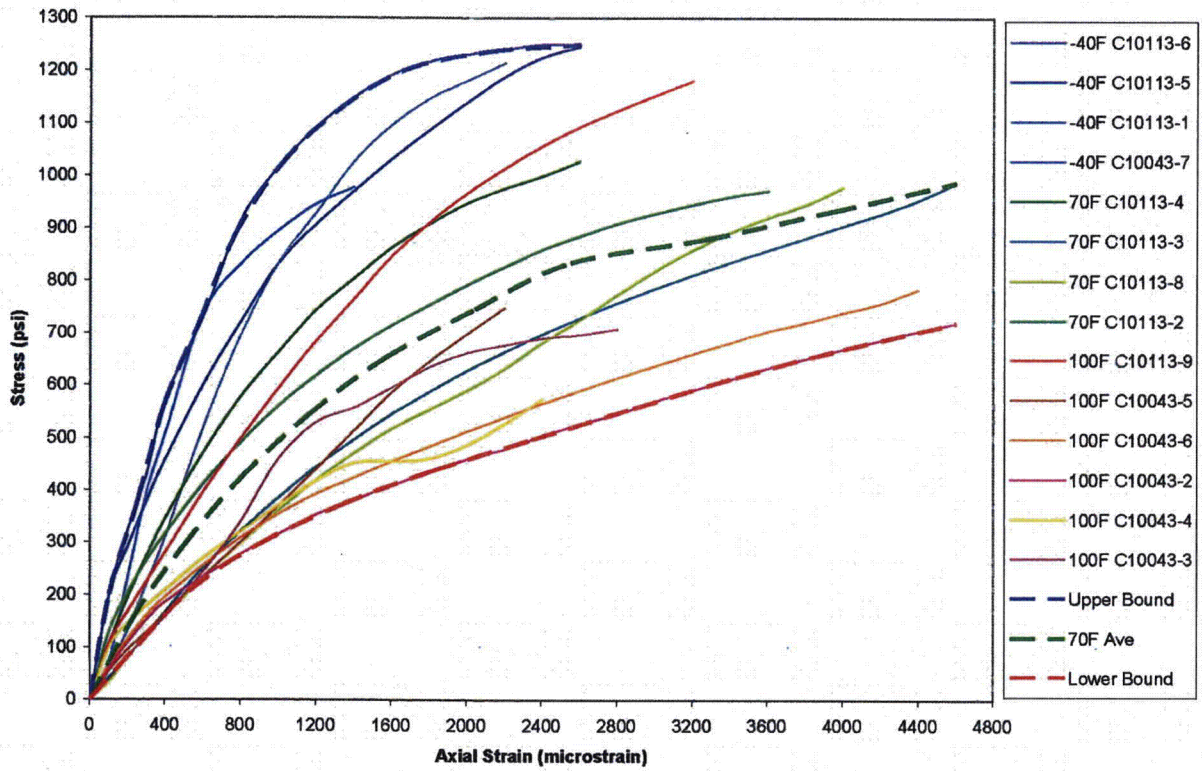**Fig. 2. Boundary and average stress-strain curves.**

7

Fig. 3. All specimen and boundary curves.

8

DISCUSSION

Tables 1 through 3 give compressive strength values in order of increasing density, under the assumption there would be a strong correlation between the two. However, a better predictor of strength is the casting date. Cubes cast on October 11 were generally stronger than those cast on October 4. This contradicts the generalization that cements increase in strength with age. Except for the specimens tested at 70°F, the tensile specimens cast on October 11 were generally stronger than the ones cast on October 4. Without information on the casting procedure or steps taken to control extraneous variables (ambient temperature, humidity, etc.) it is impossible to determine the reason for the difference in strengths.

Tables 4 through 6 give the location of the tensile specimen fracture, either at the narrow middle portion, or at the wider section that contacts the cylindrical grip. This test was loosely based on ASTM C 307, which states that "jawbreaks should be rejected" in paragraph 11.2. This requirement is understandable due to localized deformation and stress concentrations at the grips, which have the potential of introducing fracture toughness as a variable. Only a few aspects of C 307 were used for this study, such as the specimen shape, grip shape, and testing speed. Thus, the information on break location is included for the reader's information only.

9

REFERENCES

1. ASTM International. *Standard Test Method for Compressive Strength of Hydraulic Cement Mortars (Using 2-in. or [50-mm] Cube Specimens)*. ASTM Standard C 109/C 109M-02.

2. ASTM International. *Standard Test Method for Tensile Strength of Chemical-Resistant Mortar, Grouts, and Monolithic Surfacings*. ASTM Standard C 307-03.

10

APPENDIX

SURFACE PREPARATION AND STRAIN GAGE APPLICATION

Note: All cleaners and adhesives were purchased from Vishay Intertechnology, Inc.

1. Partially coat one face of 18 cubes with M-Bond AE-10 epoxy adhesive. Cure for 3 h at 125°F.

2. Nine cubes still tacky three days later. These were given a second coat of adhesive. All 18 cubes heated at 80°F for 2 h.

3. Smooth coating as much as practical by abrading with silicon-carbide paper.

4. Degrease coating with M-Line GC-6 Isopropyl Alcohol.

5. Wet-abrade coating with 400-grit silicon-carbide paper and M-Prep Conditioner A phosphoric acid solution. Wipe off residue with cotton gauze sponge.

6. Apply gage location layout lines.

7. Scrub with M-Prep Conditioner A using cotton swabs. Wipe off solution with cotton gauze sponge.

8. Scrub with M-Prep Neutralizer 5A ammonia solution. Wipe off solution with cotton gauze sponge.

9. Temporarily tape strain gage to cube and line up with layout lines.

10. Apply a small amount of M-Bond AE-10 epoxy adhesive to prepared face of cube and gage.

11. Clamp assembly together and cure overnight.

12. With clamp still on, cure adhesive for 1 h at 145°F.

13. Remove clamp and tape and solder on leadwires. Use M-Flux AR to aid soldering.

14. Thoroughly clean off flux with rosin solvent (toluene/isopropanol mix) and let dry.

15. Apply M-Coat A polyurethane protective coating. Let dry overnight.

11

DISTRIBUTION

Y-12 National Security Complex

1. C. M. Amonett
2. J. C. Anderson
3. J. G. Arbital
4. M. L. Baker
5. P. A. Bales
6. W. D. Brosey
7. G. A. Byington (2)
8. S. N. Cramer
9. M. D. Crenshaw
10. J. F. DeClue
11. G. W. Eckert
12. M. L. Goins (2)
13. K. D. Handy
14. C. N. Heatherly
15. S. T. Holder
16. D. T. Johnson
17. D. B. Miller
18. G. Perkins
19. G. B. Singleton
20. B. F. Smith
21. R. H. Smith
22. D. P. Sooter
23. S. K. Thomas
24. D. A. Tollefson
25. S. B. Turner
26. T. L. Warren
27. Y-12 Central Files (RC)

2-580

Volatile Components from Packing Materials, Rev.2

R. A. Smith

Compatibility & Surveillance Technology Development

December 22, 2004

Prepared by the
Y-12 National Security Complex
Oak Ridge, TN 37831-8169
Managed by
BWXT Y-12, L.L.C.
for the
U. S. DEPARTMENT OF ENERGY
under contract DE-AC05-00OR22800

DISCLAIMER

Volatile Components from Packing Materials, Rev.2

R. A. Smith

Compatibility & Surveillance
Technology Development

December 22, 2004

TABLE OF CONTENTS

i

LIST OF FIGURES

LIST OF TABLES

ii

SUMMARY

An outgassing study was conducted on five packing materials, comprising two experiments. These materials comprised 277-4 borated concrete, Borobond4 concrete, polyethylene bags, silica-filled silicone rubber seals, and silicone foam padding. The purpose was to measure the volume of gases which diffuse from packaging materials when sealed in containers. Two heating profiles were used to study the offgassing quantities in a set of accelerated aging tests. It was determined that the concretes contain a large quantity of water. The plastic materials hold much less moisture, with the silicone materials even consuming water, possibly due to the presence of silica filler. Polyethylene tends to degrade as the temperature is elevated and the foam stiffens.

INTRODUCTION

A variety of materials are required for safely packaging items for transport or storage. These materials must physically protect components while not causing damage by virtue of their own compositions. According to de Premare, "Sensitive products can begin to deteriorate at just 30% relative humidity (RH). Many products require a constant RH of 10-15% or less for stability and an extended shelf life."

The current study utilizes small samples of ceramic and polymeric packaging materials contained in measured volumes within stainless steel containers. Each container is then attached to a capacitance manometer or "baratron" for on-going measurement of the internal container pressure as the temperature is increased. This method allows determination of the volatiles quantity within the materials, which is most likely moisture but also decomposition products of the some materials. While such moisture is not immediately apparent under ambient conditions, the water contained in packaging is available to diffuse out over long time frames, such as years. To this extent, the maximum or "worst-case" amount can be calculated.

Two heating profiles were used and data calculated in terms of volume of gas at standard temperature and pressure, per material mass, a unit called "specific volume." This quantity was plotted versus time, as was the temperature profile. Visual observation of aged materials was conducted to ascertain obvious changes.

Experimental

Standard vacuum hardware is used to seal randomly sized specimens of each material (from 0.2 to 5 g) in air after they are weighed on a calibrated scale. In most cases, the experiment was repeated, but time limitations made this difficult. Additionally a "blank" container was tested under each experimental condition. Each container comprised a 5-inch height stainless steel retort of 1.3" diameter, in which was placed 3.75 – 4.0 inch heights of stainless steel block cylinders. This "filler" provided a smaller open volume of which the pressure was measured. This volume could be theoretically estimated, but was experimentally measured by expanding air from each unit into a known volume and measuring the resulting pressures. For experiments, each unit was attached to a pressure measurement system comprising a) and MKS Instruments Type 690A14TRB 10,000 torr baratron; b) MKS 670 signal conditioner electronics for data collection through an Omega datalogger; and c) a computer for data download and storage. The heating steps were conducted in a Despatch LAC 1-67-6 programmable laboratory oven which uses a Protocol Plus microprocessor control. A thermocouple was used to independently track and download the oven temperature to the aforementioned datalogger in concurrence with the pressure data. Upon experiment completion, containers remained sealed until disassembly. Material specimens were re-weighed and stored in labeled plastic bags.

1

Experimental Procedures:

I. A thermocouple is incorporated with the baratron such that the pressure is measured as the temperature is increased in a stepwise manner, from ambient to 300°F (23 – 150°C). Use 50°F increments and hold for 120 minutes before each rise. The outgassing pressure in torr is tracked for reporting in specific volume units of $cm^3(STP)/g$ as a function of time and temperature. The planned 300°F upper limit was actually recorded at 338°F.

II. Perform another set of experiments where test materials are held at 180°F for two hours; measure pressure over that time frame. Present total offgassing quantity for each material (two specimens each) in specific volume units of $cm^3(STP)/g$.

Data and Results

The data was collected by Omega Hyperware, then downloaded and analyzed using Microsoft Excel. For all materials, charts were produced giving outgassing volume in $cm^3(STP)/g$ and temperature in °F from ambient to 338°F, as a function of time; a text table for outgassing quantity at 180°F is provided. The outgassing curves are adjusted for linear rise in background outgassing from the container and filler materials which was measured at a total 19.2 cm^3 (STP). A similar background quantity of 4.0 cm^3 (STP) is subtracted from the 180°F outgas volumes.

I. Experiment 1 (Use 50°F increments and hold for 120 minutes before each rise up to 338°F). Figures 1 through 5 are provided for polyethylene, foam, elastomer, Borobond4, and 277-4 Borated concrete. Table 2 provides typical weight changes in specimens before and after the 13-hour heating experiments to 338°F were conducted.

II. Experiment 2 (Reach 180°F and hold for two hours; measure pressure over that time). Table 1 summarizes the total quantity of outgassing in this test. Several materials render negative results, indicating an overall reduction in gas due to absorption or reaction with the material at this temperature. The silicone foam and elastomer contain silica filler (SiO_2) which is known for its reactivity with water. The polyethylene is most likely reacting with the oxygen as its chains fragment and degrade. This material was the most obviously physically changed from this test – the originally flexible and clear film became brittle and slightly cloudy.

CONCLUSIONS

The concrete materials demonstrate the most massive degree of water content, outgassing under each experimental condition. The Borobond4 did not change much in appearance, although it was slightly darker in color after heating. However the 277-4 Borated concrete became extremely friable and more sandy than its original texture. It also turned a very light gray color.

The polyethylene film was least likely to hold moisture, but did degrade in each case. This material became glassy and yellowed due to heating, with outgassing observed in the longer duration 338°F test. This may result from degradation products, rather than water.

The silicone foam did retain some moisture content over a longer period of time and outgassed at higher temperatures. The silicone elastomer outgas quantity was very small.

Further information about gas composition could be obtained from headspace gas analysis of the captured outgassing products.

2

Polyethylene - 338°F Outgassing (170°C)
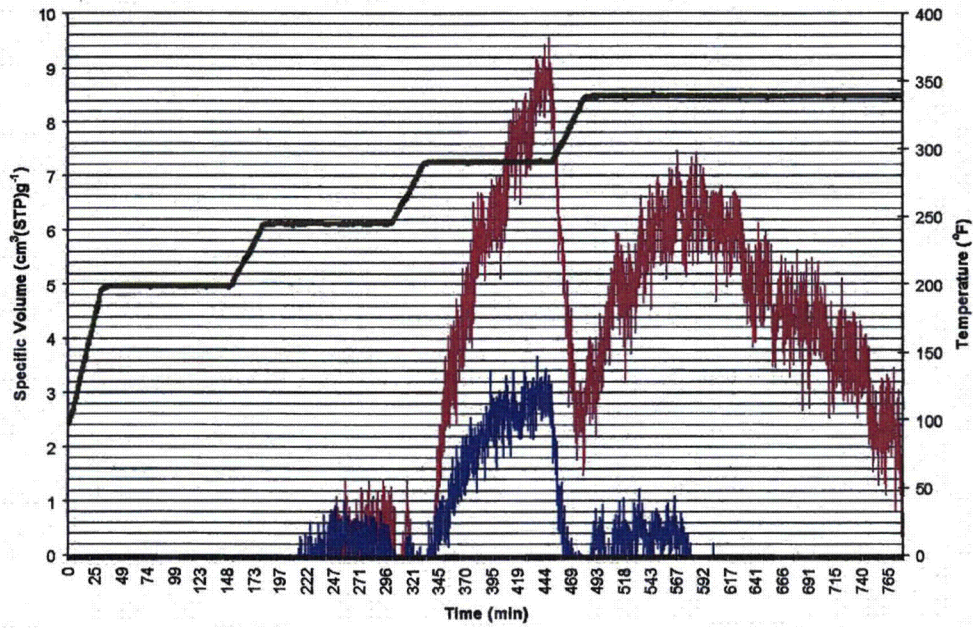### (Subtracts a linearly increasing blank outgassing STP volume to 19.2 cm³)

Figure 1. Outgassing of two polyethylene film specimens at 338 degrees F.

3

2-588

Silicone Foam - 338°F Outgassing (170°C)
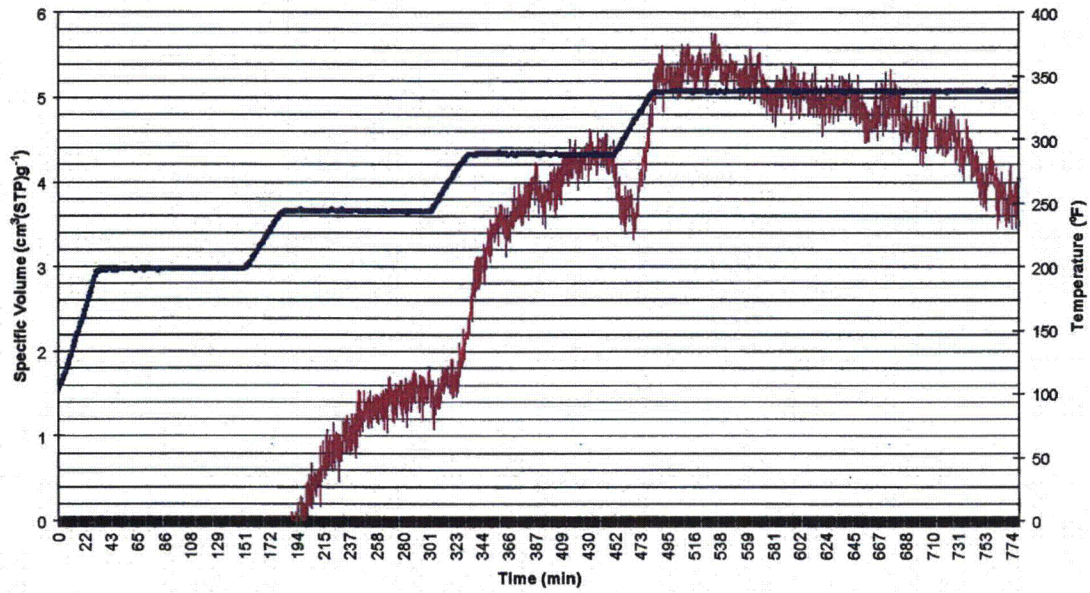### (Subtracts a linearly increasing blank outgassing STP volume to 19.2 cm^3)

Figure 2. Outgassing of two silicone foam specimens at 338 degrees F.

4

Silicone Elastomer - 338°F Outgassing (170°C)
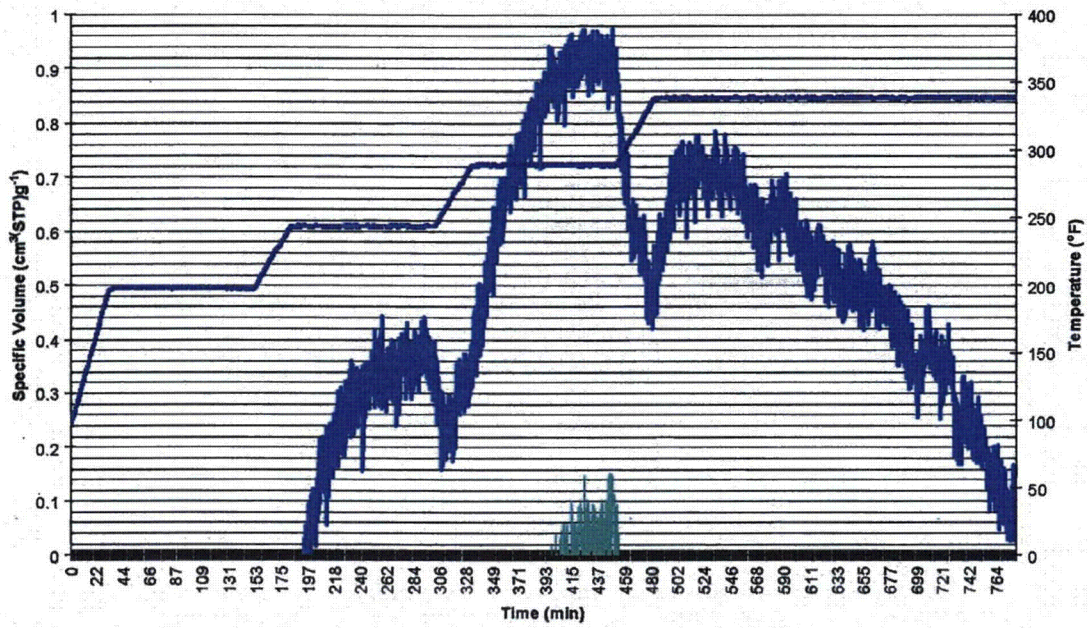### (Substracts a linearly increasing blank outgassing STP volume to 19.2 cm^3)

Figure 3. Outgassing of two silicone elastomer specimens at 338 degrees F.

5

2-590

Borobond4 Concrete - 338°F Outgassing (170°C)
(Subtracts a linearly increasing blank outgassing STP volume to 19.2 cm³)
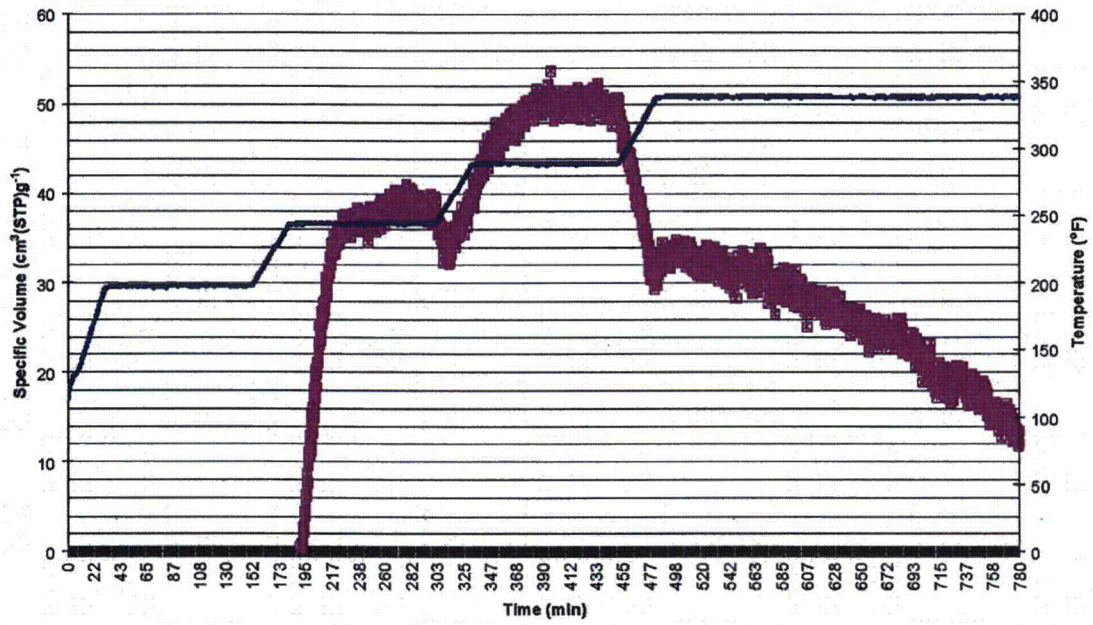

Figure 4. Outgassing of a Borobond4 concrete at 338 degrees F.

6

277-4 Borated Concrete - 338°F Outgassing (170°C)
(Subtracts a linearly increasing blank outgassing STP volume to 19.2 cm^3)
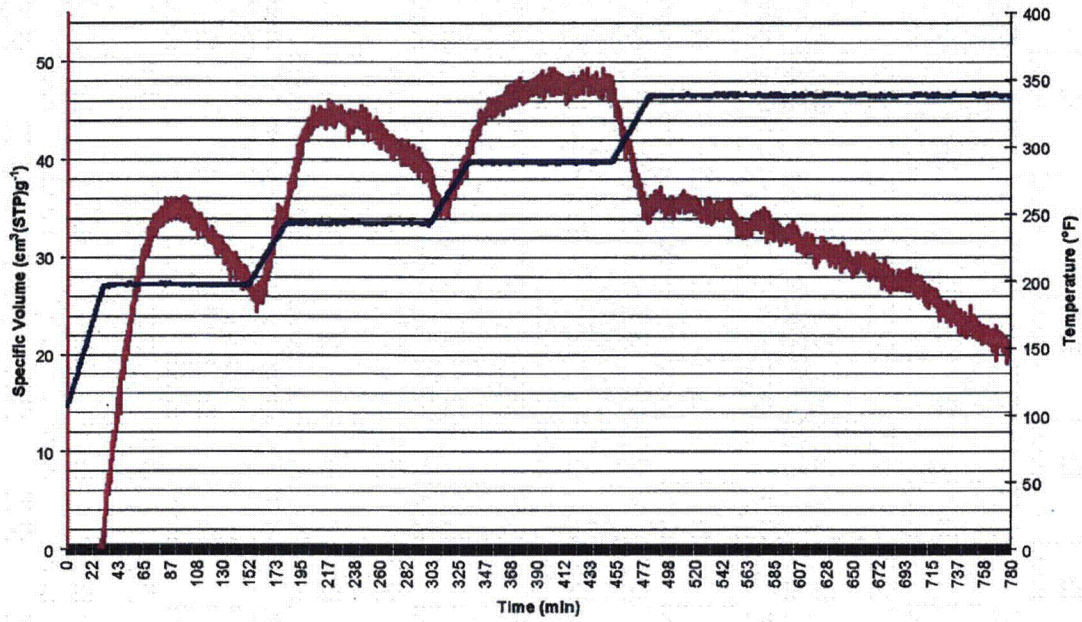

Figure 5. Outgassing of a 277-4 Borated concrete at 338 degrees F.

7

Table 1. Outgassing at 180°F at standard temperature (298K) and pressure (1 atm).

Specimen	Quantity (in units cm^{-3}(STP)/g)
Polyethylene – 1	0
Polyethylene – 2	0
Silicone Foam – 1	0
Silicone Foam – 2	0
Silicone Elastomer – 1	0
Silicone Elastomer – 2	0
Borobond4 – 1	29.3
Borobond4 – 2	32.0
277-4 Borated Concrete – 1	20.3
277-4 Borated Concrete - 2	46.9

Table 2. Weight Changes in grams after Experiment #1 (338°F or 170°C).

Material	Before	After	Weight Δ	Fractional Loss	mol H$_2$O*
borobond4	4.04	3.35	0.69	0.17	0.038
borobond4	1.99	1.69	0.3	0.15	0.017
elastomer	2.38	2.38	0	0.00	0.000
elastomer	1.45	1.45	0	0.00	0.000
277 borated	4.7	3.93	0.77	0.16	0.043
277 borated	2.82	2.34	0.48	0.17	0.027
polyethylene	0.26	0.26	0	0.00	0.000
polyethylene	0.19	0.2	-0.01	(0.05)	(0.001)
foam	0.72	0.75	-0.03	(0.04)	(0.002)

*Assumed outgas identity - should be verified with headspace gas analysis

8

2-593

Table 3. Material Information Summary.

Material \ Property	277-4 borated concrete	Borobond4	Polyethylene	Silica-filled polysiloxane elastomer	Fire-Retardant Polysiloxane foam
Composition	Hi-alumina cement	Phosphated cement	LDPE	Polysiloxane compression molded jar seal	Polysiloxane foam with carbon black
Application	Spacers between HEU parts for shipping (inside tin cans)	RT cure and neutron absorber. This is baseline material	Storage	Cap for cans; fits on top of paint cans used to ship broken pieces	Liner materials to cushion impact
Density**	120 lb/ft³ (1.93 g/cm³)	120 lb/ft³ (1.93 g/cm³)	~0.92 g/cm³	1.16 g/cm³	10 lb/ft³ (0.16 g/cm³)
Appearance	2"x2" block of gray ceramic-looking solid. Porous appearance	2"x2" block of dark gray metallic-looking solid. Very hard	Clear plastic bags as in "zip-loc"	Dark gray elastomeric pliable ring	Medium gray smooth skinned small-celled foam, soft with adhesive backed paper
Temperature of interest and durations	300°F (150°C) ramp in 50°F (10°C) increments – "Experiment 1" (Oven Profile 2) 180°F (82 °C) for 2 hrs – "Experiment 2" (Oven Profile 3)				
Amount received	203.30 g	259.36 g	2 bags = 32.95 g	38.37 g	5.95 g

**Density data not measured – for reference only.

9

2-594

DISTRIBUTION

1. Amonett, C. M.
2. Anderson, J. C.
3. Arbital, J. G.
4. Baker, M. L.
5. Bales, P. A.
6. Byington, G. A.
7. Cramer, N.
8. Crenshaw, M. D.
9. DeClue, J. F.
10. Eckert, G. W.
11. Goins, M. L.
12. Handy, K. D.
13. Heatherly, C. N.
14. Holder, S. T.
15. Johnson, D. T.
16. Leckey, J. H.
17. McKenzie, P. E.
18. Miller, D. B.
19. Perkins, G.
20. Singleton, G. B.
21. Smith, R. A.
22. Smith, R. H.
23. Sooter, D. P.
24. Thomas, S. K.
25. Tollefson, D. A.
26. Turner, S. B.
27. Warren, T. L.
28. Y-12 Central Files – RC

10

2-596

CANBERRA

Canberra Oak Ridge, LLC
1133-C Oak Ridge Turnpike, Suite 260
Oak Ridge, TN 37830-6442

Date: January 5, 2005

To: D. B. Miller

c: G. A. Byington, J. F. DeClue, L. C. Ostrowski, D. A. Tollefson, File

From: R. W. Brandenburg

Ref: BWXT-4300038751

Subject: Results of Prompt Gamma-ray Neutron Activation Analysis and Neutron Transmission Measurements on Prototype Confinement Vessel Inner Liners and Spacers

INTRODUCTION

Canberra was contracted by BWXT to perform prompt gamma-ray neutron activation analysis (PGNAA) on confinement vessel inner liners (CVIL) for the ES-3100 prototype replacement for the 6M shipping container and spacers to be used in the containers. Neutron transmission measurements on the CVILs are also part of the project. The CVILs are cylinders with an inside diameter of 6.5 in. and outer diameter of 8.5 in. The shell of the CVIL is made of 304L stainless steel and the annulus is filled with high alumina-content cement. For test purposes Canberra was supplied with three CVILs and ten spacers. The cement in two of the test CVILs contains boron in the form of 4 wt% boron carbide (B_4C). The third CVIL contains no boron. The portion of the CVIL filled with the cement is approximately 31 in. tall. The spacers are in 4-in. diameter tin coated steel cans that are 1.25 in. thick. Four of the ten spacers contain 4 wt% boron carbide while the other six contain no boron. Some of the cement mixture from each pour is used to make spacers as well as fill the annulus of the cylinder.

The measurements for the project had three parts:

1. Twelve PGNAA measurements using a BEGe gamma-ray detector were made at 30° increments around each CVIL at the center height of the CVIL.

2. Two PGNAA measurements using a BEGe gamma-ray detector were made on each spacer with a 180° rotation of the spacer between the measurements.

Page 1 of 11

3. Sixty neutron transmission measurements were made on each CVIL using a BF$_3$ neutron detector. The measurements were made at 30° increments around each CVIL at five heights starting at five inches from the bottom of the CVIL and at five inch increments up the CVIL.

NEUTRON SOURCE CONFIGURATION

A 1.8-µg ^{252}Cf spontaneous fission neutron source was purchased from AEA Technology to be the neutron source for the tests. The source was rated at 4.4 * 10^6 neutrons/sec. The source is sealed in a 32.5 mm long, 9.4 mm diameter stainless steel cylinder (Fig. 1).

X.224 · stainless steel capsule

10-32-UNF-1A   32.5   0.8   1.7   9.4   5.0
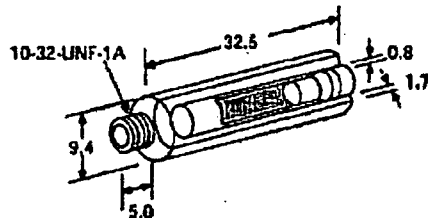
Safety performance testing

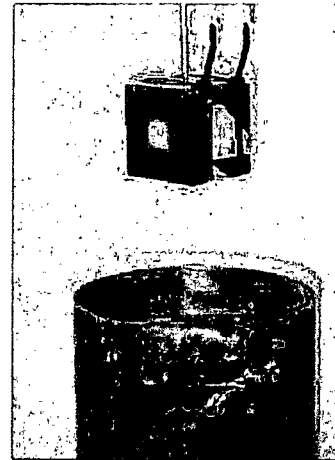| ANSI/ISO classification	IAEA special form	Model no.
C64545	GB/204/S	CVN.CY8

Fig. 1. Neutron Source Capsule

Fig. 2. Neutron Source Holder

A collimator was fabricated from high density polyethylene to hold the source. The collimator is a 3-in. cube of polyethylene covered on five sides with 2 mm of cadmium. The sixth side is covered with cadmium except for a 1-in. square in the center. A 9.5-mm hole in the center of the 1-in. square is the source location (Fig. 2). The collimator, which is suspended from a rod attached to the ceiling, is small enough to fit down the center of the CVILs. The source in the collimator is approximately 54 in. from the concrete floor. The detectors were placed on a Genie lift and centered on the source. The CVIL was placed on a second Genie lift and centered within ± 1/16 in. under the collimator. The lift was used to raise the CVIL to the designated height within ± 1/16 in. for the measurements. The spacers were clamped in a small vise and placed on the second lift and centered 1/2 ± 1/16 in. in front of the source. For the gamma-ray measurements, the detector to CVIL distance was 30 ± 1/8 in. and the detector to spacer distance was 20 ± 1/8 in. The neutron detector to CVIL distance was 4 ± 1/8 in.

GAMMA-RAY METHOD

The gamma-ray detector was a BEGe detector from Canberra in a 2-in thick lead shield. The shield covered the sides of the detector but did not collimate the field-of-view of the detector (Fig. 3). Quality assurance (QA) measurements for the gamma-ray detector were made using the QA software that is part of the Genie2K gamma-ray analysis software package from Canberra. Three small sources (^{137}Cs, ^{60}Co, and ^{109}Cd) were

attached to the face of the detector and counted for 60 seconds. One gamma-ray peak from each of the sources was analyzed for peak area and width (FWHM) and compared with previous measurements.

Prompt neutron activation of boron (specifically ^{10}B) gives rise to a 478 keV gamma ray produced by the recoil of the lithium nucleus from the neutrons captured in ^{10}B. The gamma ray is Doppler broadened by 10-15 keV. Gamma-ray spectrum collection and analysis was performed using the Genie2K gamma-ray analysis software package from Canberra. The peak fitting routine in Genie2K does not expect a peak as broad as 10-15 keV, therefore a region-of-interest (ROI) was set around the broad boron neutron activation peak. The data has three components. The gross count is the total count of the gamma rays detected with an energy that falls within the ROI. The Compton background is the portion of the gross count that is caused by scattered gamma rays. The net count is the portion of the total count that is from the boron. The net count is the difference between the gross and Compton counts.
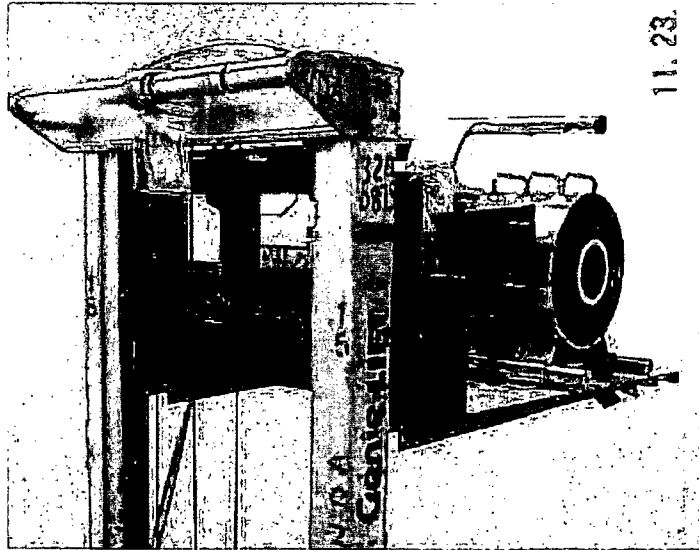

Fig. 3. BEGe Gamma-Ray Detector and Collimator

GAMMA-RAY RESULTS

The two CVILs containing boron were labeled 277-4-C1 and 277-4-C2. The CVIL containing no boron was labeled 277-0. CVIL 277-4-C1 was filled with three pours. CVILs 177-4-C2 and 277-0 were each filled with one continuous pour. Each CVIL in-turn was centered under the source collimator on the turntable on the Genie lift. The CVIL was raised to position the center of the CVIL at the level of the source for the twelve measurements (Fig. 4). Each measurement consisted of collecting a spectrum for 10 minutes. The spectrum was saved and counts in the ROI were recorded. Table 1 contains the results of the PGNAA measurements on the three CVILs. Chart 1 is a plot of the results. The average net counts for the two boron containing CVILs, agree very well. The net count for the non-boron containing CVIL is small and probably due to some minor activation of other materials in or near the CVIL. In all cases, CVILs and spacers, the standard deviation of the net counts and gross counts was less than or close to the standard deviation that would be expected based on counting statistics. The Compton background for all three CVILs agrees well, implying that there are no major effects from other materials.
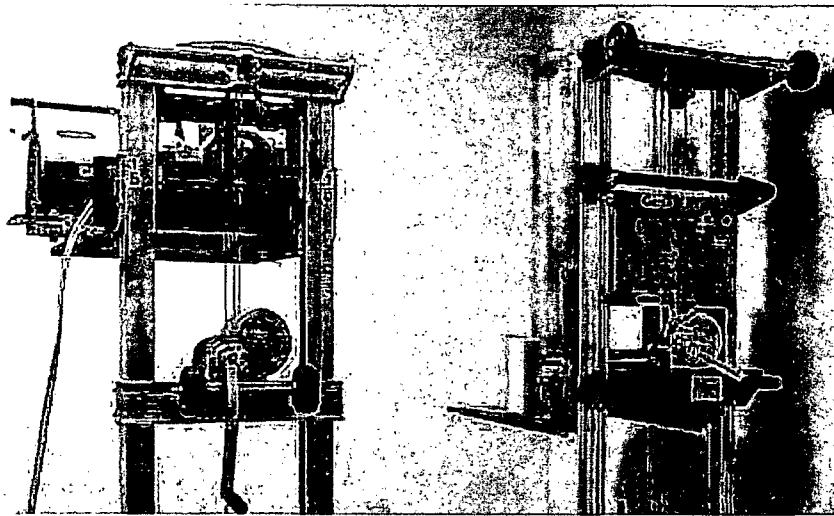
2-599

Fig. 4 BEGe Detector and CVIL Positioned for PGNAA Measurement

| CVIL	277-4-C1			277-4-C2			277-0		
Angle	Gross Counts	Compton	Net Counts	Gross Counts	Compton	Net Counts	Gross Counts	Compton	Net Counts
0	39,002	20,658	18,344	39,403	20,816	18,587	21,552	20,066	1,486
30	39,038	21,152	17,886	39,681	21,211	18,470	21,394	20,392	1,002
60	39,378	21,429	17,949	39,110	20,925	18,185	21,145	20,184	961
90	39,306	20,036	19,270	39,890	21,732	18,158	21,347	21,123	224
120	39,287	20,421	18,866	39,407	21,123	18,284	21,463	19,661	1,802
150	39,126	20,895	18,231	39,573	20,905	18,668	21,367	20,500	867
180	39,218	21,241	17,977	39,696	21,093	18,603	21,327	19,977	1,350
210	39,356	21,468	17,888	39,693	20,856	18,837	21,547	19,682	1,865
240	39,258	20,570	18,688	39,565	20,965	18,600	21,317	20,382	935
270	39,351	20,658	18,693	39,762	21,300	18,462	21,424	19,918	1,506
300	39,281	20,431	18,850	39,470	20,955	18,515	21,576	20,155	1,421
330	39,406	21,034	18,372	39,574	20,708	18,866	21,460	20,984	476
Average	39,251	20,833	18,418	39,569	21,049	18,520	21,410	20,252	1,158
Std. Dev.	132	444	456	204	274	227	122	457	503
Rel SD	0.3%	2.1%	2.5%	0.5%	1.3%	1.2%	0.6%	2.3%	43.4%

Table 1. Results of PGNAA on CVILs

2-600
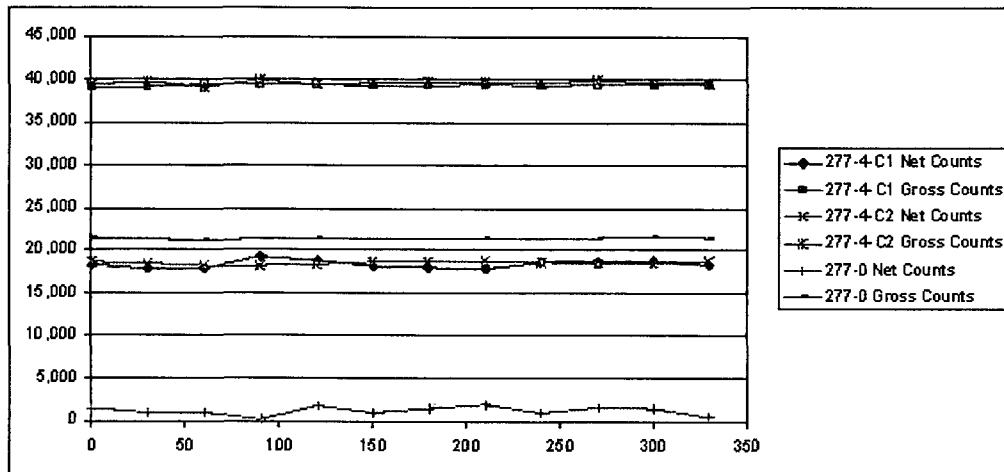
Chart 1: Results of PGNAA on CVILs

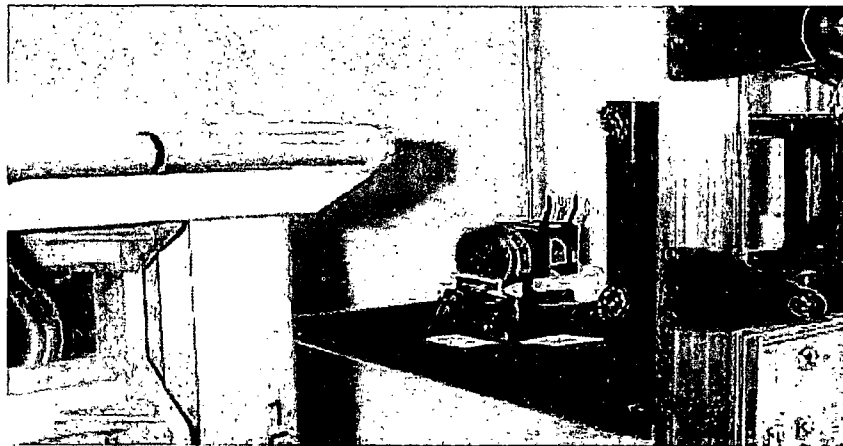The spacers were measured by centering them vertically in front of the source (Fig. 5).

Fig. 5. Spacer Positioned for PGNAA Measurement

A 15-minute spectrum was collected then the spacer was rotated 180° and a second 15-minute spectrum collected. Each spectrum was saved and the counts in the ROI were recorded. The spacers with no boron were labeled 277-0-S1 through –S6 and the boron containing spacers were labeled 277-4-S1 through –S4. Side A is with the cover of the can facing the detector and side B is with the cover facing the source. Table 2 contains the results from the measurements of the ten spacers. Chart 2 is a plot of the results.

Spacer Number	Gross Count	Compton	Net Count	Spacer Number	Gross Count	Compton	Net Count
277-4-S1-A	72,749	61,156	11,593	277-0-S1-A	65,385	61,738	3,647
277-4-S1-B	71,471	59,605	11,866	277-0-S1-B	63,964	59,280	4,684
277-4-S2-A	74,181	62,844	11,337	277-0-S2-A	63,861	59,744	4,117
277-4-S2-B	73,478	60,761	12,717	277-0-S2-B	62,261	56,850	5,411
277-4-S3-A	75,877	62,548	13,329	277-0-S3-A	64,510	59,526	4,984
277-4-S3-B	73,651	60,415	13,236	277-0-S3-B	63,653	59,684	3,969
277-4-S4-A	75,194	61,778	13,416	277-0-S4-A	64,952	60,544	4,408
277-4-S4-B	72,634	59,833	12,801	277-0-S4-B	62,865	59,961	2,904
Average	73,654	61,118	12,537	277-0-S5-A	65,635	60,188	5,447
Std Dev	1,427	1,197	826	277-0-S5-B	63,881	59,161	4,720
Rel SD	1.9%	2.0%	6.6%	277-0-S6-A	64,041	59,921	4,120
				277-0-S6-B	64,154	60,366	3,788
				Average	64,211	59,919	4,293
				Std Dev	839	455	786
				Rel SD	1.3%	0.8%	18.3%

Table 2. Results of PGNAA on Spacers
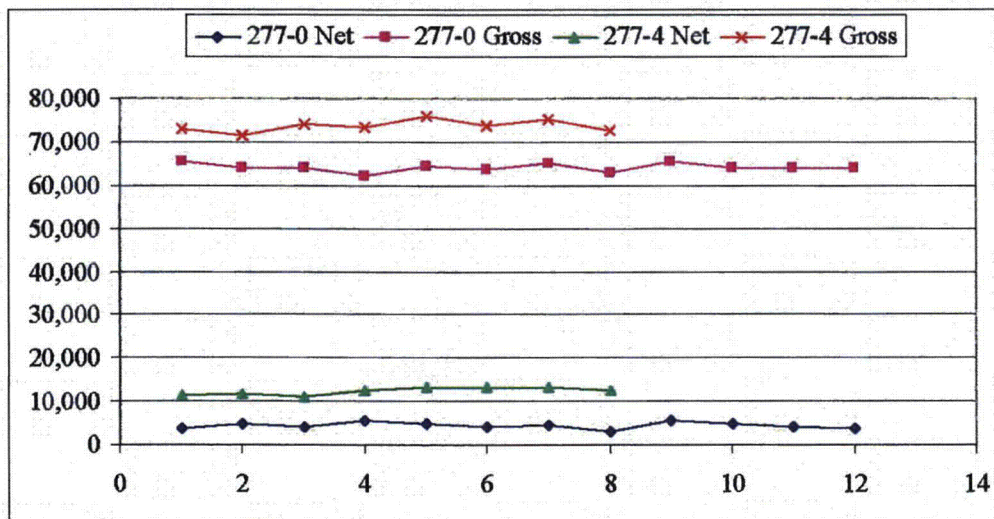
Chart 2. Results of PGNAA on Spacers

The results for the spacers show less difference between the spacers with and without boron than the CVILs. The variation among the measurements is larger for the spacers. Direct comparison between the CVIL results and the spacer results is difficult because the source to sample distance, the detector to sample distance, the area of the sample exposed to the source, and the count times are all different.

NEUTRON METHOD

The neutron detector was a 1-in.diameter BF_3 tube surrounded by a cylindrical block of polyethylene. The polyethylene is inside an aluminum case lined with a sheet of cadmium. The cadmium liner is intended to stop thermal neutrons from the surroundings and allow only fast neutrons from the source through to be moderated by the polyethylene and detected by the BF_3 tube. There was no additional shielding around the detector (Fig. 6). The detector assembly and 2241-7 handheld electronics package were from Ludlum Measurements, Inc. Quality assurance (QA) measurements were made by counting the neutron source with no CVIL in the beam of neutrons. The measurement results were entered into the Measurement Control software used by Canberra at ETTP.

The CVIL was positioned as in the gamma-ray measurements. Measurements were made at 60 points on each CVIL. As with the gamma-ray measurements, 12 measurements were made at 30° increments around the CVIL but these measurements were made at five different heights on the CVIL. The measurements were made at heights of 5, 10, 15, 20, and 25 inches from the bottom of the CVIL. The neutrons were counted for five minutes at each position then the CVIL was rotated to the next measurement position. The zero degree starting positioned was remeasured after the full rotation. The CVIL was the moved to the next height and the process repeated.

NEUTRON RESULTS

For all three CVILs, the standard deviation of the counts at any level on the CVILs was about 1.5 times the standard deviation expected from counting statistics. This indicates that there is little true variation in the neutron transmission around the circumference of the CVILs. The variation of the counts with height was larger. The standard deviation of the counts at different heights was 3 to 4 times the standard deviation expected from counting statistics for CVILs 277-4-C1 and 277-0, the three pour CVILs, but only 1.7 for 277-4-C2, the one pour CVIL. For both of the CVILs containing boron, the measurements 5 inches from the bottom yielded the highest transmission and the measurement at 25 inches from the bottom yielded the lowest transmission. This effect is presumed to be due to neutron scattering from the floor. The floor was more exposed to the neutron source when the CVIL was at maximum height (the 5-in position) than when the CVIL was down further and provided some shielding. The average transmission when compared to the measurement of the source with no CVIL is 81.4% for 277-4-C1, 83.6% for 277-4-C2, and 85.3% for 277-0. One interesting point is on 277-4-C1 at 150° and 25 inches. The results for that point were 4.4% higher that the average at the 25-in. level (Chart 3). The measurement was repeated with similar results. No clear cause of this anomaly could be determined without further investigation. Tables 3, 4, and 5 and Charts 3, 4, and 5 show the results of the neutron measurements on the three CVILs.
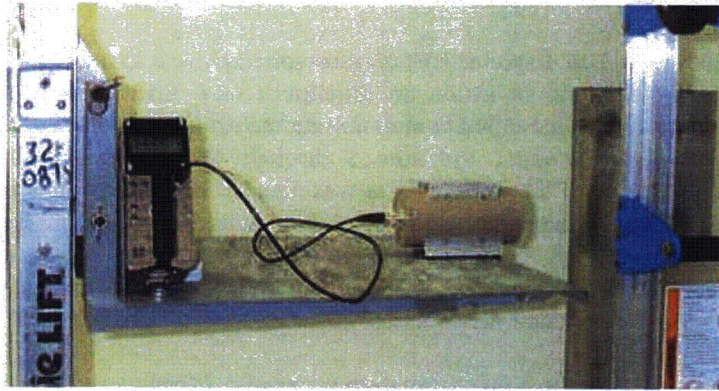
Fig. 6. Neutron Detector and CVIL Positioned for Transmission Measurements

Angle (°)	Height (in)	Counts	Height (in)	Counts	Height (in)	Counts	Height (in)	Counts	Height (in)	Counts	Mean	Std Dev
0	5	20,954	10	20,249	15	20,142	20	20,041	25	19,544	20,186	507
30		21,072		20,319		20,463		20,329		19,533	20,343	548
60		21,387		20,600		20,739		20,260		19,655	20,528	637
90		21,310		20,371		20,398		19,889		19,620	20,318	645
120		21,168		20,834		20,500		20,500		19,425	20,485	654
150		21,288		20,665		20,741		20,434		20,398	20,705	357
180		21,185		20,675		20,840		20,282		19,624	20,521	598
210		21,237		20,581		20,162		20,025		19,361	20,273	695
240		20,980		20,593		20,273		20,046		19,300	20,238	631
270		20,933		20,342		20,189		19,966		19,287	20,143	598
300		21,126		20,754		20,404		20,064		19,586	20,387	597
330		20,909		20,345		20,295		20,086		19,707	20,268	437
360		20,831		20,220		20,490		20,111		19,725	20,275	415
Mean		21,106		20,504		20,434		20,156		19,597	20,359	
Std Dev		175		204		229		187		282	538	

Table 3. Results of Neutron Transmission Measurements on CVIL 277-4-C1
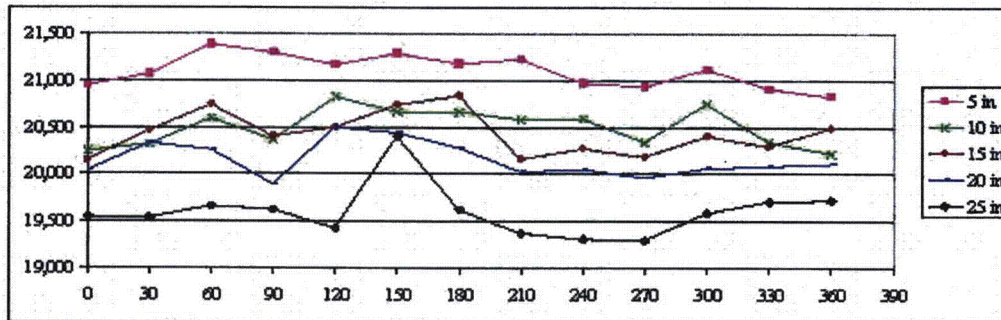
Chart 3. Results of Neutron Transmission Measurements on CVIL 277-4-C1

Page 8 of 11

2-604

Angle (°)	Height (in)	Counts	Height (in)	Counts	Height (in)	Counts	Height (in)	Counts	Height (in)	Counts	Mean	Std Dev
0	5	21,451	10	20,985	15	20,857	20	20,916	25	20,188	20,879	452
30		21,444		21,094		20,998		21,028		20,259	20,965	433
60		21,382		20,974		20,714		20,674		19,978	20,744	513
90		21,563		20,960		20,819		20,655		20,230	20,845	486
120		21,280		21,172		20,926		20,839		20,334	20,910	368
150		21,416		20,998		21,149		20,697		20,371	20,926	405
180		21,420		20,947		20,802		20,782		19,874	20,765	768
210		21,737		21,140		20,833		20,598		19,915	20,845	737
240		22,032		21,211		20,904		20,911		20,250	21,062	460
270		21,925		21,252		21,269		21,105		20,415	21,193	389
300		21,484		21,243		20,886		20,952		20,417	20,996	377
330		21,391		21,010		20,600		21,085		19,990	20,815	581
360		21,394		20,957		20,609		20,858		20,341	20,832	395
Mean		21,532		21,073		20,874		20,854		20,197	20,906	
Std Dev		226		117		190		166		193	468	

Table 4. Results of Neutron Transmission Measurements on CVIL 277-4-C2
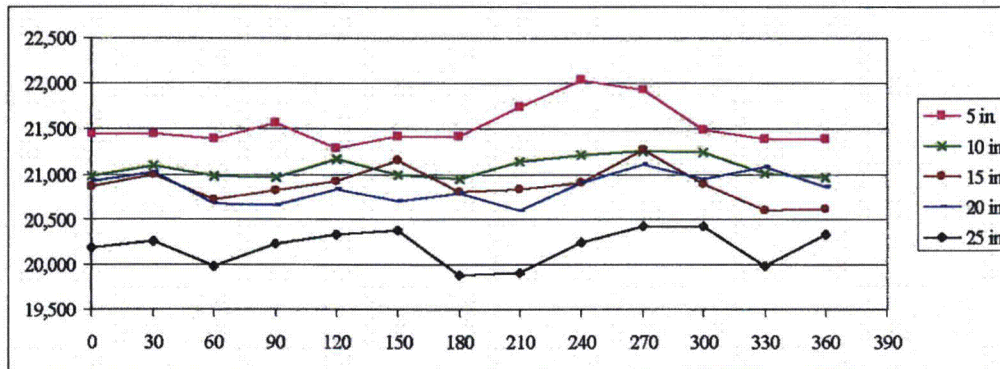
Chart 4. Results of Neutron Transmission Measurements on CVIL 277-4-C2

Angle (°)	Height (in)	Counts	Height (in)	Counts	Height (in)	Counts	Height (in)	Counts	Height (in)	Counts	Mean	Std Dev
0	5	21,752	10	21,329	15	21,377	20	20,946	25	20,624	21,206	433
30		21,376		21,848		21,084		21,243		20,576	21,225	462
60		21,129		21,518		21,172		21,085		20,378	21,056	416
90		21,437		21,482		21,472		21,138		20,588	21,223	383
120		21,743		21,685		21,765		21,265		20,679	21,427	465
150		21,550		21,867		21,535		21,298		20,637	21,377	461
180		21,359		21,939		21,385		21,009		20,524	21,243	522
210		21,456		21,898		21,434		21,346		20,616	21,350	463
240		21,043		21,888		21,754		21,319		20,640	21,329	512
270		21,415		21,954		21,446		21,132		20,682	21,326	466
300		21,495		22,037		21,674		21,411		20,898	21,503	415
330		21,443		22,399		21,847		21,828		20,894	21,682	557
360		21,259		21,542		21,864		21,511		21,022	21,440	317
Mean		21,420		21,799		21,524		21,272		20,674	21,338	
Std Dev		204		283		246		231		172	438	

Table 5. Results of Neutron Transmission Measurements on CVIL 277-0
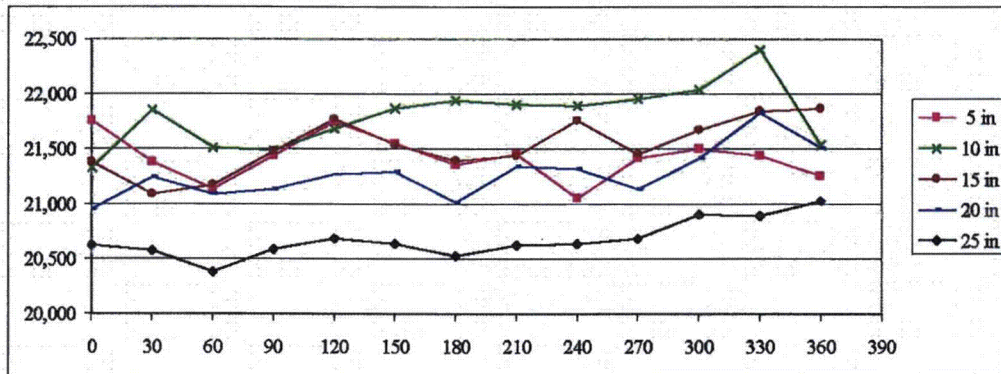
Chart 5. Results of Neutron Transmission Measurements on CVIL 277-0

SUMMARY AND CONCLUSIONS

For the measurement of gamma rays resulting from the prompt neutron activation of ^{10}B, the average net counts for the two boron containing CVILs, agreed very well. The net count for the non-boron containing CVIL is small and probably due to some minor activation of other materials in or near the CVIL. In all cases, CVILs and spacers, the standard deviation of the net counts and gross counts were less than or close to the standard deviation that would be expected based on counting statistics. The Compton background for all three CVILs agreed well, implying that there are no major effects from other materials.

Page 10 of 11

The results for the spacers showed less difference between the spacers with and without boron than the CVILs. The variation among the measurements was larger for the spacers. Direct comparison between the CVIL results and the spacer results is difficult because the source to sample distance, the detector to sample distance, the area of the sample exposed to the source, and the count times were all different.

In the neutron transmission measurements for all three CVILs, the standard deviation of the counts at any level on the CVILs was about 1.5 times the standard deviation expected from counting statistics. This indicates that there was little true variation in the neutron transmission around the circumference of the CVILs. The variation of the counts with height was larger. The standard deviation of the counts at different heights was 3 to 4 times the standard deviation expected from counting statistics for CVILs 277-4-C1 and 277-0, the three pour CVILs, but only 1.7 for 277-4-C2, the one pour CVIL. The result for the measurement on 277-4-C1 at 150° and 25 inches is 4.4% higher that the average at the 25-in. level (Chart 3), but this anomalous result does not lead to any different conclusions than those derived from the other CVIL measurements.

For both of the CVILs containing boron, the measurements 5 inches from the bottom yielded the highest transmission and the measurement at 25 inches from the bottom yielded the lowest transmission. The average transmission when compared to the measurement of the source with no CVIL was in the range from 81.4 to 85.3%.

2-608

Y/DV-1914

(BWXT
Y12
A BWXT/Bechtel Enterprise

Y-12
NATIONAL
SECURITY
COMPLEX

Summary of TGA Testing of Borated Concrete and Adhesive-Backed Silicone Foam

L. M. Thompson
J. D. Brown

Technology Development

January 2005

SUMMARY

A request was made by personnel in Engineering to conduct thermogravimetric analys is (TGA) on three different materials being evaluated for use. Two of the materials were boron loaded concrete: borated concrete 277-4 and Borobond 4. The third material was an adhesive-backed silicone foam. The samples were heated to 800°C at a ramp rate of 10°C/min. The borated concrete 277-4 showed some variability in the results. The variability was thought to be due to varying amounts of moisture that was coming off of the material initially. The experiment was repeated using borated concrete that had been allowed to air dry for approximately 1 month. Much more consistent results were obtained on these samples. There also appears to be up to 5 different types of decomposition occurring in the material over this temperature range. The Borobond 4 and the adhesive-backed silicone foam were much more consistent. The Borobond 4 had only one type of decomposition occurring over the temperature range. The amount of residue from this material was approximately 76%. The adhesive-backed silicone foam had three different areas of decomposition These were thought to be due to the adhesive, the silicone and possibly a filler or wetting agent. The amount of residue from this material was approximately 29%.

INTRODUCTION

A request was made by personnel in Engineering to conduct thermogravimetric analysis (TGA) on three different materials that may be used in the new Highly Enriched Uranium (HEU) storage facility. The materials included two boron-loaded concretes: borated concrete 277-4 and Borobond 4. The third material was an adhesive-backed silicone foam. Initially, three tests were conducted on each material type using a TA Instruments TGA 2950. An additional three tests were conducted on the borated concrete 277-4 due to the variability seen in the initial set of samples. These still showed some variability so another three tests were conducted on material that had been allowed to air dry for one month. The material was tested using a temperature sweep with a ramp rate of 10°C/min from room temperature to 800°C.

RESULTS

Borated Concrete 277-4

An overlay of the results obtained on the initial six samples of borated concrete 277-4 is shown in Fig.1.
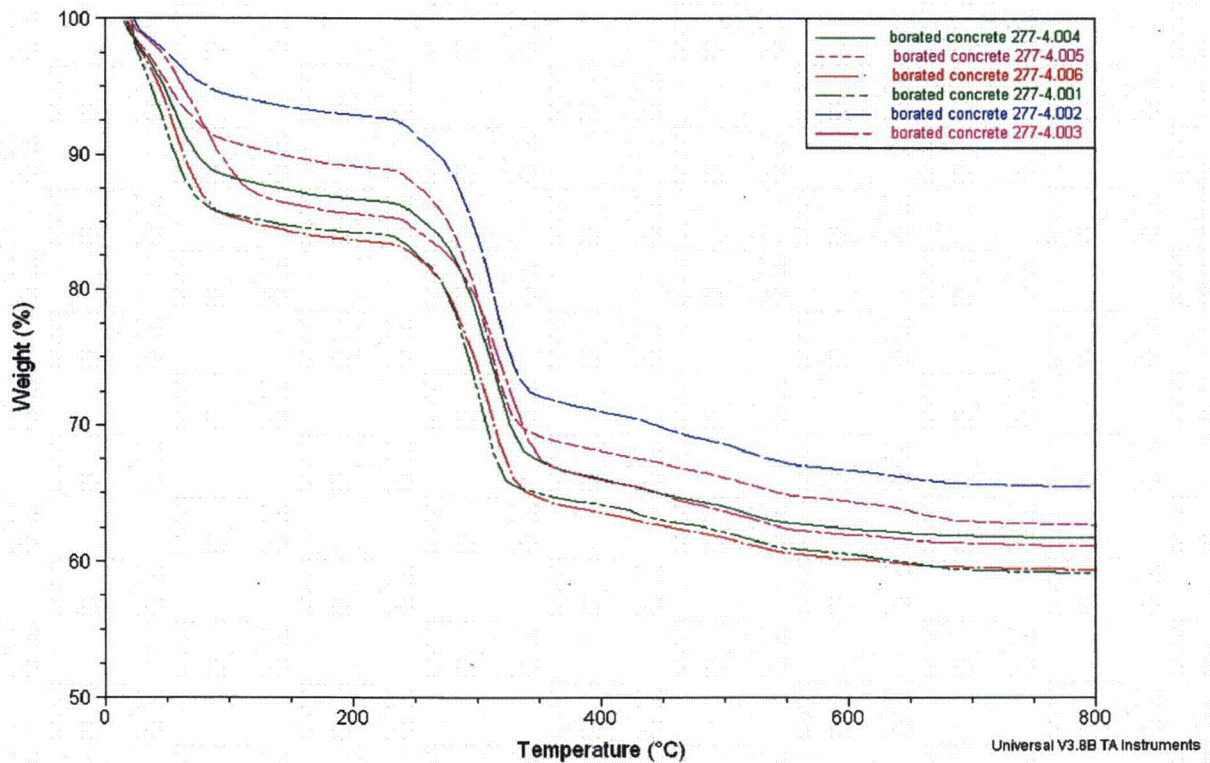
Fig. 1. Overlay of TGA results obtained on several samples of borated concrete 277-4.

2-611

The initial weight loss is thought to be due to water. The onset of decomposition occurred at approximately 265°C. The residue from the material varied from 59.2 to 65.6%. Table One summarizes the results obtained on the six samples. By taking a derivative of the weight percent curve as a function of temperature, four separate areas of decomposition were noted for the curves with the exception of the curve for samples 3, 4 and 6 which had five separate areas. Graphs of the results for each sample are contained in Appendix A.

Table 1. Results of TGA Testing of Borated Concrete 277-4

Sample Number	Weight Loss prior to Decomposition (%)	Onset of Decomposition (°C)	Residue (%)	Peaks on Derivative Curve for Weight Loss (°C)
1	14.74	269	59.22	302.74, 432.96, 523.12, 653.27
2	6.974	262.42	65.56	312.84, 442.98, 523.12, 653.27
3	14.28	267	61.13	70.49, 321.11, 451.24, 531.35, 651.5
4	13.74	257.49	61.73	56.76, 306.46, 436.7, 526.84, 636.97
5	11.33	250.21	62.7	48.98, 307.88, 518.2, 658.36
6	16.94	270.91	59.4	59.04, 309.01, 429.2, 519.34, 649.5

This material had been stored in a plastic bag and was still visibly damp. Because of this variability that was thought to be due to water, another three samples were run using material that had been air dried. The material was removed from the plastic bag and allowed to dry at room temperature for approximately 1 month. An overlay of the results obtained on these samples is shown in Fig. 2.
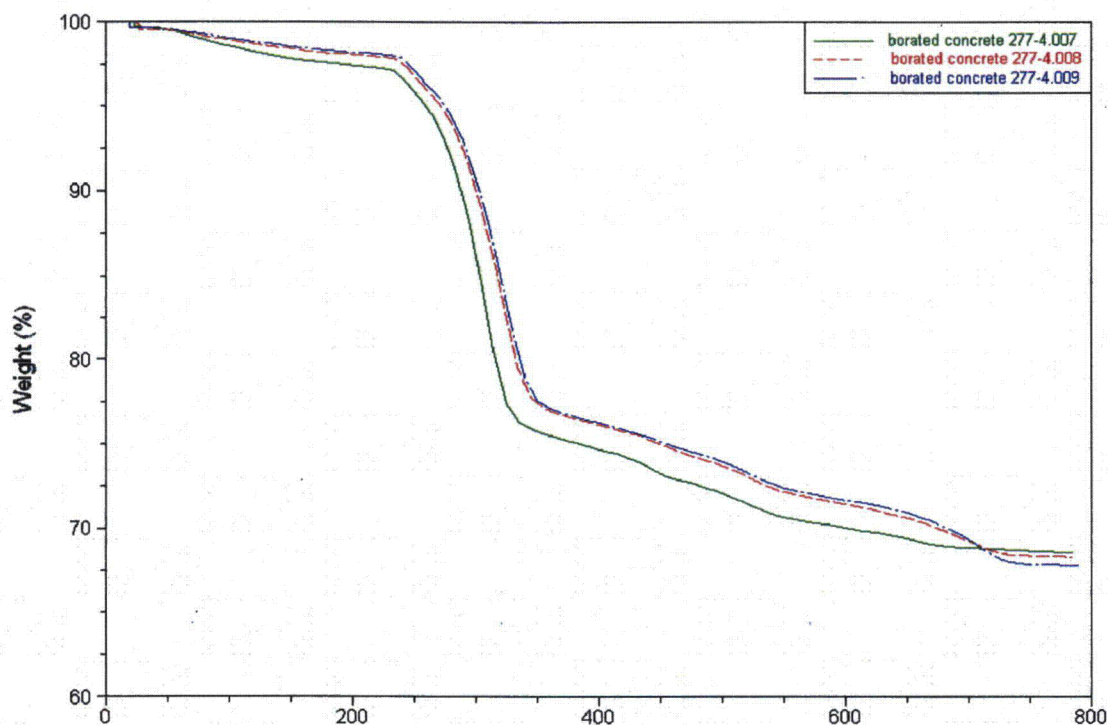
Fig. 2. Overlay of TGA results obtained on samples of borated concrete 277-4 that had been air dried for approximately 1 month.

These results were more repeatable than the previous samples. However, we still see an initial weight loss. A summary of the results are shown in Table Two. The individual graphs for each sample are contained in Appendix B.

Table 2. TGA Results Obtained on "Dried" Borated Concrete 277-4

Sample Number	Weight Loss prior to Decomposition (%)	Onset of Decomposition (°C)	Residue (%)	Peaks on Derivative Curve for Weight Loss (°C)
7	2.78	235.16	68.57	73.03, 303.91, 434.11, 514.24, 654.39
8	2.53	269.75	68.32	313.42, 453.63, 523.72, 693.9
9	2.00	239.35	67.8	319.65, 449.8, 519.9, 710.09

A Balzers mass spectrometer was run in conjunction with the TGA on these samples to determine the elements present in the sample offgas. The mass spectrometer was baked out prior to use in order to minimize gases from materials in the lines and instrument. Continuous scans were generated from masses 1 to 100 with an argon carrier gas. Initially, water (masses 16, 17 and 18) and air are the main gases that are coming off. A small amount of an alcohol (mass 30) and CxHy (mass 41) are also present in the offgases. During the first decomposition that occurs, water, hydrogen (masses 1 and 2) and CxHy (masses 41 and 30) are the main offgases with water again being the dominant material. As the material reaches approximately 440°C, water and

carbon dioxide (masses 44 and 12) appear to be the main offgases. Figure 3 is a graph of the mass spec data obtained on one of the samples. Only the masses that exhibited some changes are shown in this graph.
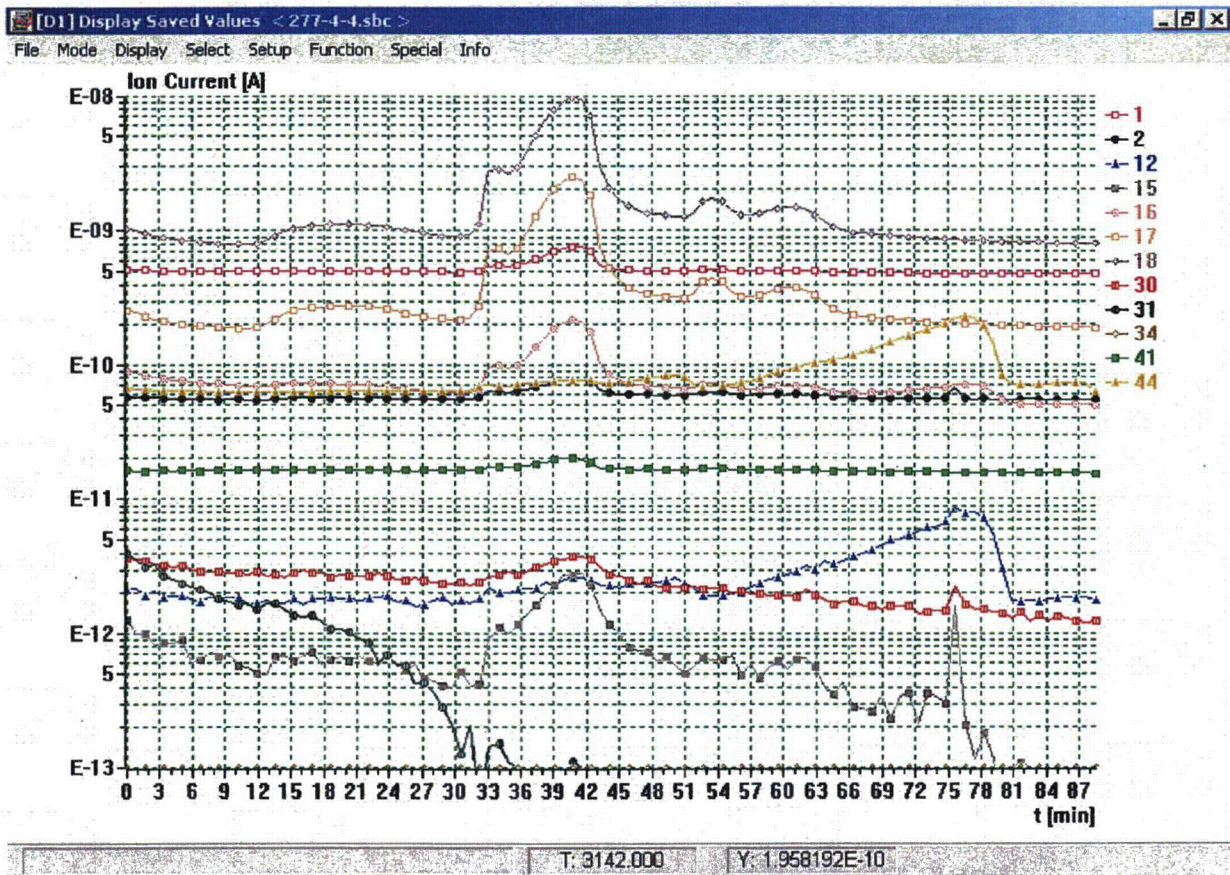
Fig. 3. Mass spectrum obtained from TGA testing of borated concrete 277-4.

A request was also made to obtain a density on this material. The density was calculated using three different techniques. The density was initially determined by weighing the material and dividing this by a calculated volume of the material obtained by measuring the cylindrical piece of the material. The density obtained using this technique was 1.51 g/cc (94.3 lb/ft^3). The second technique was to weigh a piece of the material. This piece was then submerged in a graduated cylinder of liquid and the volume determined by the amount of water displaced. The density obtained using this technique was 2.65 g/cc (165.4 lb/ft^3). The material does have some open pores so the volume obtained from this technique would be affected by these pores. The third technique used to obtain the density is to weigh the sample dry, weigh the sample submerged in water and calculate the density based upon the buoyancy of the material. The density obtained using this technique was 2.05 g/cc (128.0 lb/ft^3).

Borobond 4
Results for the sample of Borobond 4 are shown in Fig. 4.
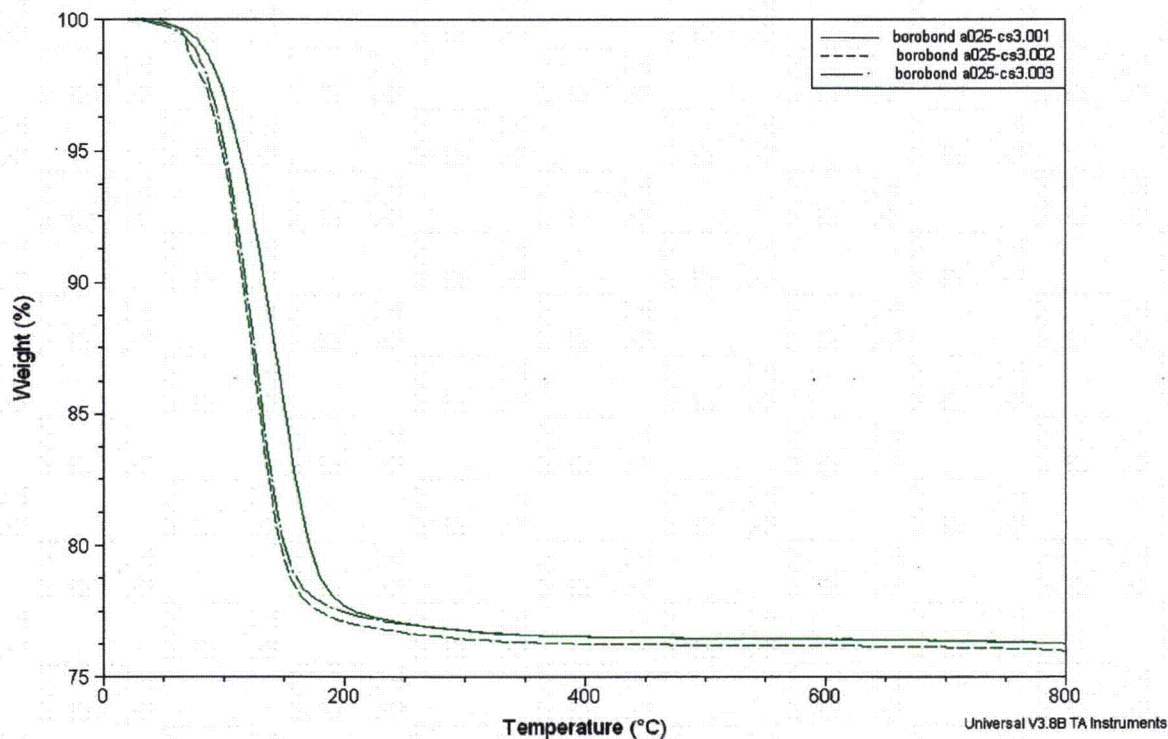
Fig. 4. Overlay of TGA Results Obtained on Three Samples of Borobond 4

The onset of decomposition occurred at approximately 70°C. The amount of residue was very similar for the three samples and averaged 76.2%. Table Three summarizes the results obtained on each sample. When the derivative of the weight loss curve as a function of temperature was taken, only one area of decomposition was noted for this material. Graphs of the results for each sample are contained in Appendix C.

Table 3. TGA Results for Borobond 4

Sample Number	Onset of Decomposition (°C)	Residue (%)	Peak on Derivative Curve (°C)
1	70.58	76.29	138.64
2	67.03	76.02	123.32
3	69.46	76.28	125.34

Adhesive Backed Silicone Foam

The third material tested was an adhesive backed silicone foam rubber. The material is part number 85925K541 from McMaster Carr. The foam was gray in color indicating some type of filler. The adhesive backing is acrylic per the material description. An overlay of the TGA results is shown in Fig. 5.
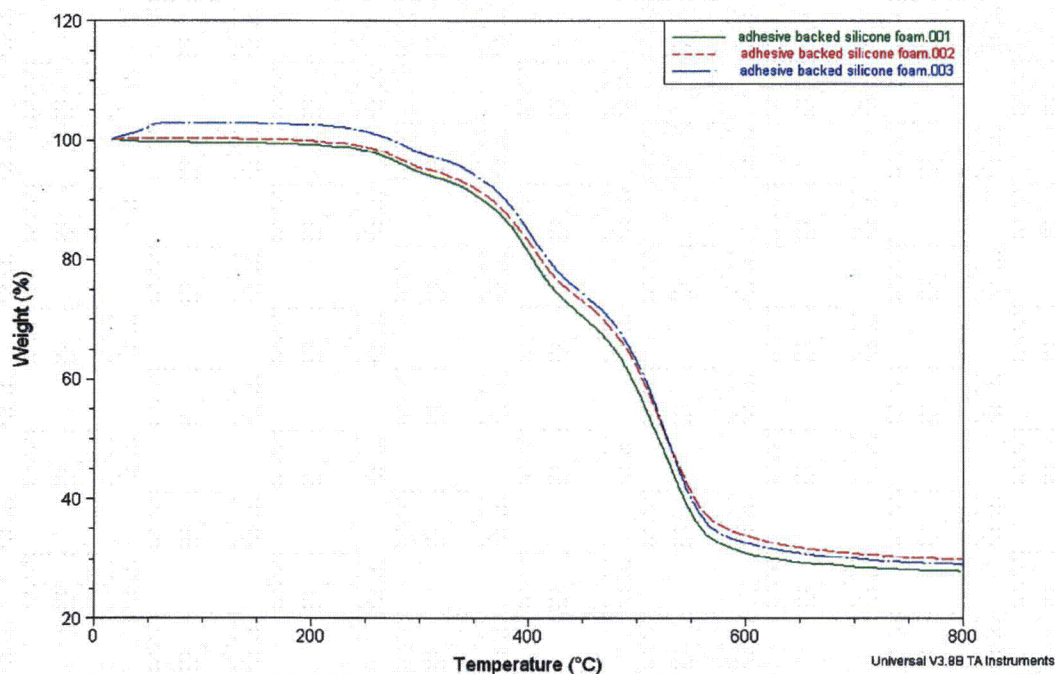
Fig. 5. Overlay of TGA results obtained on three samples of adhesive-backed silicone foam.

Three areas of decomposition are noted on these results. They are probably due to the adhesive, the silicone foam and either the filler or some type of wetting agent associated with the filler. Table Four summarizes the results obtained on these samples. Graphs for the results for each sample are located in Appendix D.

Table 4. Results of TGA Conducted on Adhesive-backed Silicone Foam

Sample Number	First Onset of Decomposition (°C)	Second Onset of Decomposition (°C)	Third Onset of Decomposition (°C)	Residue (%)	Peaks on Derivative Curve (°C)
1	254.5	361.38	487.26	28.06	283.91, 414.18 and 524.37
2	255.42	368.69	478.07	30.07	278.48, 398.78, and 528.98
3	243.96	367.94	496.69	29.26	276.11, 396.41, and 526.63

2-616

CONCLUSIONS

TGA was conducted on three different materials types: borated concrete 277-4, Borobond 4 and an adhesive-backed silicone foam. The Borobond 4 and adhesive-backed silicone foam had very repeatable results. Initial results from the borated concrete 277-4 had some variability from sample to sample. The variability was thought to be due to the evolution of water from the samples. Four to five different areas of decomposition appeared to occur over the temperature range of room temperature to 800°C for the borated concrete 277-4. Tests were repeated on a sample of borated concrete 277-4 that had been allowed to dry in open air for approximately 1 month. These results were more repeatable although there was some still initial weight loss that was thought to be due to water. The Borobond 4 had only one incident of decomposition with an onset at approximately 70°C. The adhesive-backed silicone foam appeared to have three different areas of decomposition. These were thought to be due to the adhesive, the foam and possibly a filler or additive.

2-617

2-618

Appendix A
TGA Results for Borated Concrete 277-4

2-620

Sample: borated concrete 277-4
Size: 19.1070 mg
Method: caox

TGA

File: \\...\TGA\borated concrete 277-4.001

Run Date: 3-Nov-04 09:36
Instrument: 2950 TGA HR V6.1A

302.74°C

269.00°C
83.70%

432.96°C

523.12°C

653.27°C

Residue:
59.22%
(11.32mg)

Weight (%)

Deriv. Weight (%/°C)

Temperature (°C)

Universal V3.8B TA Instruments
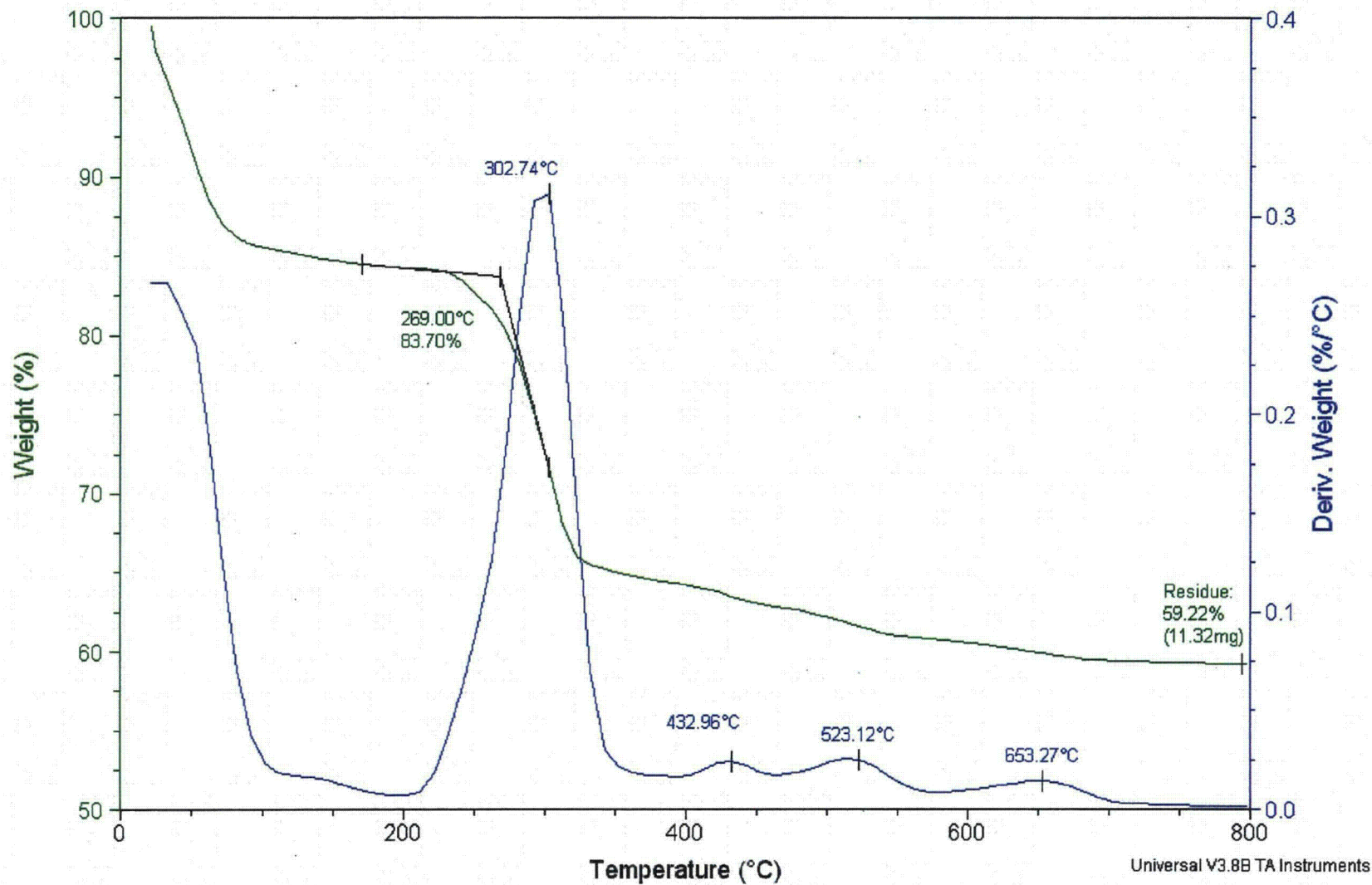
2-621

Sample: borated concrete 277-4
Size: 50.8480 mg
Method: caox

TGA

File: \\...\TGA\borated concrete 277-4.002

Run Date: 3-Nov-04 13:45
Instrument: 2950 TGA HR V6.1A

262.42°C

312.84°C

Residue:
65.56%
(33.33mg)

442.98°C   523.12°C

653.27°C

Universal V3.8B TA Instruments
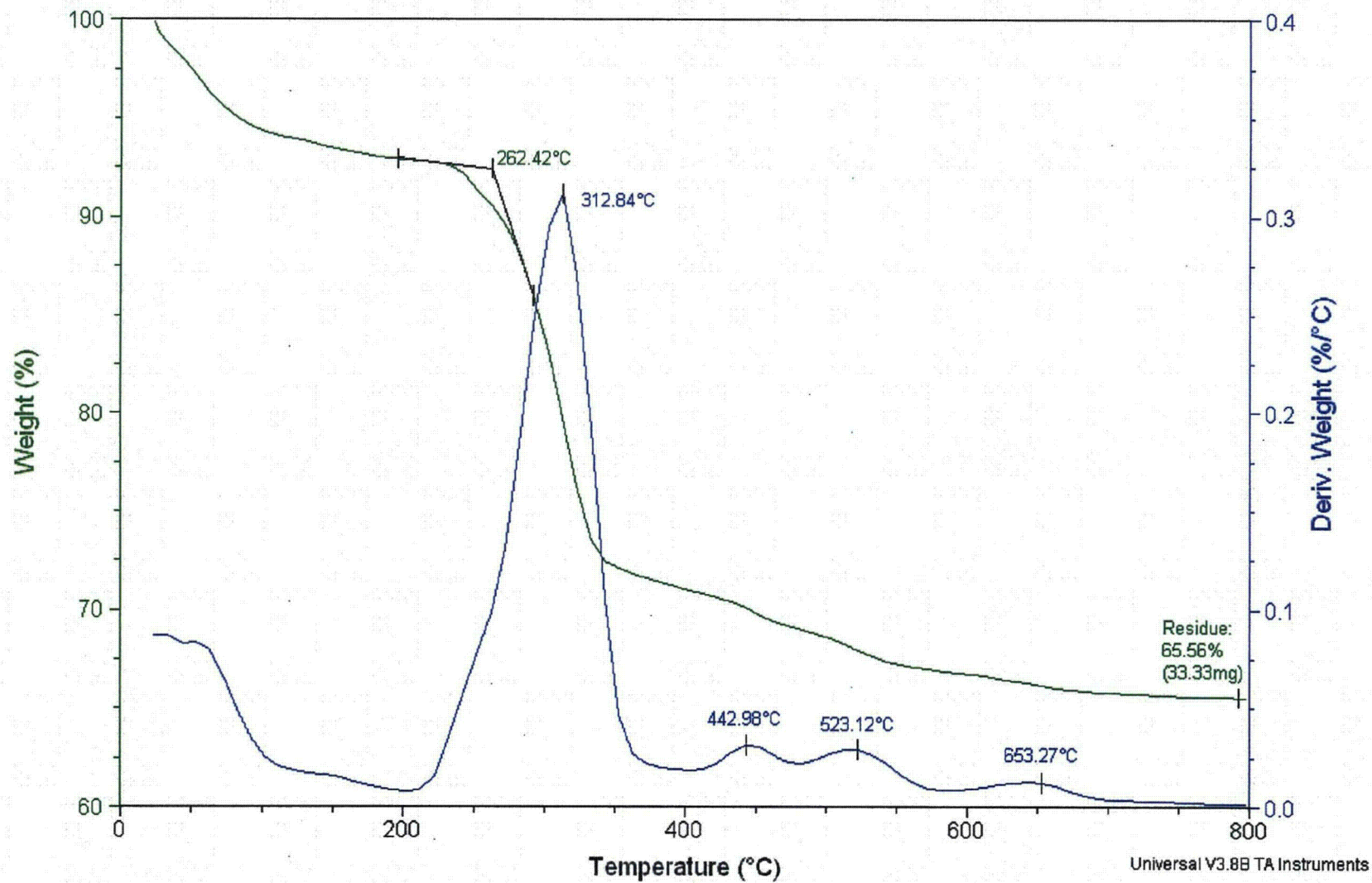
Sample: borated concrete 277-4
Size: 96.4490 mg
Method: caox

TGA

File: \\...\TGA\borated concrete 277-4.003

Run Date: 4-Nov-04 13:14
Instrument: 2950 TGA HR V6.1A

Universal V3.8B TA Instruments

2-623
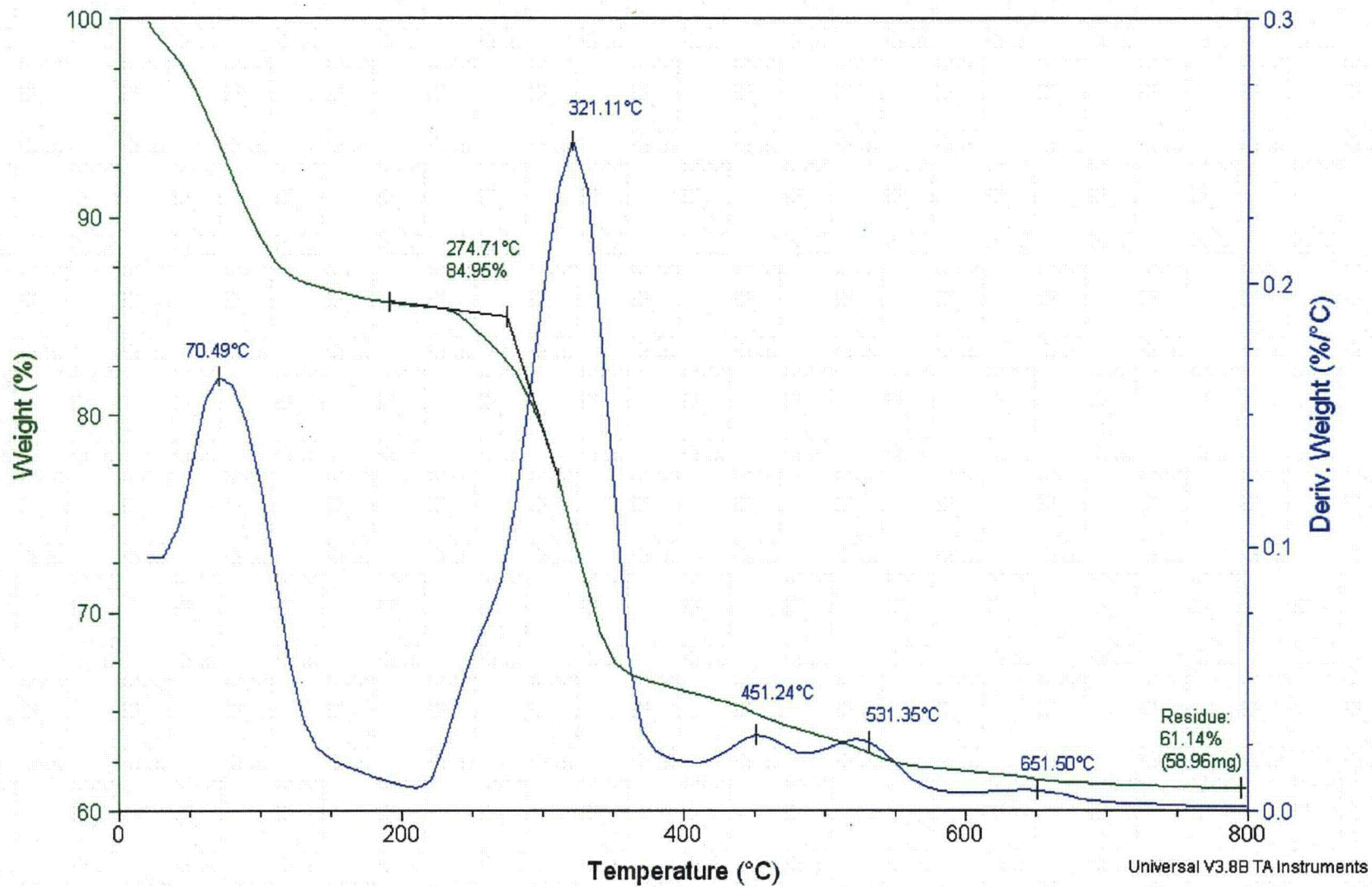
Sample: borated concrete 277-4
Size: 43.5340 mg
Method: caox

TGA

File: \\...\TGA\borated concrete 277-4.004

Run Date: 29-Nov-04 15:11
Instrument: 2950 TGA HR V6.1A

306.46°C

257.49°C
86.26%

56.76°C

436.70°C

526.84°C

636.97°C

Residue:
61.73%
(26.87 mg)

Weight (%)

Deriv. Weight (%/°C)

Temperature (°C)

Universal V3.8B TA Instruments

2-624

Y/LF-717/Rev 2/ES-3100 HEU SAR/Ch-2/rlw/3-06-08
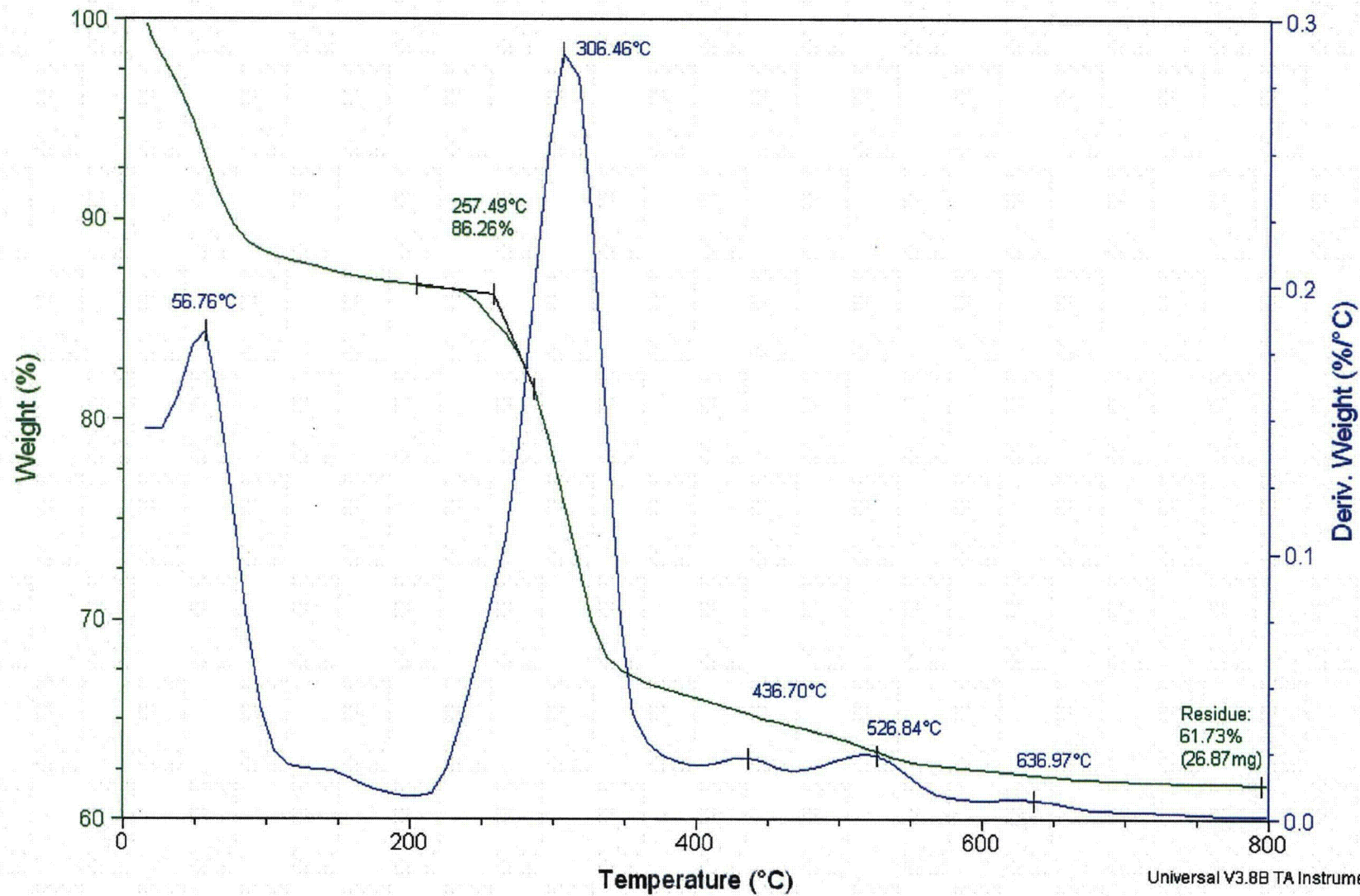
Sample: borated concrete 277-4
Size: 33.3660 mg
Method: caox

TGA

File: \\...\TGA\borated concrete 277-4.005

Run Date: 30-Nov-04 08:38
Instrument: 2950 TGA HR V6.1A

Plot labels:
48.98°C
250.21°C
88.67%
307.88°C
518.20°C
658.36°C
Residue:
62.70%
(20.92mg)

Weight (%) (left axis)
Deriv. Weight (%/°C) (right axis)
Temperature (°C)

Universal V3.8B TA Instruments
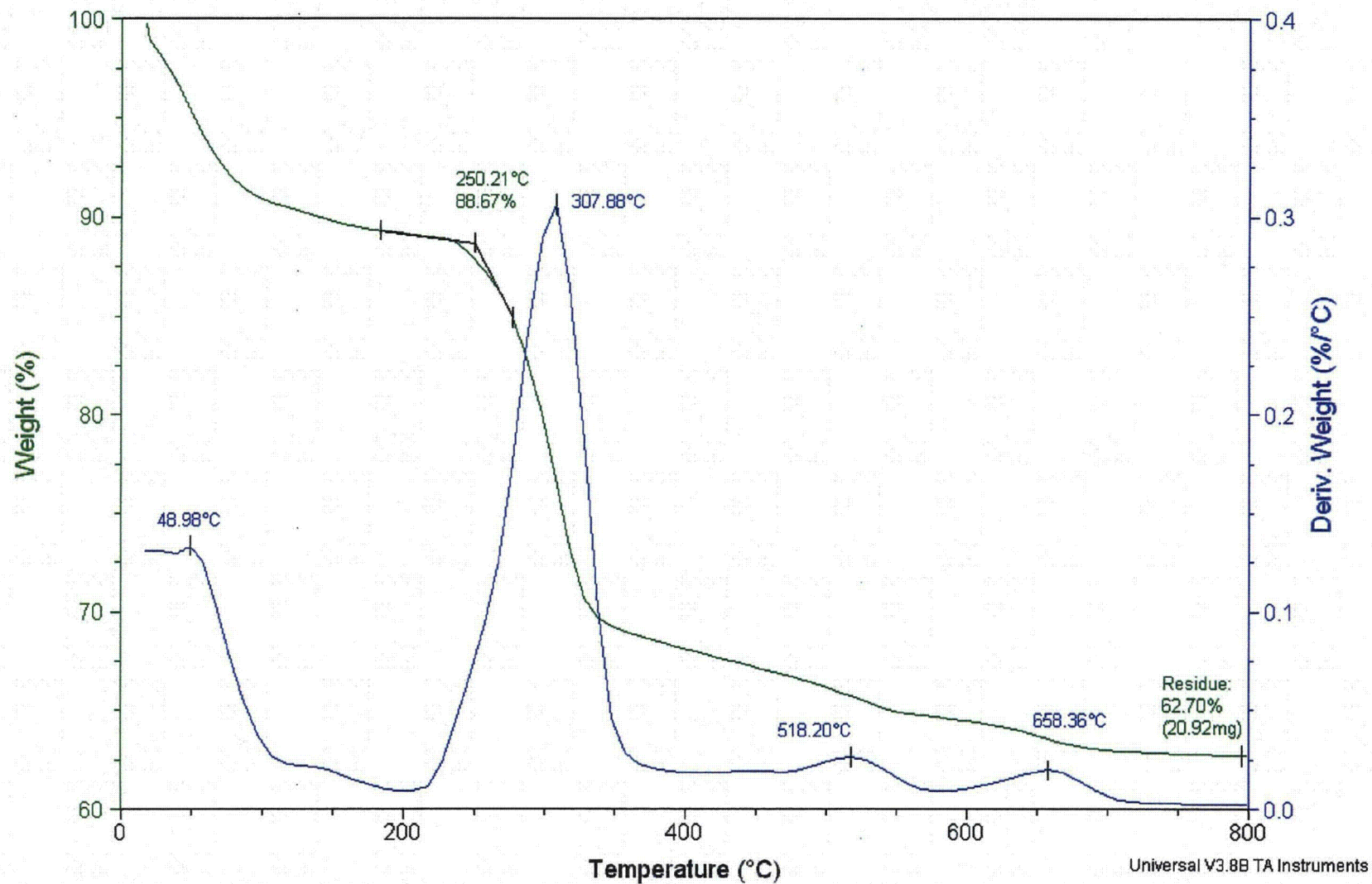
2-625

Sample: borated concrete 277-4
Size: 36.3460 mg
Method: caox

TGA

File: \\...\TGA\borated concrete 277-4.006

Run Date: 30-Nov-04 13:53
Instrument: 2950 TGA HR V6.1A

59.04°C

270.91°C
83.06%

309.01°C

Residue:
59.40%
(21.59mg)

429.20°C   519.34°C

649.50°C

Weight (%)

Deriv. Weight (%/°C)

Temperature (°C)

Universal V3.8B TA Instruments

2-626
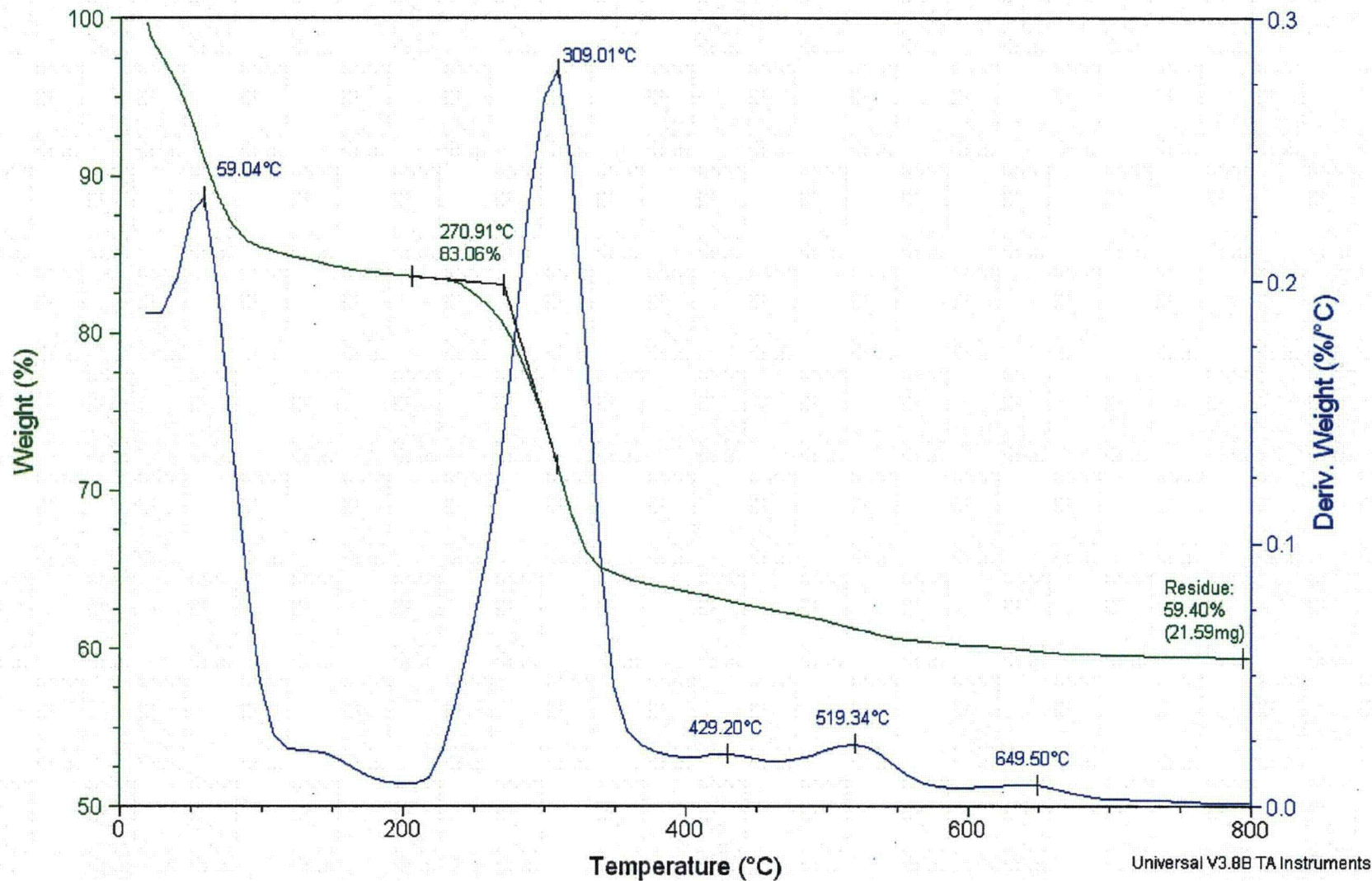
Appendix B
TGA Results Obtained on "Dried" Borated Concrete 277-4

2-628

Sample: borated 277-4
Size: 27.2660 mg
Method: caox

TGA

File: \\...\TGA\borated concrete 277-4.007

Run Date: 10-Dec-04 08:48
Instrument: 2950 TGA HR V6.1A

235.16°C
97.22%

303.91°C

Residue:
68.57%
(18.70mg)

73.03°C

434.11°C   514.24°C

654.39°C

Weight (%)

Deriv. Weight (%/°C)

Temperature (°C)

Universal V3.8B TA Instruments
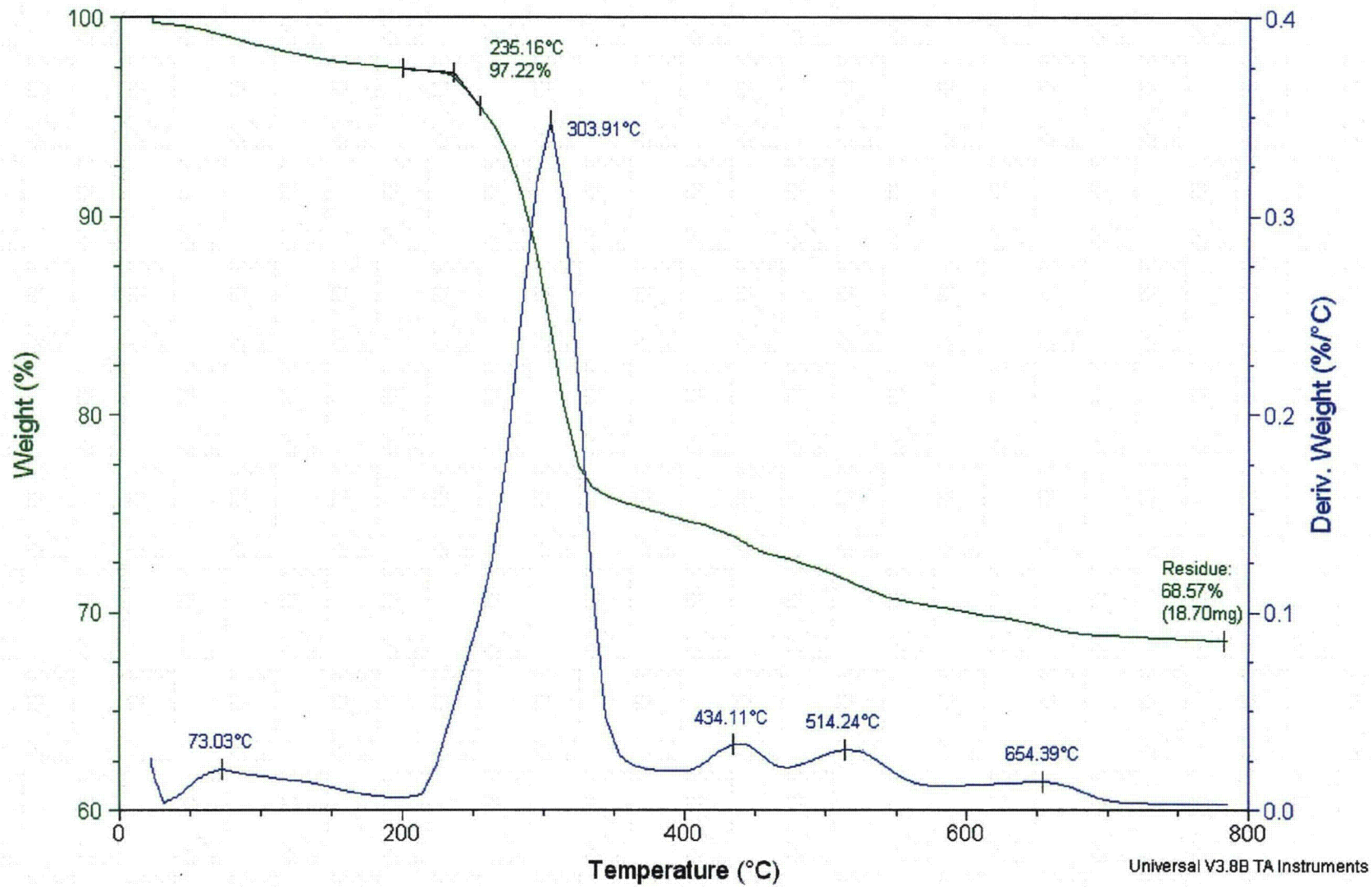
2-629

Sample: borated 277-4
Size: 52.4320 mg
Method: caox

TGA

File: \\...\TGA\borated concrete 277-4.008

Run Date: 10-Dec-04 12:28
Instrument: 2950 TGA HR V6.1A

269.75°C
97.47%

313.42°C

523.72°C

453.63°C

693.90°C

Residue:
68.32%
(35.82mg)

Weight (%)

Deriv. Weight (%/°C)

Temperature (°C)

Universal V3.8B TA Instruments
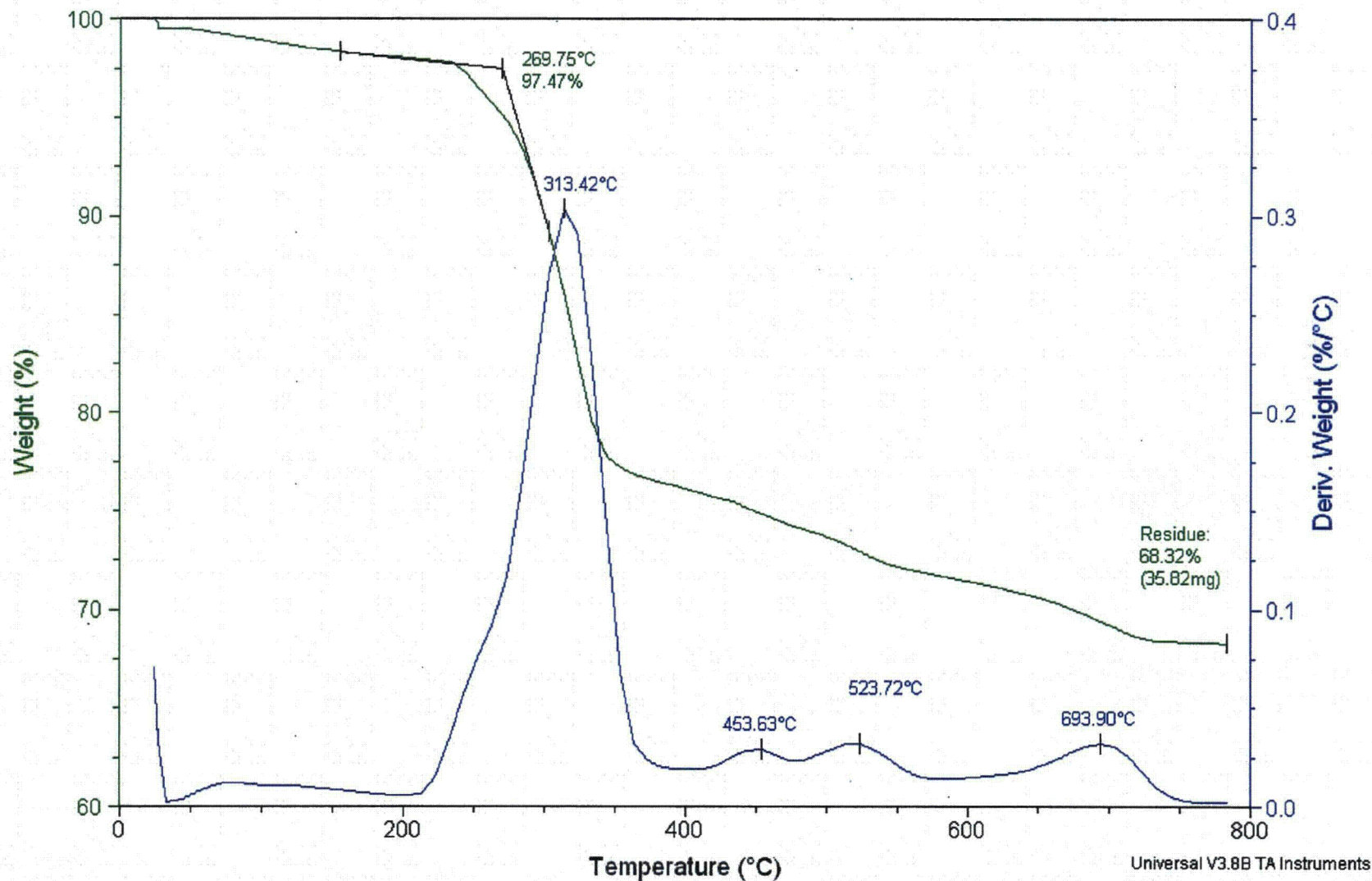
2-630

Sample: borated 277-4
Size: 53.1920 mg
Method: caox

TGA

File: \\...\TGA\borated concrete 277-4.009

Run Date: 13-Dec-04 08:16
Instrument: 2950 TGA HR V6.1A

239.35°C
98.00%

319.65°C

449.80°C   519.90°C

710.09°C

Residue:
67.80%
(36.06mg)

Weight (%)

Deriv. Weight (%/°C)

Temperature (°C)

Universal V3.8B TA Instruments

2-631

2-632
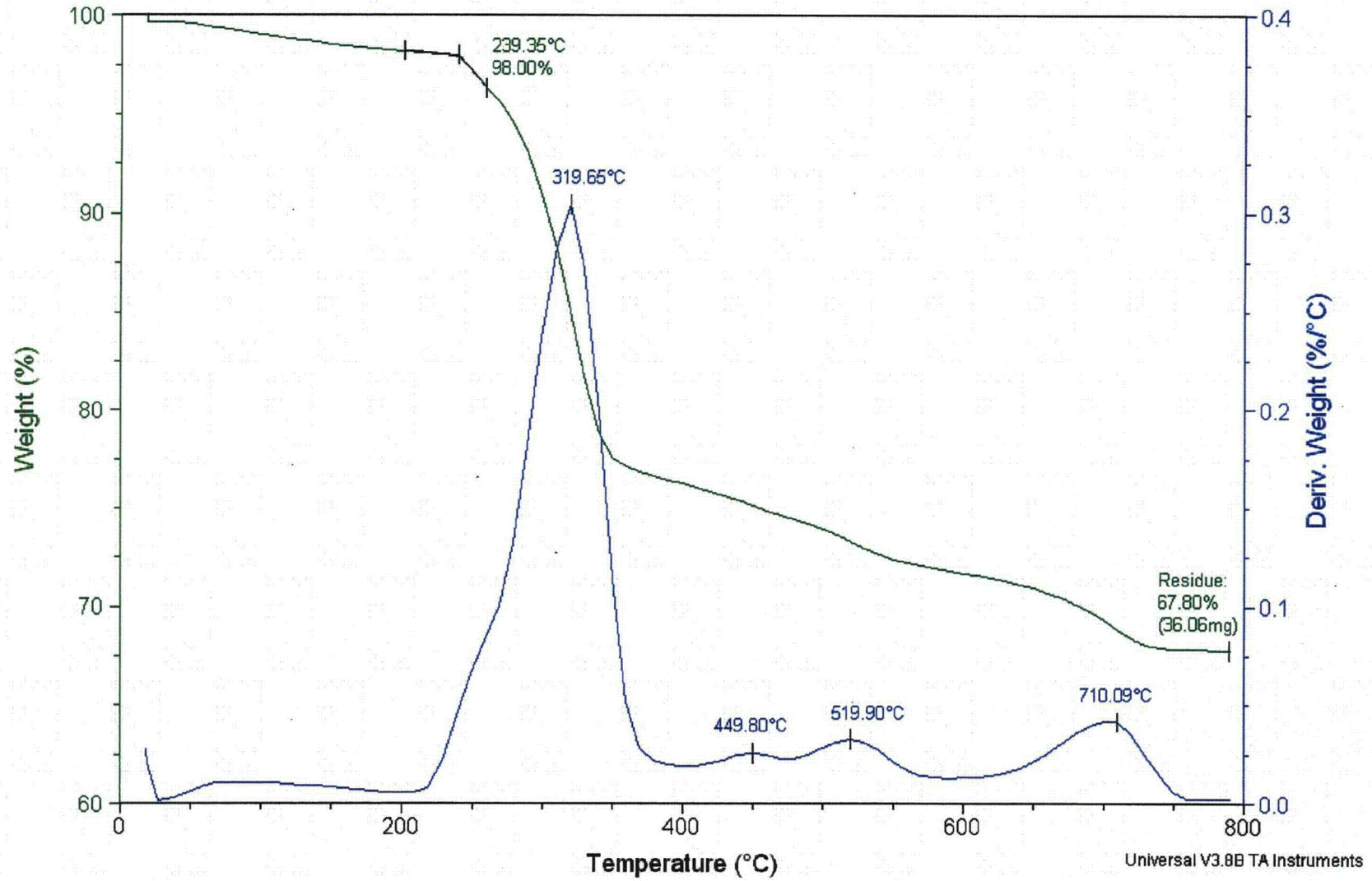
**Appendix C -
TGA Results Obtained on Borobond 4**

2-633

2-634

Sample: borobond a025-cs3
Size: 81.4390 mg
Method: caox

TGA

File: \\...\TA\Data\TGA\borobond a025-cs3.001

Run Date: 5-Nov-04 08:38
Instrument: 2950 TGA HR V6.1A

70.58°C
99.72%

138.64°C

Residue:
76.29%
(62.13mg)

Universal V3.8B TA Instruments

2-635
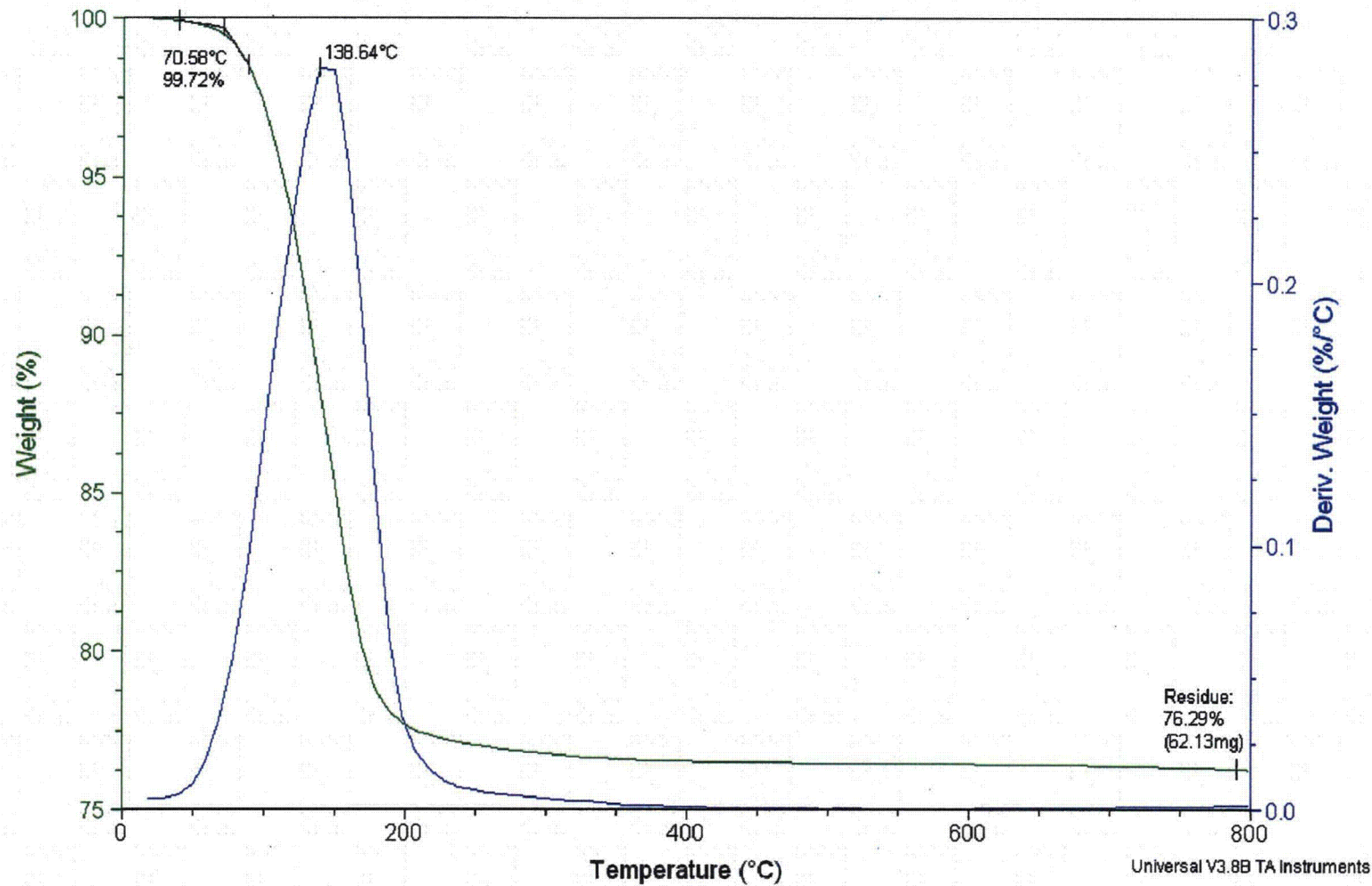
Sample: borobond a025-cs3
Size: 35.9800 mg
Method: caox

TGA

File: \\...\TA\Data\TGA\borobond a025-cs3.002

Run Date: 5-Nov-04 11:02
Instrument: 2950 TGA HR V6.1A

67.03°C
99.57%

123.32°C

Residue:
76.02%
(27.35mg)

Temperature (°C)

Weight (%)

Deriv. Weight (%/°C)

Universal V3.8B TA Instruments

2-636
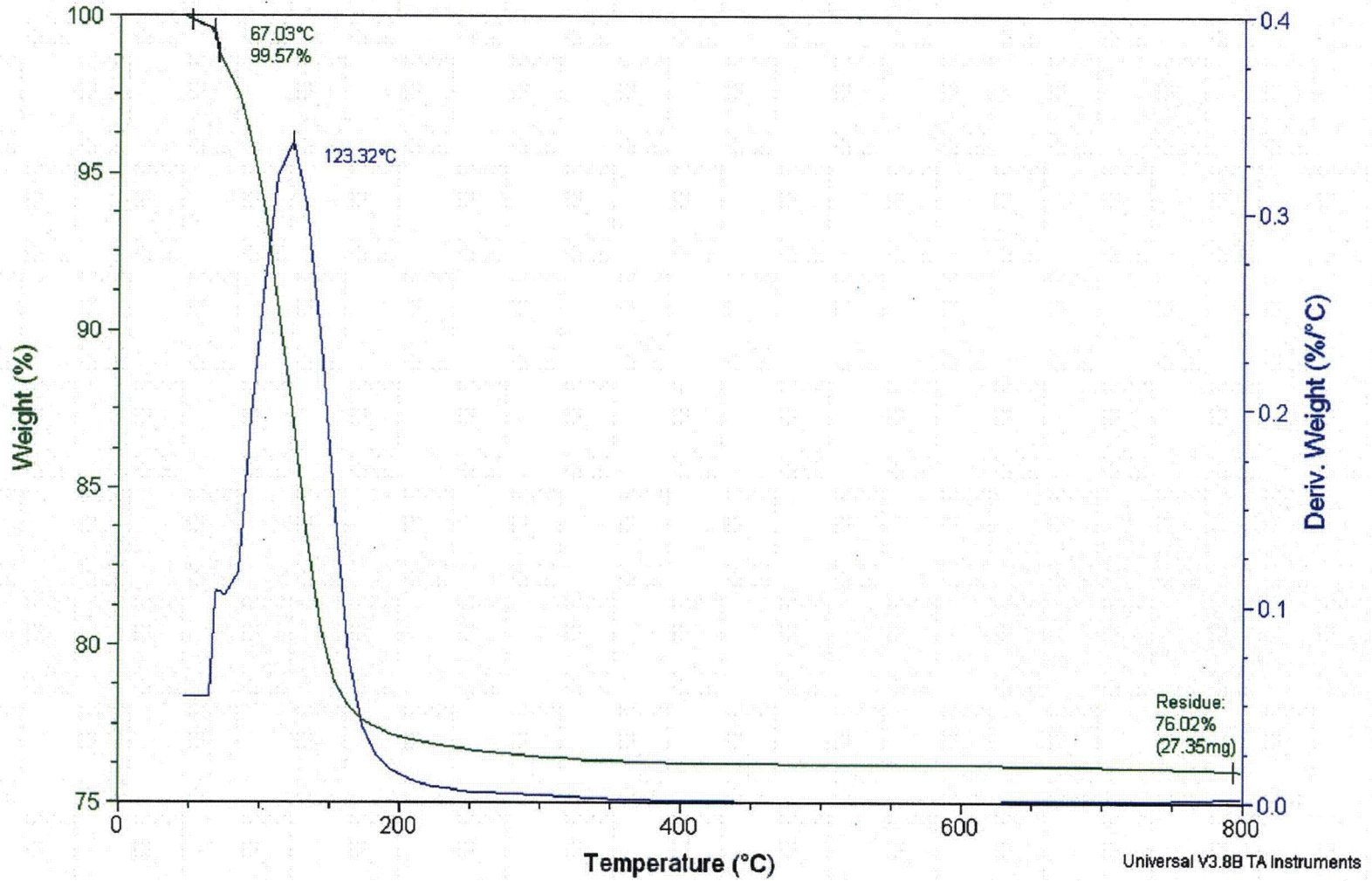
Sample: borobond a025-cs3
Size: 34.0020 mg
Method: caox

TGA

File: \\...\TA\Data\TGA\borobond a025-cs3.003

Run Date: 5-Nov-04 13:50
Instrument: 2950 TGA HR V6.1A

69.46°C

125.34°C

Residue:
76.28%
(25.94mg)

Weight (%)

Deriv. Weight (%/°C)

Temperature (°C)

Universal V3.8B TA Instruments

2-637

2-638
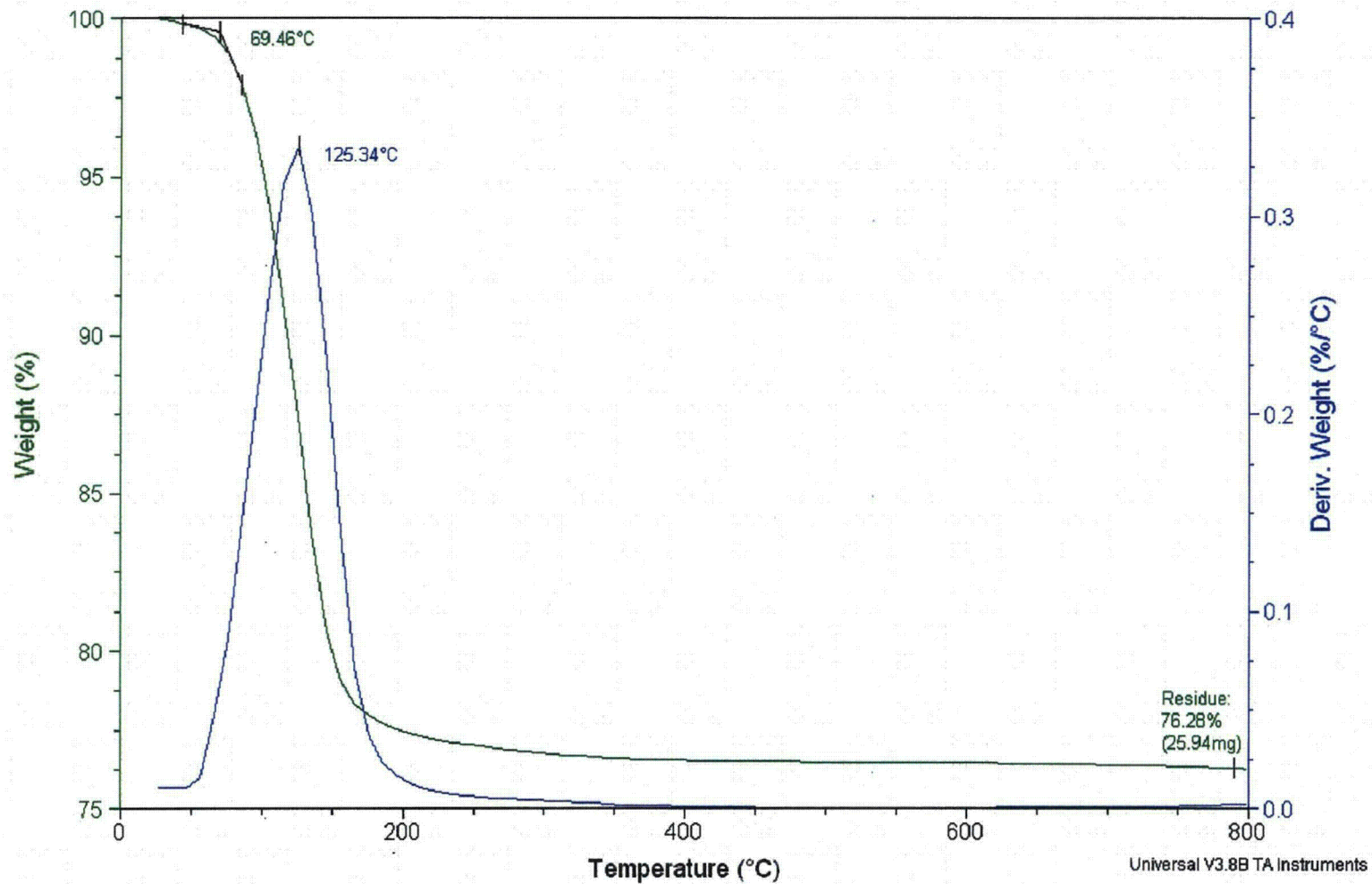
Appendix D
TGA Results for Adhesive Backed Silicone Foam

2-639

Sample: adhesive backed silicon foam
Size: 21.9230 mg
Method: caox

TGA

File: \\...\adhesive backed silicone foam.001

Run Date: 2-Nov-04 14:17
Instrument: 2950 TGA HR V6.1A

254.50°C
98.62%

361.38°C
91.42%

524.37°C

487.26°C
64.66%

404.18°C

283.91°C

Residue:
28.06%
(6.151mg)

Universal V3.8B TA Instruments

2-641
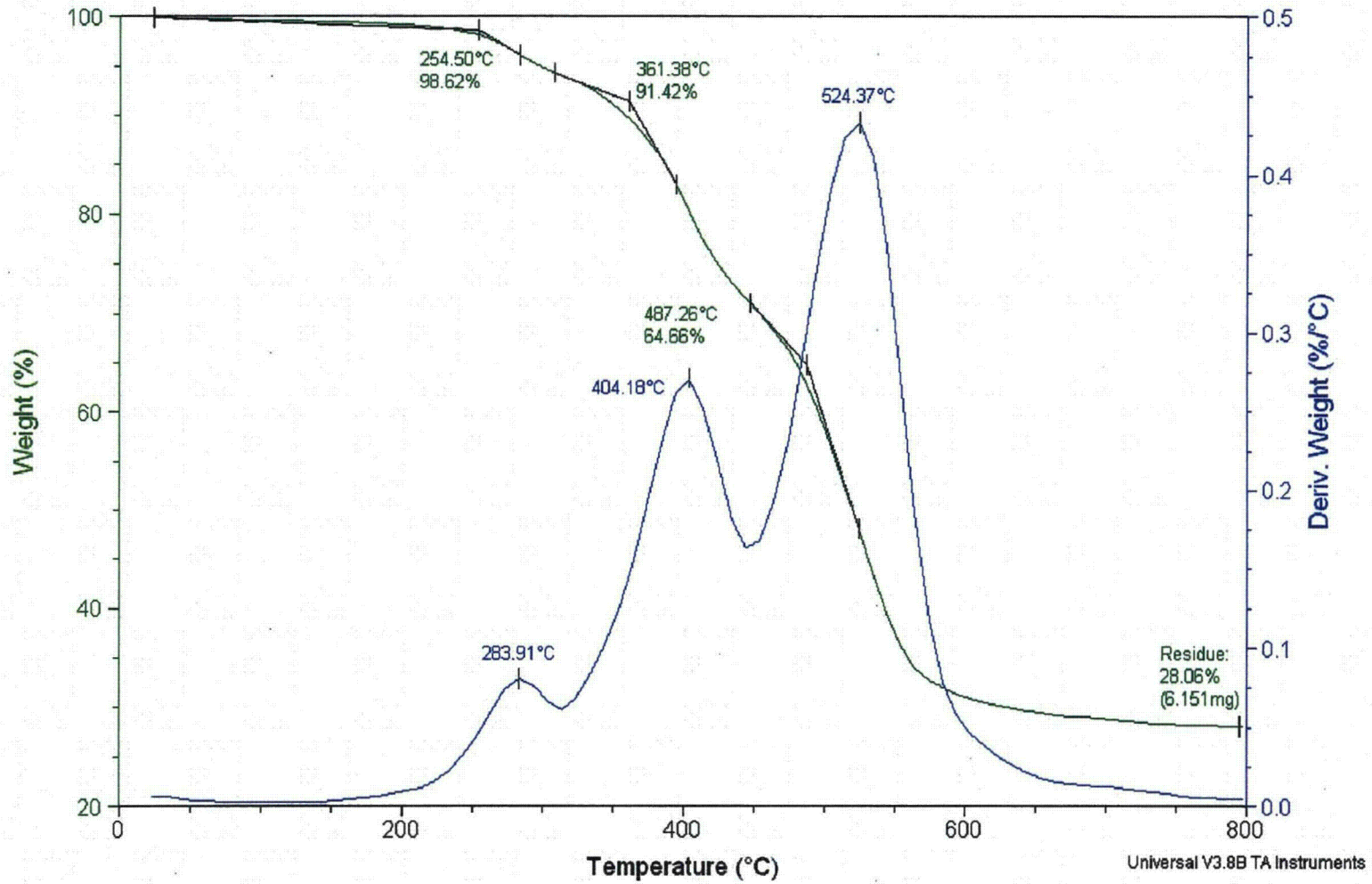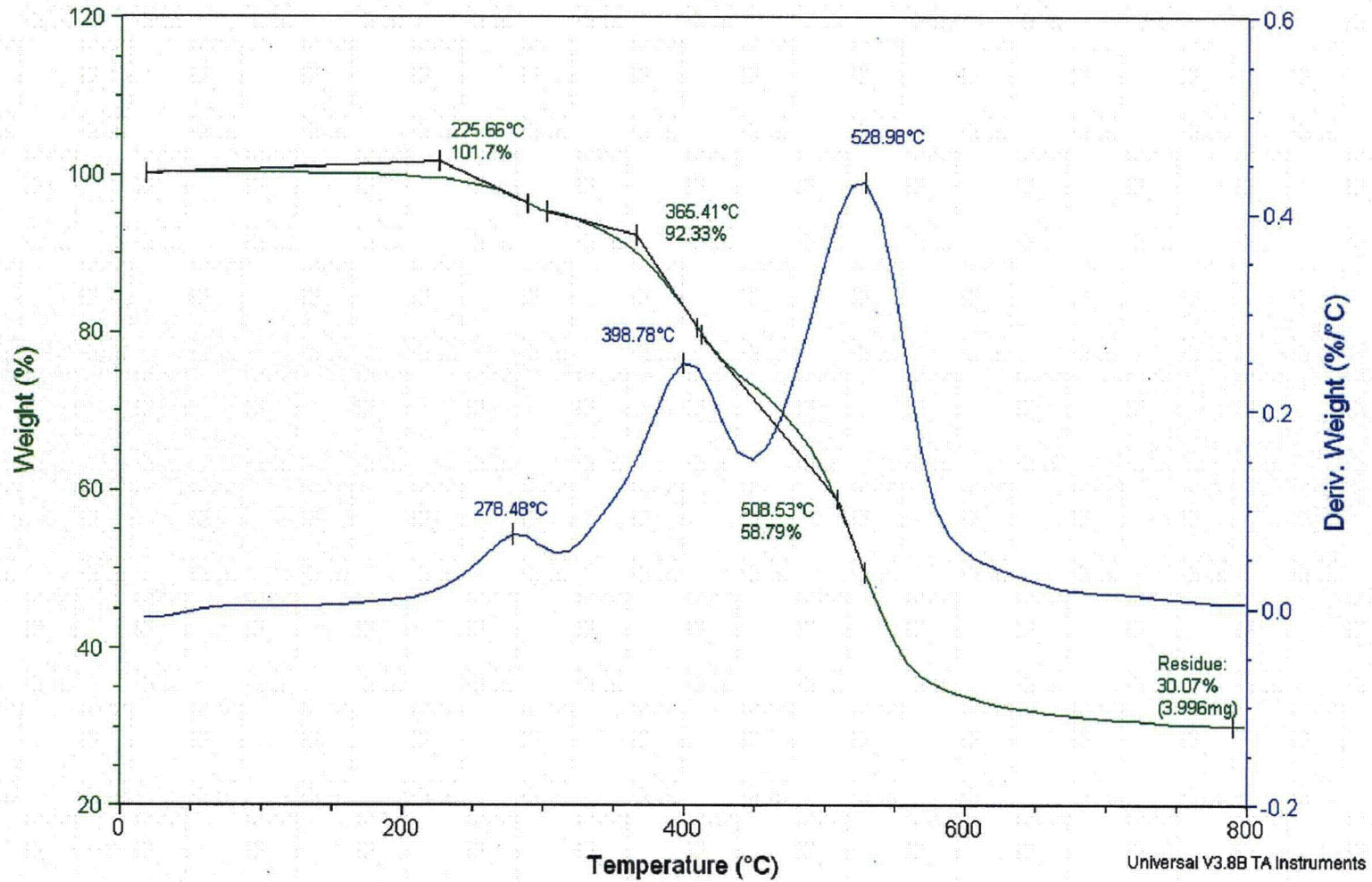
2-642

Sample: adhesive backed silicon foam
Size: 14.2630 mg
Method: caox

TGA

File: \\...\adhesive backed silicone foam.003

Run Date: 9-Nov-04 08:23
Instrument: 2950 TGA HR V6.1A

243.96°C
102.7%

367.94°C
93.17%

396.41°C

526.63°C

276.11°C

496.69°C
65.47%

Residue:
29.26%
(4.174mg)

Weight (%)

Deriv. Weight (%/°C)

Temperature (°C)

Universal V3.8B TA Instruments

2-643
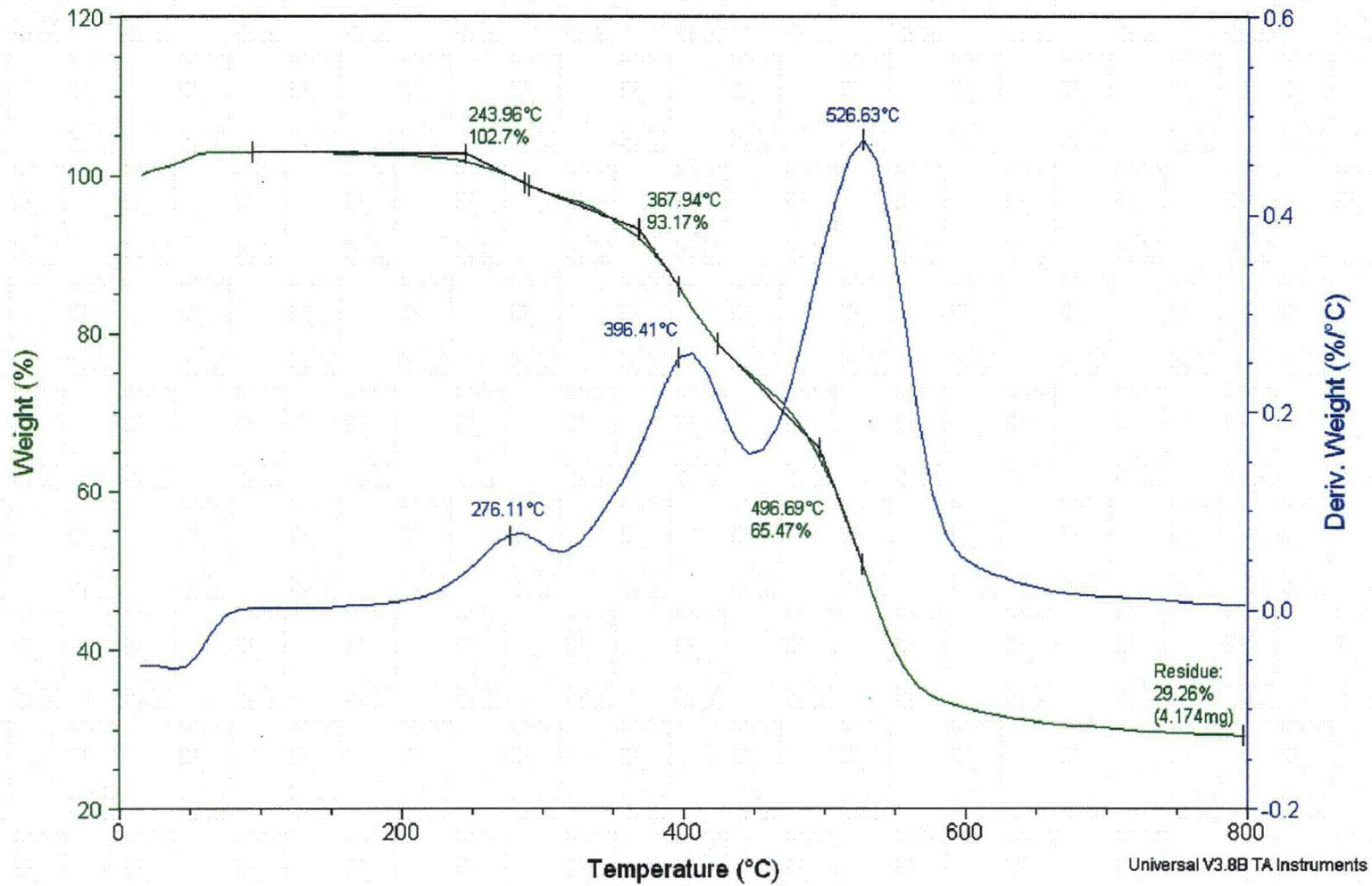
Distribution:

Amonett, C. M.
Anderson, J. C.
Arbital, J. G.
Bales, P. A.
Byington, G. A.
Cramer, Noel
Crenshaw, M. D.
DeClue, J. F.
Eckert, G. W.
Goins, M. L.
Handy, K. D.
Heatherly, C. N.
Holder, S. T.
Johnson, D. T.
Miller, D. B.
Perkins, G.
Singleton, G. B.
Smith, R. H.
Sooter, D. P.
Thomas, S. K.
Tollefson, D. A.
Turner, S. B.
Warren, T. L.
Y-12 Central Files

Appendix 2.10.5

BOROBOND4 PROPERTIES

B. F. Smith, *Compressive Strength and Coefficient of Thermal Expansion of BoroBond4*, Y/DW-1968, BWXT Y-12, Y-12 Natl. Security Complex, Jan. 19, 2005.

Note: For BoroBond4 outgassing properties, see Appendix 2.10.4: R. A. Smith, *Volatile Components from Packing Materials*, Y/DZ-2585, rev. 2, BWXT Y-12, Y-12 Natl. Security Complex, Dec. 22, 2004.

2-646

Compressive Strength and Coefficient of Thermal Expansion of BoroBond4

B. F. Smith
Characterization and Analysis Technology
Technology Development

August 11, 2004

COMPRESSIVE STRENGTH AND COEFFICIENT
OF THERMAL EXPANSION OF BOROBOND4

B. F. Smith
Characterization and Analysis Technology
Technology Development

Date of Issue: August 11, 2004

Y/LF-717/Rev 2/ES-3100 HEU SAR/Ch-2/rlw/3-06-08

CONTENTS

iii

2-650

FIGURES

TABLES

iv

INTRODUCTION

BoroBond4 is used as a neutron absorber in the ES-3100 packaging system. Mechanical and Manufacturing Engineering requested that Technology Development provide measurements of the compressive strength and rough estimates of the coefficient of thermal expansion (CTE) of BoroBond4 for use in simulations. The compressive strength measurements were to be done at room temperature (approximately 70°F), at -40°F, and at 100°F. Estimates of CTEs were to be done at -40°F, 100°F, and 200°F.

EXPERIMENTAL PROCEDURE

ASTM C 109[1] was used as a guide in measuring the compressive strength of BoroBond4. This standard provides an outline for measuring the maximum stress a two inch cube will experience before fracture. Fifty-six two inch cube specimens were provided by Eagle Picher. The density of each specimen was measured to determine the temperature distribution during compression testing. Six were tested at room temperature, six were tested at -40°F, and five were tested at 100°F. Rudimentary CTE measurements were taken on the specimens that were later compression tested at -40°F. A different group of six specimens were used only for CTE estimation at 100°F and 200°F.

As recommended by ASTM C 109, each cube was placed between two platens and loaded at a rate of 200 lb/s. The upper platen was spherically seated and the bottom platen was fixed. A 200,000 lb capacity servohydraulic load frame was used with a load cell set to the +/-50,000 lb range. Each specimen was brought to its test temperature by thermally "shocking" it, whereby it was placed in an environmental chamber at a more extreme temperature than it would be tested at. The 100°F compression specimens soaked at 110°F for 75 min, after which the chamber temperature was brought down to 100°F until testing began 6.5 h later. Similarly, the -40°F compression specimens soaked at -50°F for 15.5 h, after which the chamber temperature was raised to -40°F and testing began with little delay.

In estimating the CTE of BoroBond4, no formal standard was used and a method had to be improvised due to the lack of proper specimens and equipment. Thus, the CTE values reported here are only very rough ones and are by no means certified. The same type of two inch cubes were used for estimating CTEs that were used for the compressive strength measurements. The general procedure was to place the cube against a datum while at room temperature and measure lengths along two axes by butting a set of calipers against the top of the datum. The datum would ensure the same place on the cube was being measured before and after being brought to the appropriate temperature. A vise with faces 1.315 in. tall was used as the datum. Since the datum would result in measurements not on the center of the cube face, it was critical to keep the orientation of the cube consistent. After soaking for an adequate amount of time, the axis lengths were measured as close as possible to the original location. The CTE of BoroBond4 was then calculated using these two measurements.

1

RESULTS

Tables 1 through 3 summarize the BoroBond4 compressive strengths and test conditions. Tables 4 through 6 summarize the CTEs of BoroBond4.

Table 1. Compressive Strengths of BoroBond4 at 100°F

Cube ID	Density @ Room Temp (lb/ft³)	Compressive Strength (psi)
AO19-CS1	121.84	7711.5
AO17-CS3	121.94	7508.9
AO17-CS1	122.05	7422.8
AO20-CS2	122.08	7280.8
AO15-CS3	122.18	7440.6
Average Strength		7472.9

Table 2. Compressive Strengths of BoroBond4 at 70°F

Cube ID	Density @ Room Temp (lb/ft³)	Compressive Strength (psi)
AO22-CS2	122.69	9061.3
AO18-CS1	122.70	7697.5
AO25-CS2	122.70	9587.4
AO26-CS2	122.72	9651.4
AO20-CS1	122.75	7494.5
AO21-CS4	122.76	8263.0
Average Strength		8625.9

Table 3. Compressive Strengths of BoroBond4 at -40°F

Cube ID	Density @ Room Temp (lb/ft³)	Compressive Strength (psi)
AO24-CS3	123.10	9197.1
AO23-CS3	123.10	10347.7
AO25-CS4	123.12	11180.8
AO16-CS3	123.18	8232.8
AO16-CS1	123.19	9167.8
AO16-CS2	123.57	7081.7
Average Strength		9201.3

Table 4. Coefficients of Thermal Expansion of BoroBond4 at 200°F

Cube ID	Density @ Room Temp (lb/ft³)	CTE @ 0° Face (in/in-°F)	CTE @ 90° Face (in/in-°F)
AO21-CS1	122.27	-1.50E-05	-2.99E-05
AO21-CS2	122.30	-9.99E-06	-5.00E-06
AO22-CS4	122.70	-9.99E-06	-1.99E-05
AO16-CS4	122.81	0	-2.50E-05
AO25-CS1	123.08	-1.50E-05	-2.99E-05
AO23-CS4	123.09	-1.49E-05	-2.98E-05
Average CTEs		-1.08E-05	-2.32E-05

2

Table 5. Coefficients of Thermal Expansion of BoroBond4 at 100°F

Cube ID	Density @ Room Temp (lb/ft³)	CTE @ 0° Face (in/in-°F)	CTE @ 90° Face (in/in-°F)
AO21-CS1	122.27	0	-9.22E-06
AO21-CS2	122.30	0	-1.85E-05
AO22-CS4	122.70	0	-1.84E-05
AO16-CS4	122.81	-1.84E-05	-2.77E-05
AO25-CS1	123.08	1.85E-05	-9.22E-06
AO23-CS4	123.09	0	0
Average CTEs		1.07E-08	-1.38E-05

Table 6. Coefficients of Thermal Expansion of BoroBond4 at -40°F

Cube ID	Density @ Room Temp (lb/ft³)	CTE @ 0° Face (in/in-°F)	CTE @ 90° Face (in/in-°F)
AO24-CS3	123.10	9.02E-06	9.05E-06
AO23-CS3	123.10	4.53E-06	4.51E-06
AO25-CS4	123.12	9.07E-06	1.36E-05
AO16-CS3	123.18	0	4.53E-06
AO16-CS1	123.19	2.26E-06	2.27E-06
AO16-CS2	123.57	9.06E-06	4.53E-06
Average CTEs		5.66E-06	6.41E-06

3
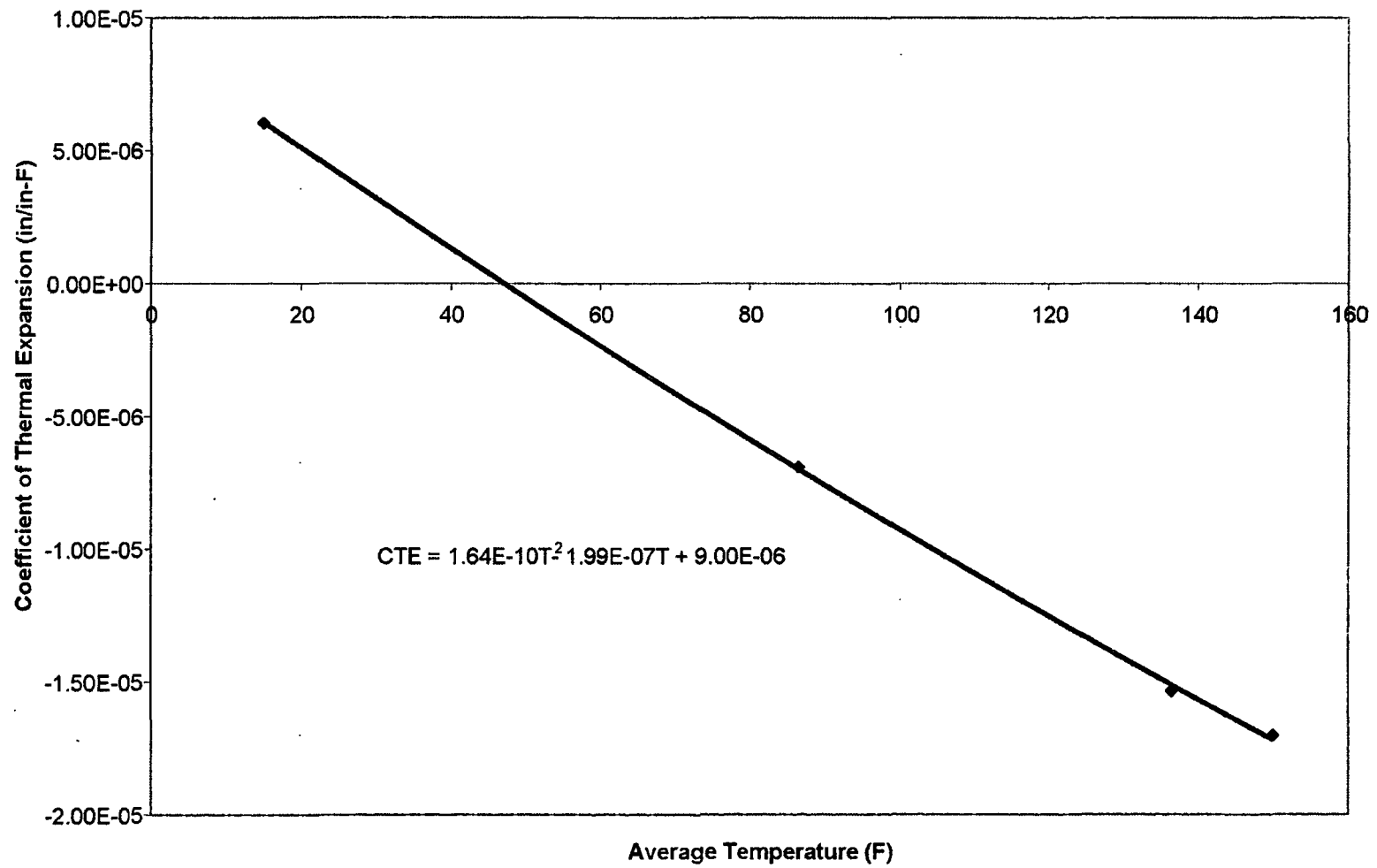
Fig. 1. Coefficient of Thermal Expansion vs. Average Temperature

4

DISCUSSION

As expected, the strength of BoroBond4 is inversely proportional to its temperature. The average strength increased from 7472.9 psi at 100°F to 9201.3 psi at -40°F.

As illustrated in Fig. 1, the coefficient of thermal expansion of BoroBond4 tends to decrease as the average temperature increases. The variation in CTE within temperature groups was very wide. The sense of the coefficient was not consistent. For example, the CTE estimated at 100°F showed that the 0° face expanded while the 90° face contracted. This may be negligible, however, since the change in temperature of only 27°F was relatively small.

The mechanism of thermal expansion or contraction is apparently due to dehydration. After measuring CTEs at 200°F and allowing the specimens to cool to room temperature, it was noted that all cubes were significantly lighter in color. Measurements showed that the cubes had not returned to their original dimensions and their masses had decreased. This could only be due to dehydration since each cube was in good condition and had not lost any noticeable mass due to chipping or rough handling. Table 7 summarizes the changes in dimensions, all taken at room temperature. All of these cubes had soaked at 110°F for 3 h followed by soaking at 100°F for 92.5 h, which was followed by a soaking at 220°F for a period of 3 h. The excessive length of time the specimens were at 100°F may explain the water loss.

Table 7. Changes in CTE Specimens

Cube ID	ΔL, 0° Face (in)	ΔL 90° Face (in)	Δ mass (g)
AO21-CS1	-0.004	-0.0055	-27.14
AO21-CS2	-0.005	-0.007	-29.295
AO22-CS4	-0.004	-0.007	-25.44
AO16-CS4	-0.006	-0.0075	-28.625
AO25-CS1	-0.004	-0.0075	-25.565
AO23-CS4	-0.001	-0.007	-27.74

REFERENCES

1. ASTM International. *Standard Test Method for Compressive Strength of Hydraulic Cement Mortars (Using 2-in. or [50-mm] Cube Specimens)*. ASTM Standard C 109/C 109M-02.

5

DISTRIBUTION

<u>Y-12 National Security Complex</u>

Anderson, J. C.
Arbital, J. G.
Bales, P. A.
Byington, G. A. (2)
DeClue, J. F. (2)
Doyle, J. H.
Goins, M. L.
Hammond, C. R.
Handy, K. D. (2)
Heatherly, C. N.
Kitzke, K. A.
Miller, D. B.
Neal, J. Y.
Smith, B. F.
Sooter, D. P.
Y-12 Plant Records - RC

6

2-658

Appendix 2.10.6

RECOMMENDED RANDOM VIBRATION AND SHOCK TEST SPECIFICATIONS FOR CARGO TRANSPORTED ON SST AND SGT TRAILERS

2-659

2-660

Sandia National Laboratories

Operated for the U.S. Department of Energy by
Sandia Corporation
Albuquerque, New Mexico 87185

date: April 19, 2002

to: Distribution

from: J. S. Cap, 9125

subject: Recommended Random Vibration and Shock Test Specifications for Cargo Transported on SST and SGT Trailers

References

[1] UNC document from J. S. Cap, 9735; to G. W. Crowder, 5512; dated 5/1/97; "Maximum Expected Mechanical Shock and Vibration Environments and Test Requirements for Cargo Transported on SSTs & SGTs."
[2] UNC Document MIL-STD-810E; "Environmental Test Methods and Engineering Guidelines."

Introduction

The primary goal of this document is to provide a set of random vibration test specifications and a set of shock test specifications for cargo being transported on the Safe-Secure Trailers (SST2/82 and SST2/90) and the Safeguards Transporter (SGT). An earlier study [1] established that the random vibration and shock profiles measured during road tests for each trailer indeed represented the Maximum Expected Environments (MEE) (i.e., statistically conservative upper bounds). That study also established the appropriate random vibration test durations for producing the equivalent fatigue damage as a function of trip distance.

copy to:

Dept	MS	Name	Dept	MS	Name
5851	0790	G. W. Crowder	8234	9035	K. E. Carbiener
5851	0790	J. K. Deuel	8234	9035	T. Harrison
8242	9014	W. R. Delameter	8727	9042	J. J. Lauffer
8242	9014	D. M. Kwon	9125	0557	T. J. Baca
8242	9014	A. H. Leung	9125	0557	File(EE6.7)
8242	9014	A. A. Ver Berkmoes			Steve Jensen (LLNL)

The raw Acceleration Spectral Densities (ASDs) and the raw Shock Response Spectra (SRS) that define the MEE for random vibration and shock respectively are not practical for use as laboratory test specifications. Therefore, reference [1] also provided a set of straight-line segment ASDs and SRS that envelop the raw MEE spectra and are suitable for use in the laboratory. However, those straight-line segment ASDs and SRS were deemed to be less than ideal, so a slightly improved set is presented in this document.

Random Vibration Test Duration

For purposes of estimation, we have identified a generic 2000-mile cross-country road trip that will last 45 hours. Of course, the cargo will not be subjected to the MEE vibration levels for the entire time, but instead will experience a distribution of input levels that is by definition at or below the MEE levels. Using the distribution of input levels for the entire road trip identified in reference [1], it is possible using fatigue theory to define a laboratory test that produces the same amount of fatigue damage in a few hours that the cargo would experience during the 2000-mile trip. The most logical initial (baseline) choice for the laboratory test specifications is the MEE ASDs (and hence the corresponding straight-line segment ASDs).

Table 1, which is taken verbatim from [1], identifies the amount of time spent on each of the different type roads during the generic 2000-mile road trip and the corresponding laboratory test durations for different types of cargo (the definition of which are explained in the table notes).

Table 1: Accelerated Laboratory Test Times for a 2000-Mile Road Trip

Road Type	Trip Time	Lab Scale Factors and Test Times (1,2,3)		
		1 dB/decade	3 dB/decade	4 dB/decade
Interstate	37 Hrs	0.23 Hrs/Axis	0.41 Hrs/Axis	0.8 Hrs/Axis
Rural Highways	6 Hrs	0.07 Hrs/Axis	0.09 Hrs/Axis	0.2 Hrs/Axis
Urban Streets & Unpaved Roads (4)	2 Hrs	1.5 Hrs/Axis	1.5 Hrs/Axis	1.5 Hrs/Axis
Total Test Times	45 Hrs	1.8 Hrs/Axis	2.0 Hrs/Axis	2.5 Hrs/Axis

Notes for Table 1:
1) Some of the laboratory test times identified in this table have been rounded up for simplicity.
2) The amount of time compression to be achieved for a given increase in test level will depend on the materials and assembly techniques present in the item being tested. The literature identifies a range of compression factors (defined in terms of the dB increase in test level per decade of time compression) that vary from 1 dB/decade for brittle materials exposed to coulomb friction (such as for un-potted bolted assemblies) to 4 dB/decade for ductile materials supported in viscoelastic media (as for encapsulated assemblies). Table 1 identifies the compressed test times for several compression factors of interest.
3) If the specifics of a system design are not known, or contain a range of materials, it is recommended that the time compression be performed using a 3 dB/decade compression factor.

4)   The environmental levels for urban streets and unpaved roads were so close in magnitude to the MEE levels that minimal time compression was possible.

It is interesting to note that the resulting test time for the 3 dB/decade compression factor (2 hours/axis for a 2000-mile trip) agrees exactly with the recommended ratio of test duration versus trip distance identified in MIL-STD-810E [2] for truck-transport.

If the total laboratory test-duration is still too long after the initial time compression has been applied (usually true for components that must make many trips on one of the trailers), then additional time compression can be achieved by increasing the test specifications by a specified number of dB to achieve additional time compression. The user is cautioned that there are risks associated with testing one's hardware to levels that are higher than they would ever expect to see in the field. However, since the absolute magnitude of the SST/SGT MEE test levels are relatively low compared with other truck transport inputs (such as MIL-STD-810E), an increase of 3-6 dB should not significantly increase the risk of a component failure, while permitting an additional time compression factor of 10-100 (assuming the 3 dB/decade compression factor).

Random Vibration Test Specifications

Figure 1 presents the recommended straight-line segment ASD random vibration test specifications for transport of cargo on SST and SGT trailers. The axes identified in the figure (LONG, LAT, and VERT) refer to the trailer coordinate system.

However, there may be instances where the orientation of the cargo relative to the longitudinal and lateral trailer axis is not unique. In such cases it is recommended that the cargo be tested in two mutually perpendicular horizontal axes using to the "HORIZ" test specifications identified in Figure 2 (the "VERT" test specification, which has been reproduced in Figure 2 for convenience, must still be applied in that axis).

These ASDs should be applied to the cargo at a point that is in intimate contact with the shaker table. Assuming that the 3 dB/decade compression factor is chosen and no additional scaling is done, the test specifications presented in Figure 1 should be applied for 1 Hr/axis for each 1000 miles of road transport.

The test specifications presented in these figures have been defined down to 1 Hz for completeness. However, the cargo need only be tested down to a frequency that is equal to one-half of its lowest resonant mode, or 10 Hz, whichever is lower. The ASDs identified in Figures 1 and 2 would be truncated accordingly.

Appendix A compares the straight-line ASD test specifications against the underlying MEE ASDs.

Figure 1: SST/SGT Random Vibration Test Specifications
Input to Base of Cargo
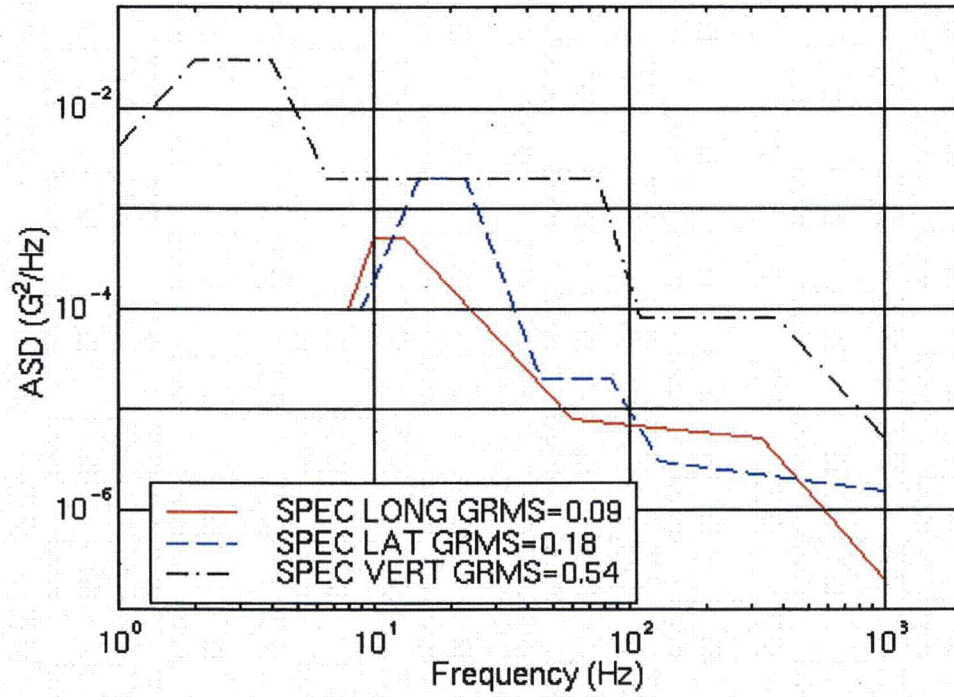
LONG		LAT		VERT	
Freq (Hz)	G²/Hz	Freq (Hz)	G²/Hz	Freq (Hz)	G²/Hz
1.0	1.0e-4	1.0	1.0e-4	1.0	4.0e-3
8.0	1.0e-4	9.0	1.0e-4	2.0	3.0e-2
10.0	5.0e-4	15.0	2.0e-3	4.0	3.0e-2
13.0	5.0e-4	23.0	2.0e-3	6.5	2.0e-3
60.0	8.0e-6	45.0	2.0e-5	75.0	2.0e-3
330.0	5.0e-6	85.0	2.0e-5	110.0	8.0e-5
1000.0	2.0e-7	130.0	3.0e-6	380.0	8.0e-5
		1000.0	1.5e-6	1000.0	5.0e-6

Figure 2: SST/SGT Random Vibration Test Specifications
Alternative Test Specifications for Cargo with a Non-Unique Horizontal Orientation
Input to Base of Cargo
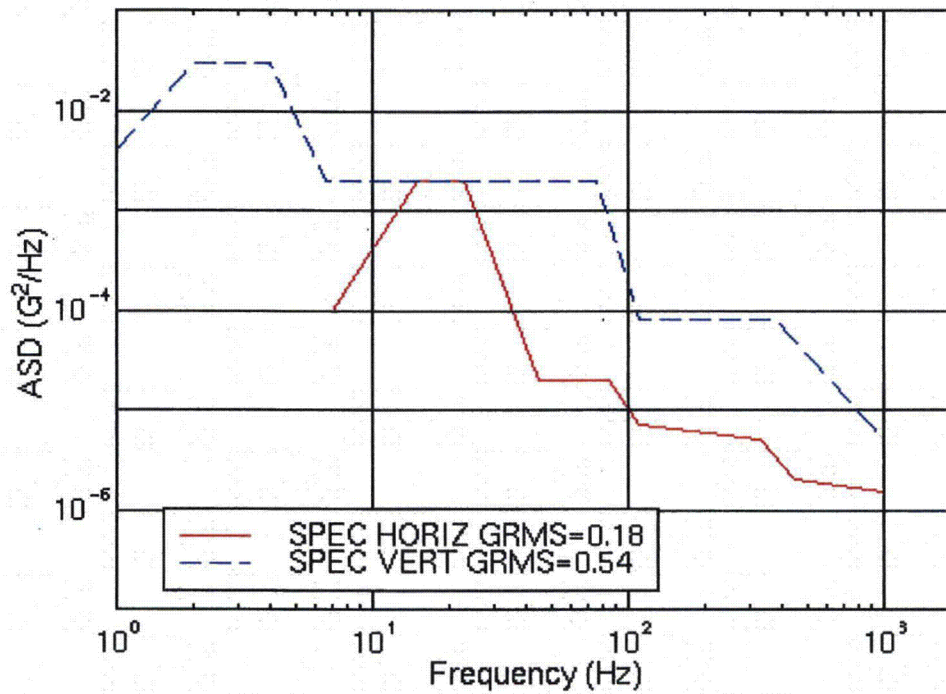
HORIZ		VERT	
Freq (Hz)	G^2/Hz	Freq (Hz)	G^2/Hz
1.0	1.0e-4	1.0	4.0e-3
7.0	1.0e-4	2.0	3.0e-2
15.0	2.0e-3	4.0	3.0e-2
23.0	2.0e-3	6.5	2.0e-3
45.0	2.0e-5	75.0	2.0e-3
85.0	2.0e-5	110.0	8.0e-5
110.0	7.0e-6	380.0	8.0e-5
330.0	5.0e-6	1000.0	5.0e-6
450.0	2.0e-6		
1000.0	1.5e-6		

Shock Test Specifications

Figure 3 presents the recommended straight-line segment SRS shock test specifications for transport of cargo on SST and SGT trailers. All of the SRS presented in this document were calculated using a Maxi-Max Absolute Acceleration (MMAA) algorithm with a 3% critical damping ratio. The axes identified in the figure (LONG, LAT, and VERT) refer to the trailer coordinate system.

However, there may be instances where the orientation of the cargo relative to the longitudinal and lateral trailer axis is not unique. In such cases it is recommended that the cargo be tested in two mutually perpendicular horizontal axes using to the "HORIZ" test specifications identified in Figure 4 (the "VERT" test specification, which has been reproduced in Figure 4 for convenience, must still be applied in that axis).

These SRS should be applied to the cargo at a point that is in intimate contact with the shaker table. It is recommended that the cargo be subjected to 5 hits/axis for every 1000 miles of trip distance (this number of hits is admittedly somewhat arbitrary and has been defined to match the guidelines in similar specifications).

The preferred method for simulating the SRS identified in these figures is with an oscillatory pulse (such as the sum of decayed sinusoids or wavelets) on a shaker table. Such a pulse is an acceptable representation of the test specification if its SRS matches the specified SRS within some tolerance range defined by the project group (typically ±3dB).

The test specifications presented in these figures have been defined down to 1 Hz for completeness. However, the cargo need only be tested down to a frequency that is equal to one-half of its lowest resonant mode, or 10 Hz, whichever is lower. The SRS identified in Figures 3 and 4 would be truncated accordingly.

Appendix B compares the straight-line SRS test specifications against the underlying MEE SRS.

Figure 3: SST/SGT Shock Test Specifications
Input to Base of Cargo
3% Damped MMAA SRS
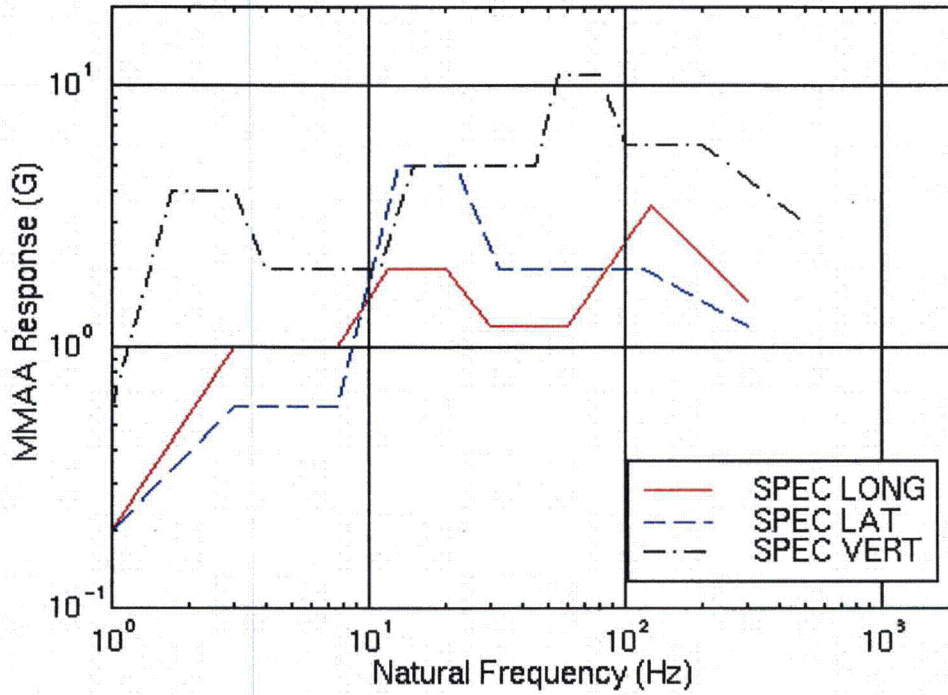
LONG		LAT		VERT	
Freq (Hz)	G^2/Hz	Freq (Hz)	G^2/Hz	Freq (Hz)	G^2/Hz
1.0	0.2	1.0	0.2	1.0	0.6
3.0	1.0	3.0	0.6	1.7	4.0
7.5	1.0	7.5	0.6	3.0	4.0
12.0	2.0	13.0	5.0	4.0	2.0
20.0	2.0	22.0	5.0	11.0	2.0
30.0	1.2	32.0	2.0	15.0	5.0
60.0	1.2	120.0	2.0	45.0	5.0
125.0	3.5	300.0	1.2	55.0	11.0
300.0	1.5			80.0	11.0
				100.0	6.0
				200.0	6.0
				500.0	3.0

Figure 4: SST/SGT Shock Test Specifications
Alternative Test Specifications for Cargo with Non-Unique Horizontal Axes
Input to Base of Cargo
3% Damped MMAA SRS
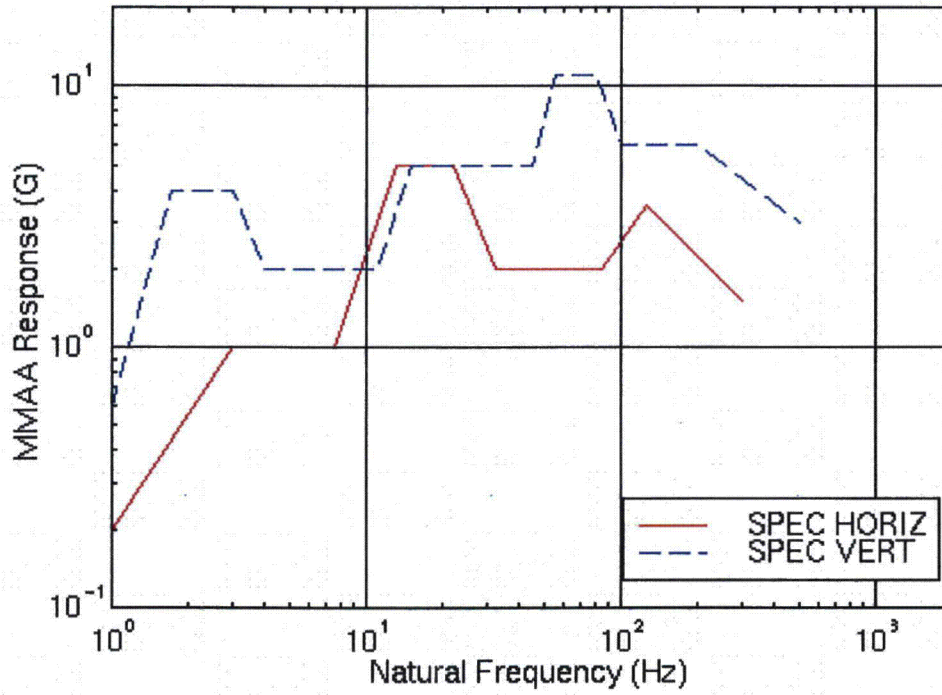
HORIZ		VERT	
Freq (Hz)	G²/Hz	Freq (Hz)	G²/Hz
1.0	0.2	1.0	0.6
3.0	1.0	1.7	4.0
7.5	1.0	3.0	4.0
13.0	5.0	4.0	2.0
22.0	5.0	11.0	2.0
32.0	2.0	15.0	5.0
85.0	2.0	45.0	5.0
125.0	3.5	55.0	11.0
300.0	1.5	80.0	11.0
		100.0	6.0
		200.0	6.0
		500.0	3.0

2-668

APPENDIX A
COMPARISON OF TEST SPECIFICATIONS AGAINST UNDERLYING MEE RESPONSE SPECTRA FOR RANDOM VIBRATION

Figures A-1, A-3, and A-5 present comparisons of the recommended test specifications identified in the main section of this document (denoted SPEC...) against the envelopes of the MEE response spectra for the individual trailers (denoted ALL...). Figures A-2, A–4, and A-6 present the MEE spectra for the individual trailers (denoted 282, 290, and SGT for the SST2/82, SST2/90, and SGT respectively).

Figure A-1: SST/SGT Random Vibration Environment
Comparison of Recommended Test Specification Versus MEE Response (All Trailers)
Trailer Floor – Longitudinal Axis
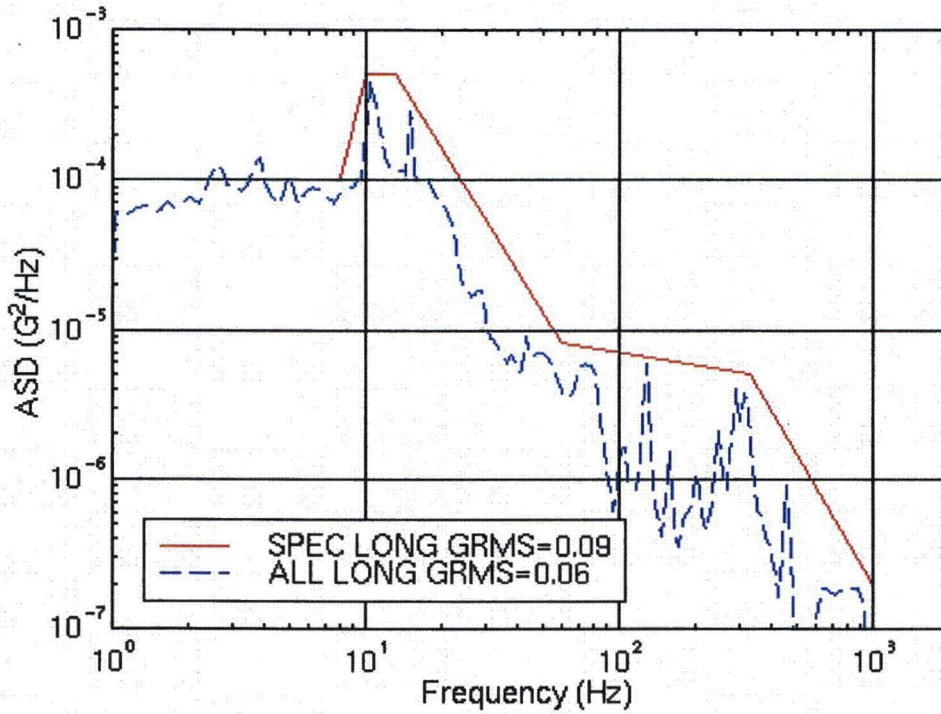
Figure A-2: SST/SGT Random Vibration Environment
Comparison of MEE Responses for SST2/82, SST2/90, and SGT
Trailer Floor – Longitudinal Axis

2-670
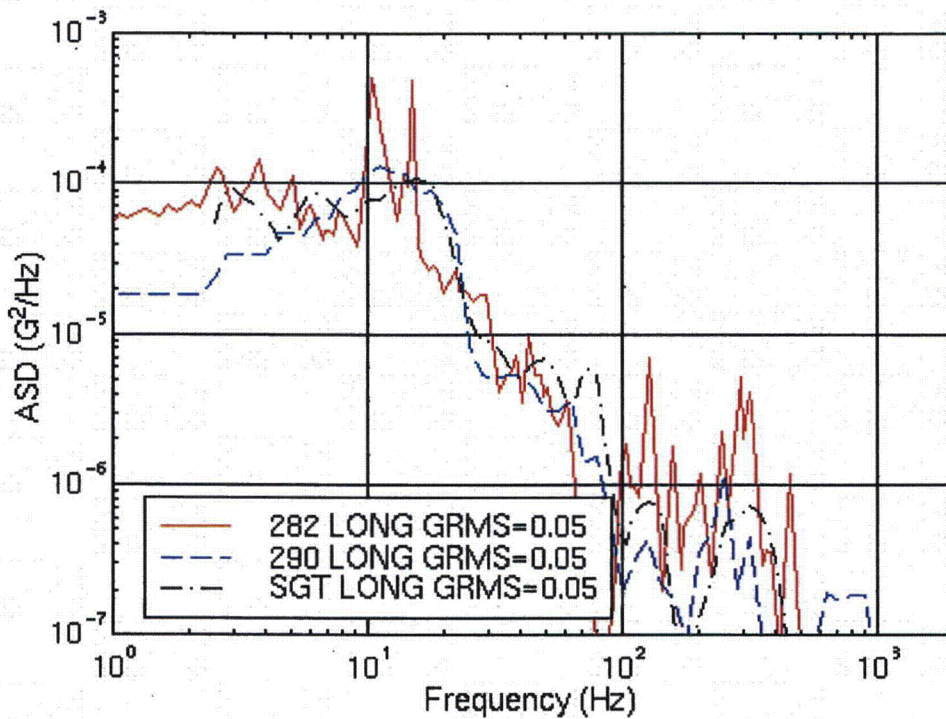
Figure A-3: SST/SGT Random Vibration Environment
Comparison of Recommended Test Specification Versus MEE Response (All Trailers)
Trailer Floor – Lateral Axis
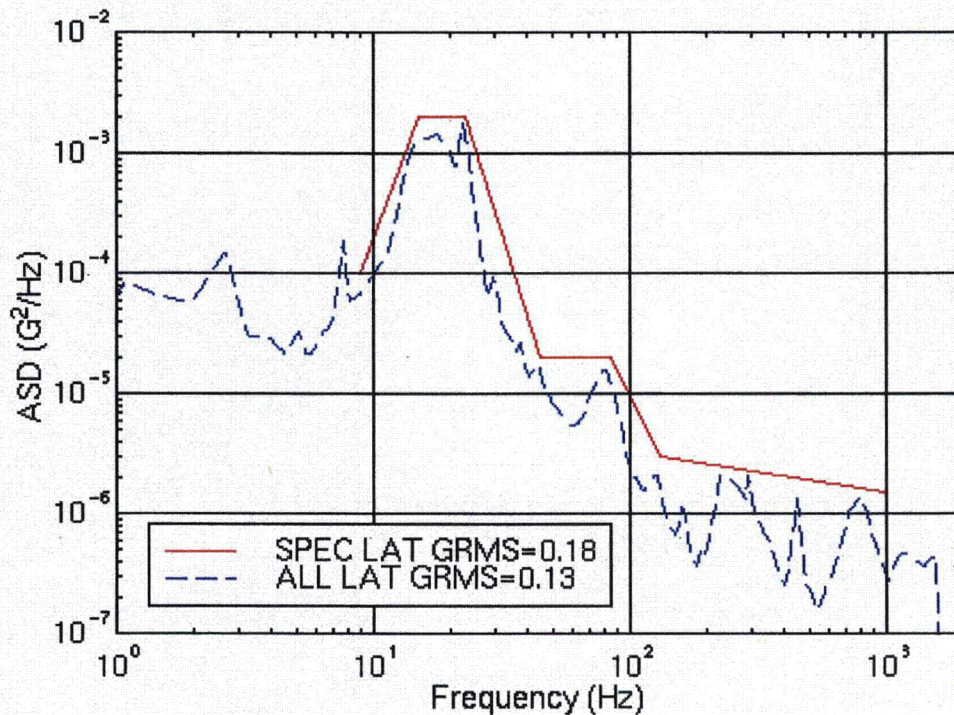
Figure A-4: SST/SGT Random Vibration Environment
Comparison of MEE Responses for SST2/82, SST2/90, and SGT
Trailer Floor – Lateral Axis

2-671
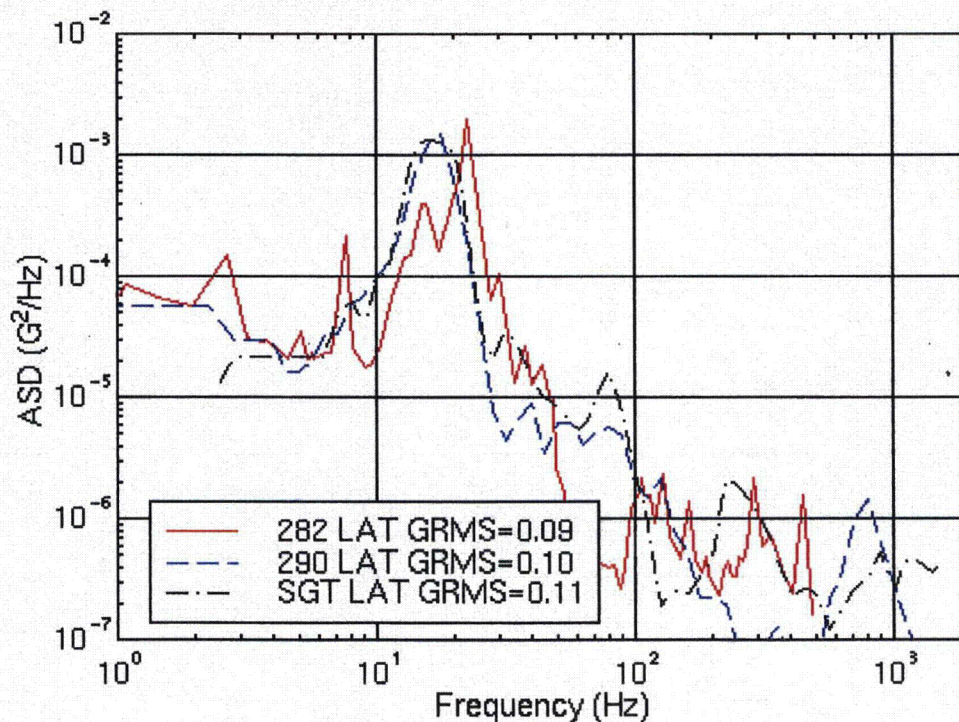
Figure A-5: SST/SGT Random Vibration Environment
Comparison of Recommended Test Specification Versus MEE Response (All Trailers)
Trailer Floor – Vertical Axis
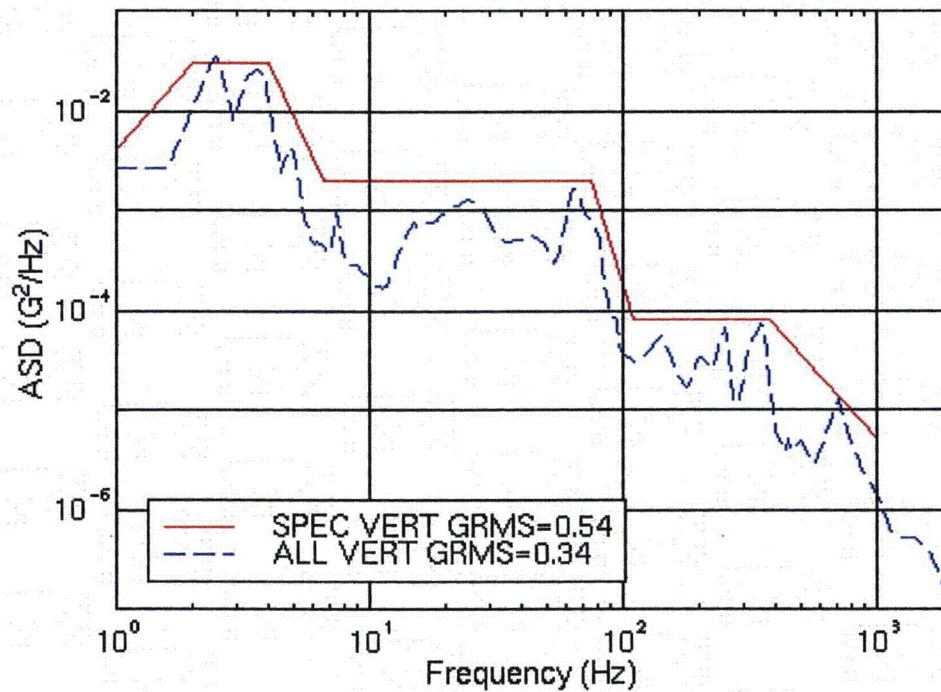
Figure A-6: SST/SGT Random Vibration Environment
Comparison of MEE Responses for SST2/82, SST2/90, and SGT
Trailer Floor – Vertical Axis

2-672
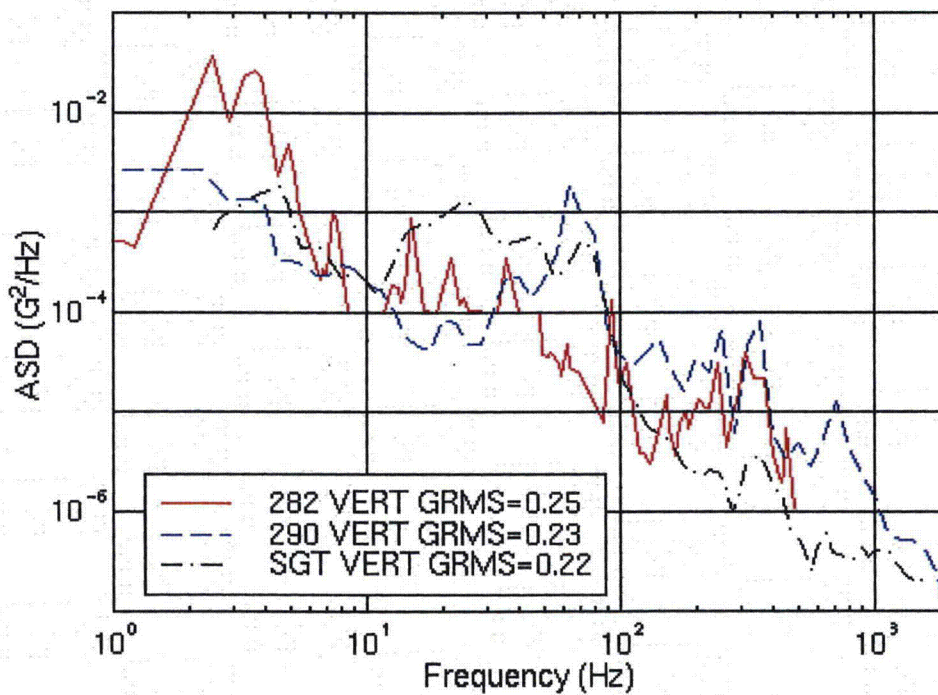
APPENDIX B
COMPARISON OF TEST SPECIFICATIONS AGAINST UNDERLYING MEE
RESPONSE SPECTRA FOR SHOCK

Figures B-1, B-3, and B-5 present comparisons of the recommended test specifications identified in the main section of this document (denoted SPEC...) against the envelopes of the MEE response spectra for the individual trailers (denoted ALL...). Figures B-2, B-4, and B-6 present the MEE spectra for the individual trailers (denoted 282, 290, and SGT for the SST2/82, SST2/90, and SGT respectively).

Figure B-1: SST/SGT Shock Environment
Comparison of Recommended Test Specification Versus MEE Response (All Trailers)
Trailer Floor – Longitudinal Axis - 3% Damped MMAA SRS
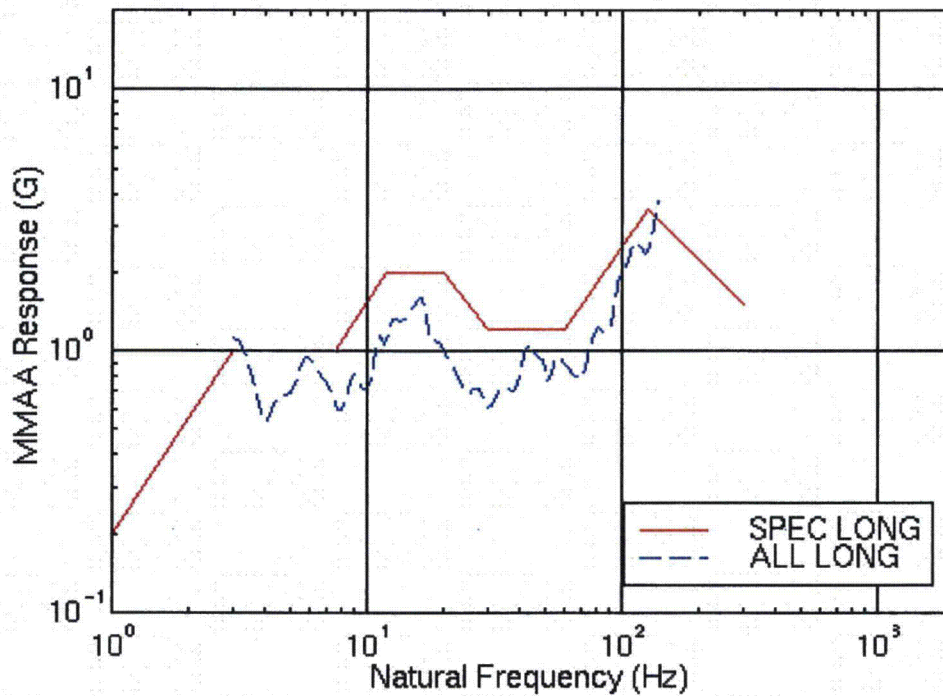
Figure B-2: SST/SGT Shock Environment
Comparison of MEE Responses for SST2/82, SST2/90, and SGT
Trailer Floor – Longitudinal Axis - 3% Damped MMAA SRS

2-674
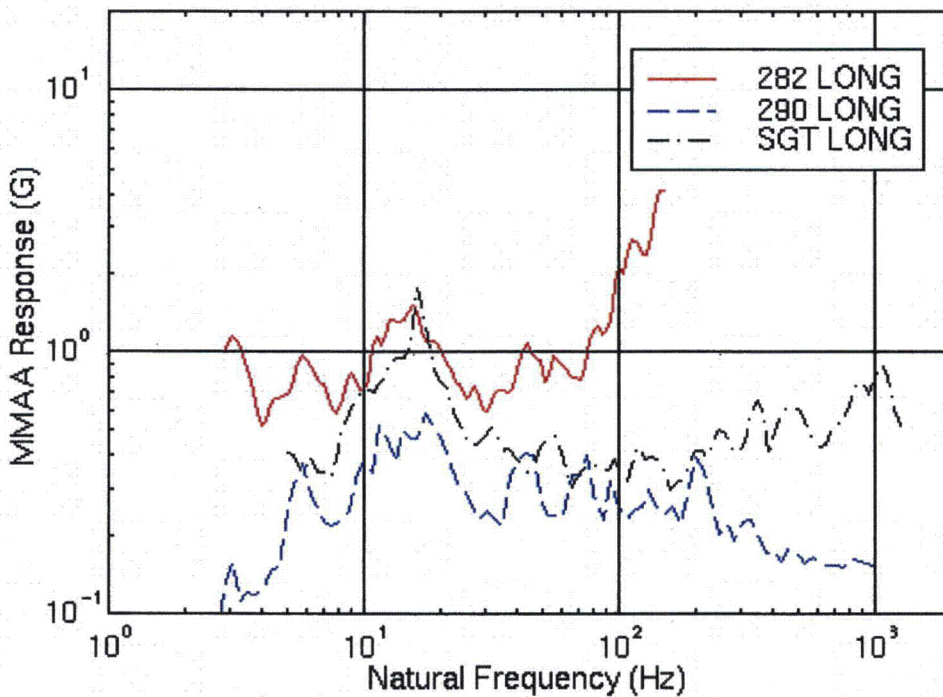
Figure B-3: SST/SGT Shock Environment
Comparison of Recommended Test Specification Versus MEE Response (All Trailers)
Trailer Floor – Lateral Axis - 3% Damped MMAA SRS
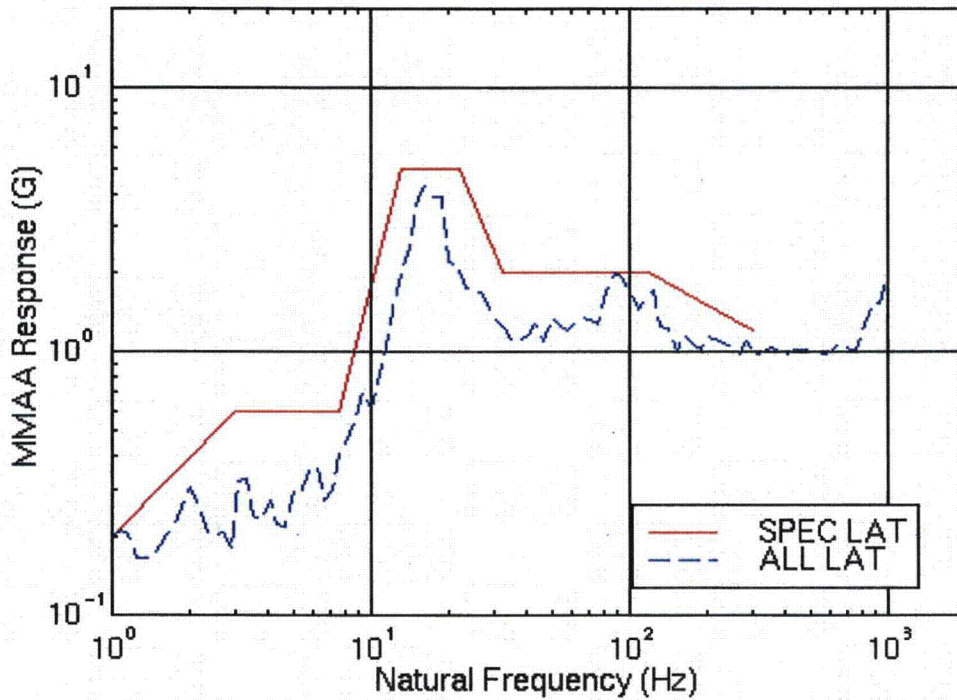
Figure B-4: SST/SGT Shock Environment
Comparison of MEE Responses for SST2/82, SST2/90, and SGT
Trailer Floor – Lateral Axis - 3% Damped MMAA SRS
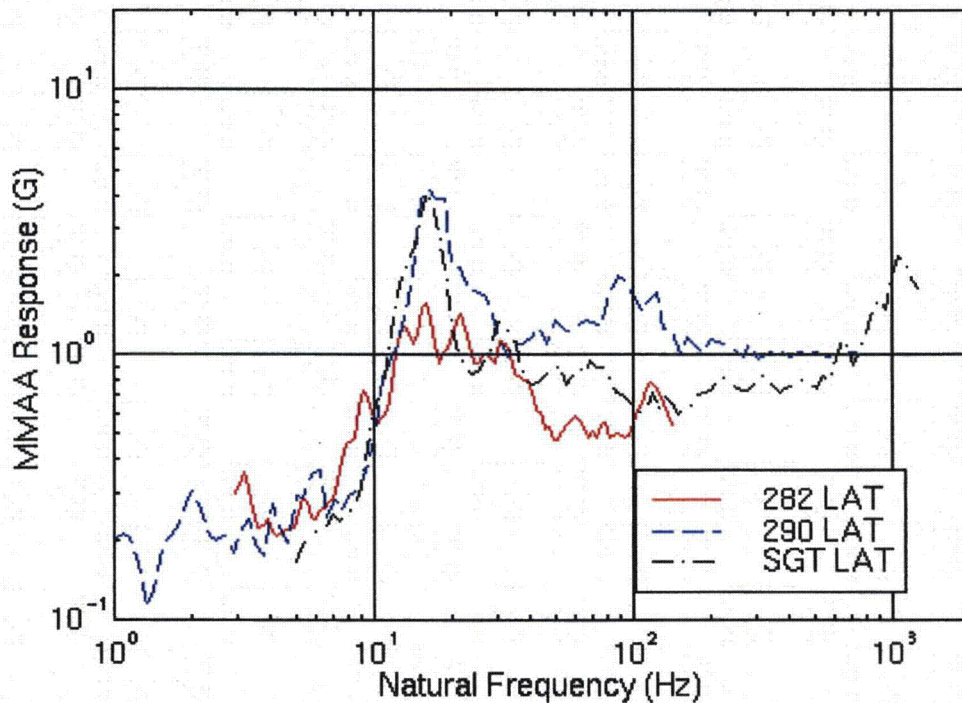
Figure B-5: SST/SGT Shock Environment
Comparison of Recommended Test Specification Versus MEE Response (All Trailers)
Trailer Floor – Vertical Axis - 3% Damped MMAA SRS
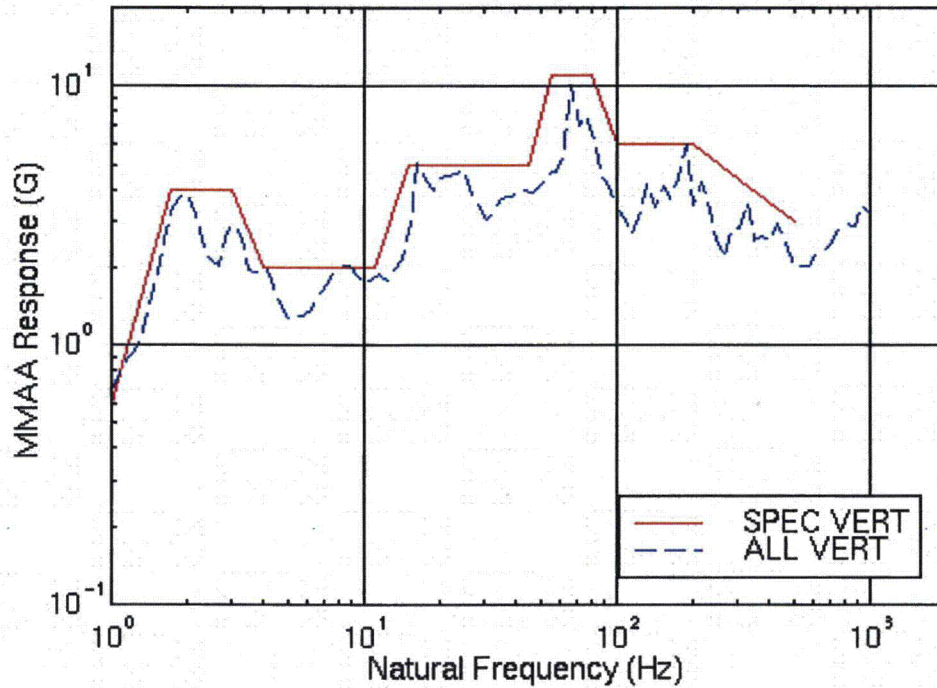
Figure B-6: SST/SGT Shock Environment
Comparison of MEE Responses for SST2/82, SST2/90, and SGT
Trailer Floor – Vertical Axis - 3% Damped MMAA SRS
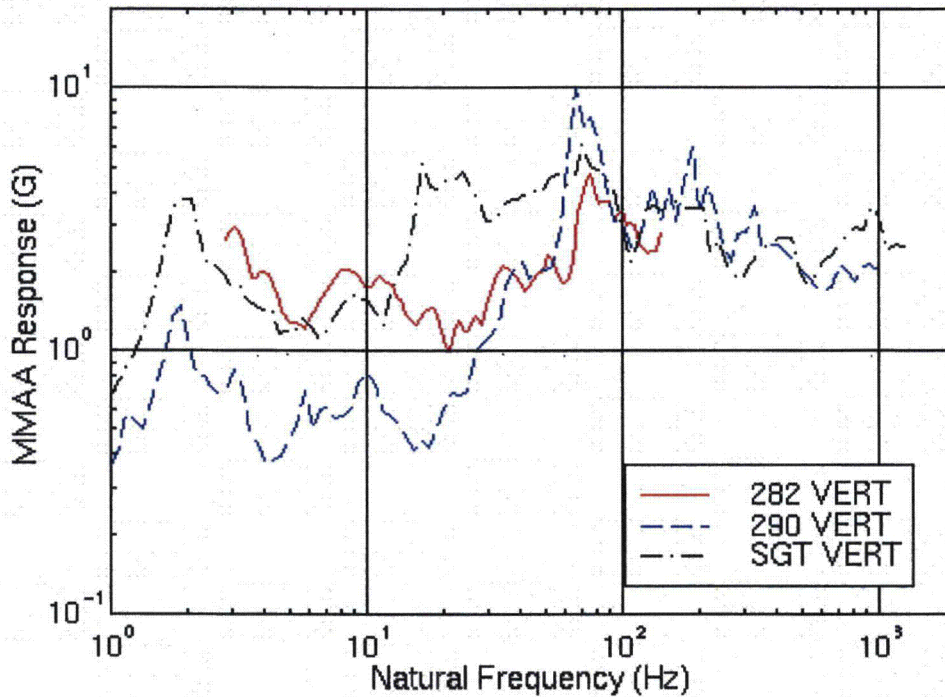
Appendix 2.10.7

**TEST REPORT OF THE ES-3100 PACKAGE, VOLUME 1 - MAIN REPORT,
ORNL/NTRC-013/V1, REV. 0, SEPTEMBER 10, 2004**

2-678

ORNL/NTRC-013/V1
Rev. 0

TEST REPORT OF
THE ES-3100 PACKAGE

Volume 1- Main Report

Revision 0
September 10, 2004

ornl

NTRC

NATIONAL TRANSPORTATION
RESEARCH CENTER

UT-BATTELLE
ORNL-27 (4-00)

Nuclear Science and Technology Division

Test Report of the ES-3100 Package
Volume 1 – Main Report

L. S. Dickerson
M. R. Feldman
R. D. Michelhaugh

September 10, 2004

Prepared for the
Y-12 National Security Complex
Highly Enriched Uranium Disposition Program Office

Prepared by
OAK RIDGE NATIONAL LABORATORY
P.O. Box 2008
Oak Ridge, Tennessee 37831-6285
Managed by UT-Battelle, LLC
For the
U.S. DEPARTMENT OF ENERGY
Under contract DE-AC05-00OR22725

Test Report of the ES-3100 Package
Volume 1 – Main Report

Prepared for the
Y-12 National Security Complex
Highly Enriched Uranium Disposition Program Office

Prepared by
L. S. Dickerson
M. R. Feldman
R. D. Michelhaugh

Oak Ridge National Laboratory
Nuclear Science and Technology Division
National Transportation Research Center

APPROVALS
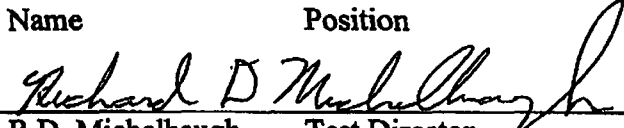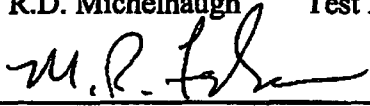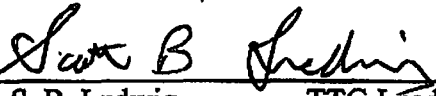
Name	Position	Date
R.D. Michelhaugh	Test Director	9-9-04
M. R. Feldman, PE	Program Manager	9/9/04
S. B. Ludwig	TTG Leader	9-9-04

TABLE OF CONTENTS

vi

TABLE OF APPENDICES

LIST OF FIGURES

x

LIST OF TABLES

Test Report of the ES-3100 Package

ABSTRACT

The Y-12 Highly Enriched Uranium Disposition Program Office (HDPO) is developing a new package design designated the ES-3100. Between May 2004 and July 2004, the Oak Ridge National Laboratory (ORNL) National Transportation Research Center (NTRC) tested six ES-3100 prototype units to the Type B performance tests prescribed in Part 71 of Title 10 Code of Federal Regulations (10 CFR). This test report documents test unit preparation, pre-test condition of each test unit, the Normal Conditions of Transport (NCT) and Hypothetical Accident Condition (HAC) testing, and the post-test measurements and observations of the damage resulting from the se tests.

1 INTRODUCTION

The Y-12 Highly Enriched Uranium Disposition Program Office (HDPO) is developing a new package designated the ES-3100. In order to support the certification of the ES-3100 package design, Y-12 contracted the ORNL Transportation Technologies Group (TTG) to perform independent testing of the ES-3100 to the requirements of 10 CFR Part 71. TTG conducted the tests according to a test plan (ORNL/NTRC-011, May 17, 2004) approved by the Y-12 Packaging Engineering and HDPO organizations and reports the testing and test results in this document. The test results will be used in the preparation of the ES-3100 package Safety Analysis Report (SAR).

Six ES-3100 packages were tested to demonstrate compliance with the requirements of Title 10, Code of Federal Regulations (CFR), Part 71.71, *Normal Conditions of Transport* (NCT), and Title 10, CFR, Part 71.73, *Hypothetical Accident Conditions* (HAC). (A seventh package was available just in case additional testing was necessary.) The packages were identified by sequential designation numbers: TU-1-05/04, TU-2-05/04, TU-3-05/04, TU-4-05/04, TU-5-05/04, and TU-6-05/04. The undamaged containment vessel of TU-6-05/04 was used for the 15-m immersion test. Hereafter in this report, the test units are identified simply by their "TU-*X*" designation.

All the NCT tests were performed on TU-4 while the NCT free drop test was performed on test units TU-1 through TU-5. All HAC drop and thermal tests were performed on TU-1 through TU-5. TU-6 (which was comprised of a CV only) was only subjected to the HAC 15-m (50-ft) immersion test. Test matrices are presented in Section 1.2.

Section 2 describes the pre-testing activities. Section 3 describes the NCT tests performed and results. Section 4 describes the HAC tests and results, and Section 5 describes the disassembly, the subsequent leak and immersion tests, and inspection and post-test measurements.

1.1 Description of the ES-3100 Shipping Package

The ES-3100 package consists of an outer drum and a containment vessel (CV) (Figure 1.1). The exterior of the package is a drum that is about 19 inches in diameter and about 44 inches in height, and is fabricated from 16-gauge, 304 stainless steel. The package has an integral annular liner that is filled with Kaolite 1600™, a mixture of Portland cement and expanded vermiculite which is cast in place. An inch thick layer of Borobond4 is located along the inner walls of the CV cavity to provide neutron absorption.

The test units will be made of drum assemblies and CV assemblies with specific serial numbers. Table 1.1 below indicates the specific serial numbers of the drums and CVs to be combined to assemble each complete test unit.

Ø19.37 [492]

STAINLESS STEEL CONFINEMENT PLUG VIBRO-CAST WITH KAOLITE 1600TM

OVERPACK LID

Ø18.25 [463.6]

5.07 [128.9]

.18 [4.6]

Ø7.50 [190.5]

4.67 [118.5]

VIBRATION ABSORBING SILICONE RUBBER SPACING PADS

.30 [7.6]

O-RINGS

CONTAINMENT VESSEL LID

32.88 [835.2]

.90 [22.9]

43.50 [1104.9]

BOROBOND4 NEUTRON ABSORBER

31.00 [787.4]

4.99 [126.6]

STAINLESS STEEL KAOLITE LINER

.06 [1.5]

Ø5.06 [128.5]

STAINLESS STEEL BOROBOND4 INNER LINER

STAINLESS STEEL CONFINEMENT BODY VIBRO-CAST WITH KAOLITE 1600TM

CONTAINMENT VESSEL BODY

.105 [2.67]

CONTAINMENT VESSEL VIBRATION ABSORBING SILICONE RUBBER PAD

3.96 [100.5]

STAINLESS STEEL CONFINEMENT BODY BOTTOM COVER

.20 [5.1]

Figure 1.1 Cut-away view of the ES-3100.

Table 1.1 Drum and CV serial numbers for each Test Unit

Test Unit	Drum Serial Number	CV Serial Number
TU-1	2	2
TU-2	4	4
TU-3	5	5
TU-4	9	9
TU-5	11	11
TU-6	N/A	1
TU-7	6	6

The test units were configured with simulated payloads in the containment vessels. For TU-1 through TU-4, the simulated payloads consisted of three product can-size test weights with a band clamp, cable lanyard and silicone vibration absorbing pad on the top of each can. The bottom test weight also had a silicone vibration absorbing pad. These test units had a "full" payload consisting of a total mass of 110 lb. BoroBond4 spacers were used between the top test weight and the middle test weight and also between the middle test weight and the bottom test weight. Test Unit 5 had a light weight test assembly which consisted of three product cans stacked together. The lower can was filled with ballast such that its total weight was 6.6 lb, and the other two cans were empty. No BoroBond4 spacers were used between the cans. TU-6 was a containment vessel (CV) with approximately 15 pounds of steel shot in a plastic bag serving as ballast weight to ensure that it would sink for the immersion test. TU-6 weighed 47 pounds.

1.2 ES-3100 Test Matrix

Table 1.2 and Table 1.3 summarize the order of the tests performed on each individual test unit along with the general orientation of each test unit when it was drop tested and crush tested. The cells containing numbers indicate that the designated test was performed on the test unit. The number in the cell indicates the sequence that the test was performed on the test unit. The NCT tests preceded the HAC tests.

TU-4 underwent the full battery of NCT tests. For the impact tests, a variety of package orientations were used to ensure that one or more test units would be subjected to impacts in "the most damaging orientation." As can be seen by reviewing Table 1.3, TU-1 through TU-5 were subjected to the full battery of HAC tests. TU-6 was an "undamaged" CV only and was only subjected to the HAC 15-m (50-ft) immersion test.

Table 1.2 Summary of NCT – 10CFR71.71 Tests performed on ES-3100 Package

Test	TU-1 (heavy) 12° Slap-down	TU-2 (heavy) Side Drop	TU-3 (heavy) CG over Top Corner	TU-4 (heavy) Top Down	TU-5 (light) 12° Slap-down
Operational Leak Test (CALT5)	1	1	1	1	1
NCT – 10CFR71.71 (c)(6) Water Spray				2	
NCT – 10CFR71.71 (c)(7) Free Drop	2	2**	2	3	2
NCT – 10CFR71.71 (c)(10) Penetration				4	
NCT – 10CFR71.71 (c)(9) Compression				5	
NCT – 10CFR71.71 (c)(5) Vibration				6	

*- TU-6 is only a containment vessel (CV)
** - TU-2 was chilled to below -40°F for this test
Note: Numbers in table indicate testing sequence

Table 1.3 Summary of HAC – 10CFR71.73 Tests performed on ES-3100 Packages

Test	TU-1 (heavy) 12° Slap-down	TU-2 (heavy) Side Drop	TU-3 (heavy) CG over Top Corner	TU-4 (heavy) Top Down	TU-5 (light) 12° Slap-down	TU-6* 15m Immerse (CV only)
HAC – 10CFR71.73 (c) (1) Free Drop – 9-m (30 ft.)	1	1**	1	1	1	
HAC – 10CFR71.73 (c) (2) Crush – 9-m (30 ft.)	2	2**	2	2	2	
HAC – 10CFR71.73 (c) (3) Puncture – 1m (40 in.)	3,4,5,6	3**	3,4†	3	3	
Preheat to above 38 °C (100 °F) before Thermal test	7	4	5	4	4	
HAC – 10CFR71.73 (c) (4) Thermal – 800°C (1475°F)	8	5	6	5	5	
Operational Leak Test of CV (CALT5)	9	6	7	6	6	1
Full Containment Boundary Leak Test (He Leak Test)	10	7	8	7	7	
HAC – 10CFR71.73 (c) (5) Immersion Test – Fissile materials – 0.9-m (3 ft.)	11	8	9	8	8	
HAC – 10CFR71.73 (c) (6) Immersion Test – All Packages – 15-m (50 ft.)						2

*- TU-6 is only a containment vessel (CV)
** - TU-2 was chilled to below -40°F for these tests
†This differs from original test plan.
Note: Numbers in table indicate testing sequence.

1.3 Test Data Records

This report (Volumes 1, 2, and 3) documents the tests performed and measurements observed from the ES-3100 testing. The general data types for these tests are:

- manually derived measurements and observations,
- automatically recorded temperatures from the thermal testing,
- digital still photography, and
- video and high-speed motion photography of drop tests.

The primary recording media for each of the general types of data are:

- Procedure Checklists and Data Sheets for data, measurements, and observations,
- Computer files (Excel spreadsheets) for the temperature records,
- Computer files (JPG format) for the digital photography, and
- VHS and DVD video media for the video and motion photography.

The completed Data Sheets and Procedure Checklists have been scanned into a digital format. The still photography, scanned data sheets and the field marked test plan are attached to this document as appendices in separate volumes (Volumes 2 and 3). There is an appendix of photographs and an appendix of completed Data Sheets and Procedure Checklists for each test unit. Additionally, Appendix G, *Pre-Thermal Test Activities Photos*, contains the collection of digital photos related to preparation of the ES-3100 packages and thermal test facility for the thermal testing and Appendix N contains the as field-marked version of the test plan. Table 1.4 provides a listing of appendices and subject matter.

Table 1.4 Listing of appendices for photos and data sheets by test unit

Test Unit	Photo Appendix (Volume 2)	Data Sheet and Procedure Checklist Appendix (Vol. 3)
TU-1	A	H
TU-2	B	I
TU-3	C	J
TU-4	D	K
TU-5	E	L
TU-6	F	M
ALL	G	N

Appendix G contains digital photos related to preparation of the ES-3100 packages for the thermal testing
Appendix N contains the field marked version of the test plan

2 PRE-TESTING ACTIVITIES

Several activities were required to prepare the test units for testing. These activities focused on documenting the initial condition of each test unit, installing data acquisition devices (temperature-indicating labels) in various locations on the test units, and assembling each test unit per operational procedures developed by the package design team.

2.1 Description of Test Units

The test units were full-scale ES-3100 packages equipped with surrogate payloads in the containment vessels. For TU-1 Through TU-4, the simulated payloads consisted of three product can size test weights with a band clamp, cable lanyard and silicone vibration absorbing pad on the top of each can. The bottom test weight also had a silicone vibration absorbing pad on its bottom. These units had a "full" payload consisting of a total mass of 110 lb. BoroBond4 spacers were used between the test weights in these four units. Figure 2.1 shows the surrogate payloads for TU-1 through TU-4.

Figure 2.1 Surrogate payload for TU-1 through TU-4

The picture shows the three solid cylindrical masses that are stacked on top of each other when put inside the containment vessel, the vibration-absorbing pads placed on top of the three cans, and the BoroBond4 spacers (to the left of the picture). The rubber silicone

cushions used to reduce metal-to-metal contact and jarring are shown between the top plug and the cans.

Test Unit 5 had a light weight test assembly which consisted of three product cans stacked together. The lower can was filled with a plastic bag of steel shot to add ballast such that its total weight was 6.6 lb, and the other two cans were empty. The cans in TU-5 had band clamps, cable lanyards and silicone vibration absorbing pads on the top of each can. The bottom can also had a silicone vibration absorbing pad on its bottom; however, no BoroBond4 spacers were used. TU-6 was only a containment vessel (CV) with 13 lbs. of steel shot ballast added, which Y-12 engineers calculated would be enough to ensure that it did not float during the immersion test. With the ballast, TU-6 weighed a total of 47 pounds.

As stated above, the test units were loaded with two different configurations of surrogate payloads. As a result the location of the center of gravity (CG) for TU-5 varied from the other test units. Table 2.1 shows the test weight configuration inside each CV and identifies the location of the CG for each test unit. The CG locations were provided by Y-12 Packaging Engineering and were not measured or independently verified by ORNL-TTG personnel.

Table 2.1 Surrogate payload vs. Test Unit

	TU-1	TU-2	TU-3	TU-4	TU-5	TU-6
Payload (heavy) M2E801580A028	X	X	X	X		
Payload (light) M2E801580A030					X	
CV + ballast (M2E801580A011)						X
Location of CG (from base of outside drum)	22.42 in.	22.42 in.	22.42 in.	22.42 in.	23.00 in.	N/A CV only

Test Units 1 through 5 had temperature-indicating labels affixed to the surrogate payload, the outside of the CV, the inside surface of the drum liner, and the top plug prior to assembly. Figure 2.2 shows the temperature labels on the inside of the outer drum for TU-3.

The vertical seam of the outside drum of TU-1 through TU-5 was marked with a 0° vertical reference line and the other three quadrants were marked with a vertical line at 90°, 180°, and 270° as measured around the top perimeter of the package in a counterclockwise direction looking down onto the top of the package. A horizontal line was also marked around the circumference of each outer drum, which designated the center-of-gravity plane of each package. The intersection of the vertical lines and the circumferential line provided CG "targets" on each quarter of the outer drum surface. Figure 2.3 shows the markings on a typical test unit.
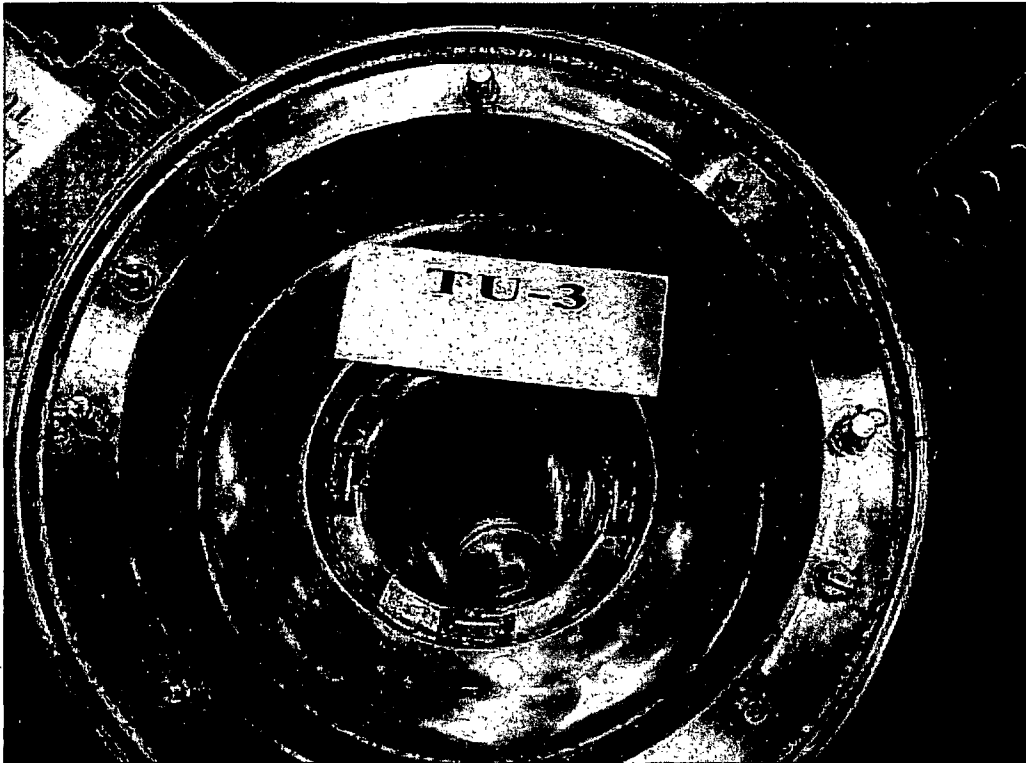
Figure 2.2 Temperature-indicating labels affixed to inner liner of TU-3

Figure 2.3 Vertical and CG markings on TU-1 and TU2

2.2 Application of Temperature Labels

Prior to assembly, an array of temperature-indicating labels was applied to the components of the test units. Type B labels (171 °F to 261 °F) were affixed to opposite sides of each surrogate payload can; 17 total temperature labels of a combination of Type B and Type C labels (270 °F to 360 °F) were placed on each CV; and an additional 18 labels were affixed to the inner surface liner of each drum. The B range labels were used on the inner wall of the drum, as specified by the test plan. A mistake was made during assembly and B range labels were used on the CV lid instead of the 125 °F to 300 °F labels specified in the test plan. The full range labels are designed with 16 indicating spots that range from 125 °F to 500 °F, in 25 ° increments. Also, full-range temperature labels were applied at the 0°, 90°, 180°, and 270° positions on the underside of the top plug. General placement of the temperature labels inside the drum can be seen in the previous Figure 2.2. Figure 2.4 shows some of the temperature labels applied to the outside of the containment vessel. Each label was affixed at a specific location and an additional strip of Teflon™ tape was placed over the label to ensure that it would remain in place during the thermal test. Details of temperature-indicating label locations are in Section 5.6.
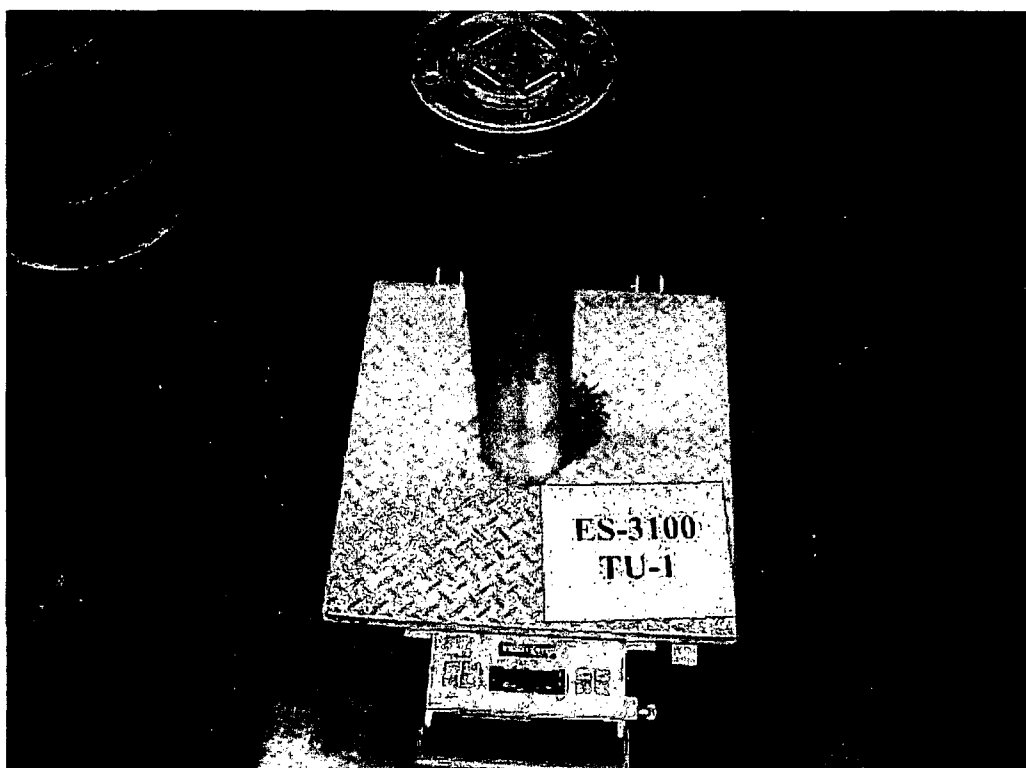
Figure 2.4 Temperature labels applied to outer CV

In addition to the use of temperature labels, after the structural testing and just prior to the thermal testing, thermocouples were also placed on the surface of the test units by fitting them underneath welded tabs. Six thermocouples were placed on the exterior of each test unit along the 0°-, 90°-, 180°-, and 270°-line, and the bottom and top of the drums.

Y/LF-717/Rev 2/ES-3100 HEU SAR/Ch-2/rlw/3-06-08

2.3 Package Assembly

Before assembly of each test unit, the components of each CV were given a visual inspection and weighed. The weights of the various components making up the package were measured and recorded on TEST FORM 1. The assembly process for each test unit was documented on TEST FORM 2. TEST FORM 3 describes assembly of the test package: placement of the CV, drum lid installation, weighing, etc. The total weight of each package is given in Table 2.2. The slight weight loss shown in the last row, *Change in weight*, could be a factor of the accuracy of the weighing scale, water loss from Kaolite, or combustion of silicone gaskets. In the table, TU-5 weighs roughly 100 lbs less than the other test units (except TU-6, of which only the weight of its CV and included ballast is shown) because its containment vessel had only a light-weight test assembly installed.

Table 2.2 Total weight of each test unit pre- and post-testing

Item	TU-1	TU-2	TU-3	TU-4	TU-5	TU-6
Pre-test total weight (lb)	446	447	449	445	347	47
Post-test total weight	446	447	448	444	346	47
Change in weight	0	0	-1	-1	-1	0

2.4 Pre-test Operational Leak Test

Prior to the initiation of testing, the O-ring seals of the CV assembly of TU-1 through TU-6 were leak tested using a CALT5 leak check system manufactured by Croft and Associates. The leak check was conducted in accordance with ANSI N14.5-1997 using a CALT5 Leak Detector and following the manufacturer's leak testing procedure. If a CV successfully passed this test (1×10^{-4} ref-cc/sec), it showed that the O-rings were installed and functioning properly.

The CALT5 pressurizes the volume between the O-rings and then uses a very precise pressure transducer to measure the pressure drop over the test period. The CALT5 will compute a leak rate; however, the ES-3100 package operating procedures call for the computation of the leak rate based on the ANSI N14.5-1997 algorithm, using data from the CALT5 as inputs for V*cm3* (*interstitial volume*), M(*length of test*), P_1atm (*initial pressure*), P_2atm (*ending pressure*), T_1 K, and T_2 K:

$$Lr = \frac{Vcm3 * 298K}{3600 * \frac{M\,min}{60\,min} * 1atm}\left(\frac{P_1atm}{T_1K} - \frac{P_2atm}{T_2K}\right)ref - cc/\sec$$

The instrument was set to a test sensitivity of 5×10^{-5} ref-cc/sec. A summary of the leak rates is given in Table 2.3. All leakage rate data and calculations resulting from the tests are documented in Appendices H, I, J, K, L and M.

Table 2.3 Pre-test leak rate for the test unit CV

Drum ID	TU-1	TU-2	TU-3	TU-4	TU-5	TU-6
Leak Rate, std-cc/sec	2.760E-5	2.102E-5	2.381E-5	2.967E-5	2.116E-5	4.772E-5

2.5 Chilling of TU-2

TU-2 was chilled before the structural tests were conducted. TU-2 was placed in an environmental chamber at ORNL and chilled to -70 °F for 24 hours and then -45 °F for 72 hours. TU-2 was then placed in an insulated box and transported to the NTRC test site. The four structural tests, NCT 1.2-m drop test, HAC 9-m drop test, HAC crush test, and the HAC puncture test, were conducted as quickly as possible after its removal from the environmental chamber. The package was removed from the environmental chamber at 8:28 a.m. The NCT drop test was conducted on it at 9:30 and the HAC drop took place 8 minutes later. The remaining crush and puncture tests concluded before 10:33 a.m. Therefore, all of the structural tests were performed within 125 minutes of removal of the test unit from the environmental chamber.

3 NCT TESTS

The applicable Normal Conditions of Transport (NCT) test sequence as specified in 10 CFR 71.71 includes a water spray test, a static compression test, a vibration test, a penetration test, and a 1.2 m (4 ft) drop test. Table 1.2 lists the NCT tests that were performed on the test units and the sequence in which they were conducted. Because the full battery of NCT tests were conducted only on TU-4, this unit will be used to guide discussion of the NCT test application.

3.1 Full NCT Test Series (TU-4 Only)

As noted above, TU-4 was the only test unit to be subjected to all of the applicable NCT tests. This section discusses only the NCT testing performed on TU-4. Drop testing will be discussed in the following Section 3.2, since it was applied to all the test units.

3.1.1 Water Spray Test

The water spray test was performed using a four-nozzle spray manifold with the four nozzles directed to spray the top as well as the four quadrants of TU-4. The water spray was conducted on the package within two hours of the subsequent tests and is noted on the test forms for the subsequent tests. The water spray test was conducted prior the free-drop, penetration, and compression testing. Figure 3.1 shows TU-4 undergoing the water spray test. (Using a rain gauge, which is positioned near the bottom of the package in Fig. 3.1, the flow rate was measured to be ~91 cm/h.) Water accumulated in the drum between the inner liner and the CV. The water drained out during the setup for the drop test.

3.1.2 Penetration Test

TU-4 was placed on its side on the center of the indoor drop pad with the 0° (drum seam) line facing upward. TU-4 was chocked to keep it from moving during the test. The 6-kg penetration bar was raised to 1 m (40 in.) above the contact point. The contact point was the "X" marking placed at the 0° line to indicate the location of the internal CV flange. Figure 3.2 shows the test setup. The bar struck the package slightly left of center and formed a ~1/4 inch deep dent in the side of the package (Figure 3.3). See the data sheets in Appendix K for results of the test.
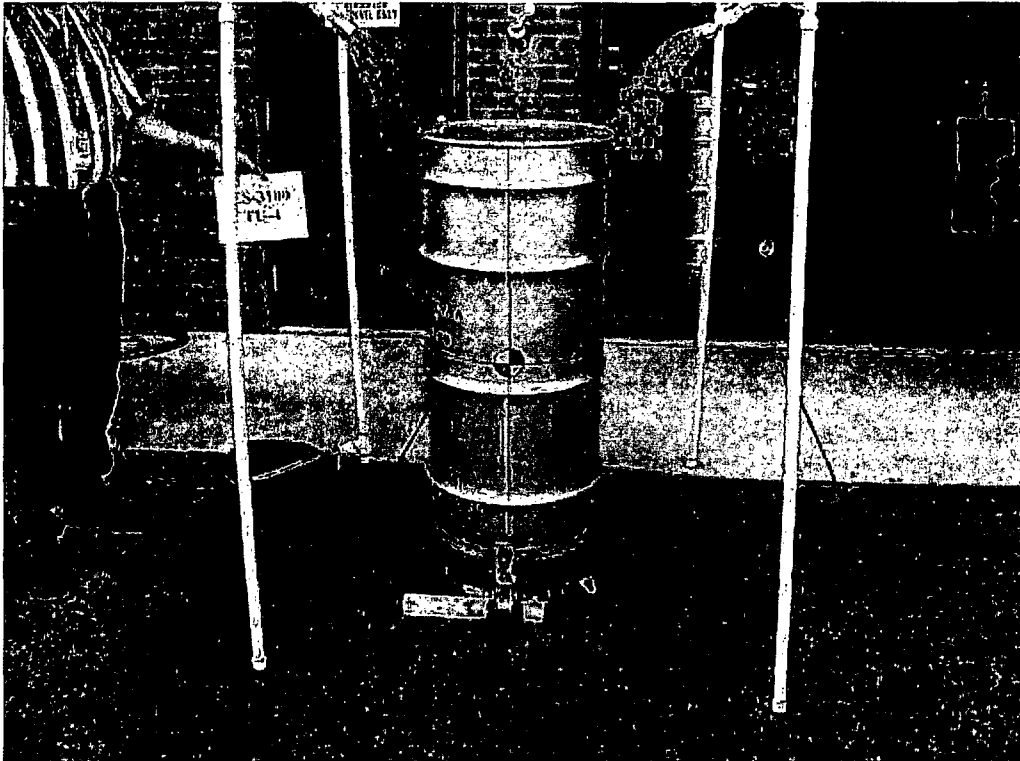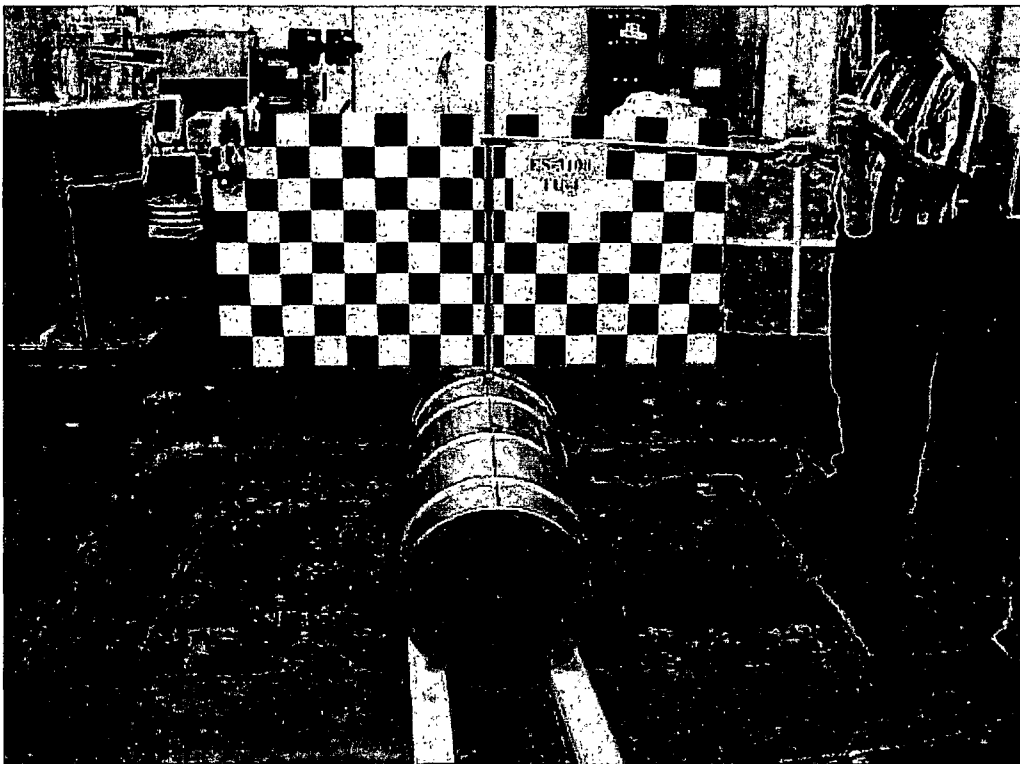
Figure 3.1 TU-4 undergoing the water spray test
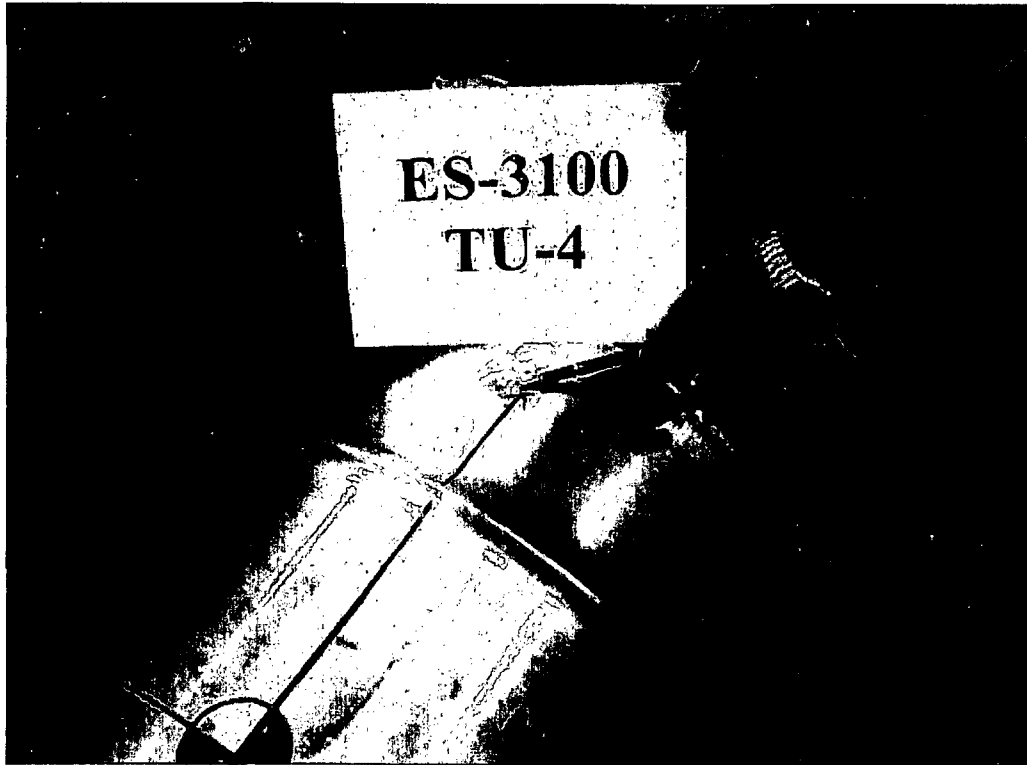

Figure 3.2 TU-4 penetration test setup

Figure 3.3 TU-4 damage from penetration test

3.1.3 Compression Test

The static compression test was performed on TU-4 using a Lansmont model 152-30K compression tester (Figure 3.4.). In accordance with 10 CFR 71.71(c)(9), 1.9 psi times the projected vertical area of the package was shown to be only 1,008 pounds; hence the more restrictive load of 5 times the maximum package weight or 2,500 pounds was applied to the package. (A maximum package weight of 500 lbs was assumed; actual maximum package weight may be lower.) After being compressed for 24 hours and 1 minute, there were no measurable effects on the package. See the data sheet in Appendix K.

Figure 3.4 TU-4 in Compression Tester.